



Western Washington University
Western CEDAR

WWU Graduate School Collection

WWU Graduate and Undergraduate Scholarship

Summer 2018

A Chemoenzymatic Approach to the Synthesis of Hemoglobin Oligomers

Johann Sigurjonsson

Western Washington University, jsigurjonsson1@gmail.com

Follow this and additional works at: <https://cedar.wwu.edu/wwuet>

 Part of the [Chemistry Commons](#)

Recommended Citation

Sigurjonsson, Johann, "A Chemoenzymatic Approach to the Synthesis of Hemoglobin Oligomers" (2018). *WWU Graduate School Collection*. 750.
<https://cedar.wwu.edu/wwuet/750>

This Masters Thesis is brought to you for free and open access by the WWU Graduate and Undergraduate Scholarship at Western CEDAR. It has been accepted for inclusion in WWU Graduate School Collection by an authorized administrator of Western CEDAR. For more information, please contact westerncedar@wwu.edu.

A Chemoenzymatic Approach to the Synthesis of Hemoglobin Oligomers

By

Johann Sigurjonsson

Accepted in Partial Completion
of the Requirements for the Degree
Master of Science

ADVISORY COMMITTEE

Chair, Dr. Spencer Anthony-Cahill

Dr. P. Clint Spiegel

Dr. John Antos

GRADUATE SCHOOL

Dr. Gautam Pillay, Dean

Master's Thesis

In presenting this thesis in partial fulfillment of the requirements for a master's degree at Western Washington University, I grant to Western Washington University the non-exclusive royalty-free right to archive, reproduce, distribute, and display the thesis in any and all forms, including electronic format, via any digital library mechanisms maintained by WWU.

I represent and warrant this is my original work, and does not infringe or violate any rights of others. I warrant that I have obtained written permissions from the owner of any third party copyrighted material included in these files.

I acknowledge that I retain ownership rights to the copyright of this work, including but not limited to the right to use all or part of this work in future works, such as articles or books.

Library users are granted permission for individual, research and non-commercial reproduction of this work for educational purposes only. Any further digital posting of this document requires specific permission from the author.

Any copying or publication of this thesis for commercial purposes, or for financial gain, is not allowed without my written permission

Johann Sigurjonsson

8/13/18

A Chemoenzymatic Approach to the Synthesis of Hemoglobin Oligomers

A Thesis
Presented to
The Faculty of
Western Washington University

In Partial Fulfillment
Of the Requirements for the Degree
Master of Science

by
Johann Sigurjonsson
August 2018

Abstract

Polymerized hemoglobin (poly-Hb) molecules have been shown to have reduced toxicity compared to cell-free hemoglobins when transfused intravenously. Poly-Hbs are typically generated with non-specific crosslinking agents that yield a product that is polydisperse in molecular weight. We propose a chemoenzymatic approach to generate poly-Hb of defined molecular weight. The proposed method employs the site-specific ligation reaction of the sortase A enzyme from *S. aureus*. A Hb mutant previously developed in our lab has been “sortagged” – modified by adding either the sortase recognition sequence (LPXTG) to the C-terminus of the α -subunit or a tetraglycine motif (GGGG) to the N-terminus. We show here that Hb subunits can be ligated directly by sortase A, using a mixture of substrate tagged (LPXTG) and nucleophile tagged (poly-G) Hbs. Additionally, using a novel approach for crosslinking Hb subunits using sortase A, we have generated a di- α construct that is functionalized with a strained cycloalkyne through an unnatural C-to-C fusion of sortagged α -subunits using a bifunctional sortase nucleophile peptide. We show that cycloalkyne-modified Hb molecules can be covalently linked to an azide functionalized fluorescein, using the well-established method of Huisgen cycloaddition. The work presented here establishes the feasibility of generating a monodisperse poly-Hb using azide decorated scaffolds.

Acknowledgements

I would like to express my sincere gratitude to Dr. Spencer Anthony-Cahill for the opportunity to work with him both as an undergraduate and graduate student. He has been a very dedicated mentor to me, always available with encouragement and assistance when the difficulties of research arose. Most of all, I am deeply appreciative of his gestures that have gone above and beyond his duties as a research advisor, offering kindness and understanding during times in my life it was needed most.

I would also like to thank my committee members, Dr. John Antos and Dr. Clint Spiegel for their guidance and support for this project. This work would not have been possible without the generous use of shared lab equipment that both Dr. Antos and Dr. Spiegel have provided. Specifically, I would like to thank Dr. Antos for his generosity in allowing the use of his HPLC and ESI-MS for this project, and the Antos Lab for their time assisting me in the use of said equipment.

In addition, I would like to thank all the past and current lab members who made this work possible and provided an enjoyable environment to work. This work would also not have been possible without the care and support I receive from loved ones at home and my family.

Table of Contents

Abstract.....	iv
Acknowledgements	v
List of Tables and Figures	vii
1. Introduction	1
1.1 Necessity for a Red Blood Cell Substitute	1
1.2 Hemoglobin-Based Oxygen Carriers	6
1.3 Overview of Modern Protein Modification Methodologies	18
1.4 Project Goals and Overview	25
2. Preparation of Sortase-Ready Hbs and Peptide Crosslinkers.....	27
2.1 Expression, purification, and characterization of sortagged α -globins	27
2.2 Design and Synthesis of GGGK(K)GGG	30
3. Sortase-Mediated Ligation of Sortagged α -subunits	32
3.1 Ligation of α -LPETG and GG- α by Sortase A.....	32
3.2 Crosslinking α -LPETG in a C-to-C Ligation by Sortase A	35
3.3 Bioorthogonal Reactivity of Crosslinked Hbs	46
4. Discussion.....	52
4.1 Implication of Termini Modification in Sortagged-Hbs	52
4.2 Functionalizing and Crosslinking Sortagged-Hbs	53
4.3 Improving the Bioorthogonal Reactivity of DBCO-Hbs.....	59
4.4 Conclusions and Future Directions	60
5. Experimental	63
5.1 Expression and Purification of Hbs	63
5.2 Staphylococcus aureus Sortase A	68
5.3 Preparation of Oligopeptide Crosslinkers.....	69
5.4 Sortase-Mediated Ligation Reactions	71
5.5 Bioorthogonal Ligation Reactions	74
Literature Cited.....	76
Appendix	85

List of Tables and Figures

Figure 1. Chemical structure of a biologically relevant PFC	5
Figure 2. Tetrameric Hb dissociation into $\alpha\beta$ heterodimers	7
Figure 3. Major pathway of NO-induced vasodilation and NO-scavenging by Hb	15
Figure 4. Sortase-mediated ligation as a protein engineering tool	22
Figure 5. Purification of sortagged-Hbs analyzed by SDS-PAGE	28
Figure 6. AEX purification of α -LPETG/cp β following Ni-IMAC	29
Figure 7. Design and synthesis of GGGK(K ^{DBCO})GGG	31
Figure 8. Sortase-catalyzed ligation of α -LPETG and GG- α	33
Figure 9. Analysis of oligomerization state of ligated α -LPETG/cp β and GG- α /cp β	35
Figure 10. Crosslinking α -LPETG with Gly-PEG4-Gly via SML	37
Figure 11. Crosslinking α -LPETG with GGGK(K ^{FITC})GGG via SML	39
Figure 12. Crosslinking α -LPETG with GGGK(K ^{FITC})GGG via wtSrtA	40
Figure 13. Crosslinking α -LPETG with GGGK(K ^{DBCO})GGG	41
Figure 14. Reaction time-course by ESI-MS for α -LPETG crosslinking	43
Figure 15. Purification of α -GGGK(K ^{DBCO})GGG- α from crude reaction mixture	45
Figure 16. Bioorthogonal conjugation of 6-FAM and DBCO modified Hbs	48
Figure 17. Reaction of α -GGGK(K ^{DBCO})GGG- α and azido-PEG5-azide	50
Figure 18. Reaction of α -GGGK(K ^{DBCO})GGG- α and 4-arm PEG azide	51
Figure 19. Circularization of GFP with high efficiency by Antos <i>et al.</i> ⁹³	54
Figure 20. C-to-C fusion of adjacent α -subunits in tetrameric Hb	56
Figure 21. Hypothetical additional crosslinking event	59
Table 1. Examples of direct and indirect transfusion-related costs	2
Table 2. A brief overview of the three HBOC types described here	8

Table 3. Summary of HBOCs and their properties and clinical development	9
Table 4. Observed and expected masses by ESI-MS	30
Table 5. Expected and ESI-MS observed masses for α -LPETG crosslinking reaction	42
Table 6. Typical abundances of α -species in purified fractions of SML mixture	46

1. Introduction

1.1 Necessity for a Red Blood Cell Substitute

Current trauma medicine completely depends on donor-derived red blood cells (RBCs), because there is no viable alternative in critical care. Although blood transfusion is a life-saving medical procedure, it can nonetheless result in medical complications that pose serious risk to the patient. Many of these risks, such as blood-borne illnesses and type mismatch, arise from a blood supply derived from a large and diverse donor population. Federal regulators have mandated measures that have significantly reduced transmission rates of some more well-known transfusion-related diseases.¹ For example, transmission of human immunodeficiency virus (HIV) occurs at rates of 1 in 1.9 million units of transfused blood and fatal ABO-incompatible transfusions are less than 1 in 1.5 million transfusions.^{2, 3} However, new potential pathogenic threats continually emerge, requiring the development of new screening tests. In one recent example, 1 in every 529 blood donations made during an outbreak of dengue in Puerto Rico was shown to contain viral RNA. Consequently, one recipient developed dengue hemorrhagic fever.⁴

Other post-transfusion complications are more common. Despite widespread testing for bacterial contamination, sepsis occurs in 1 per 100,000 platelet transfusions and clinically relevant bacterial burdens are found in 1 in 3000 units.⁵ Non-infectious complications, such as immunogenic response to donor leukocytes, potentially pose the greatest patient risk and occur much more frequently than transfusion-related infections as they are less predictable and difficult to prevent.³ Transfusions have also been linked to serious medical complications and poor outcomes, including multiple organ failure, increased mortality, and increased length of intensive care.⁶⁻⁹

From the perspective of healthcare economics, these adverse medical complications are reflected in patient costs. One study found the mean acquisition cost per unit to be approximately \$240, when adjusted for inflation.¹⁰ The direct cost, however, only reflects the cost of donor recruitment and materials, and is estimated to represent only 20% of the total patient cost.¹¹ Unaccounted for are the quality-adjusted life costs such as hospital stays, lost earnings, bacterial infection treatment, or the lifetime costs of HIV or hepatitis infections (Table 1). These contributing factors to the total cost of allogenic blood transfusions are often unconsidered and, as a result, are often unappreciated.

Table 1. Examples of direct and indirect transfusion-related costs.^a

Cost	Item(s)	Estimated Cost	Source
Direct	Collection, disease testing, compatibility, management	\$150/unit	Etchason, et al ¹²
	Overhead, materials, labor	\$469/unit	Cremieux, et al ¹¹
	Clinical compensation, overhead, acquisition, testing	\$565/unit	Cantor, et al ¹³
Indirect	Unused or Discarded Blood	\$13.59/unit	Etchason, et al ¹²
	Risk of transfusion-transmitted disease	\$4.05 (hepatitis), \$0.63 (HIV) \$4.80 total per unit	
	Infection	\$112,578 per fatal event	Denton et al ¹⁴
	Hospital Costs	\$838/visit additional if transfused	Vamvakas et al ¹⁵
	Lost Earnings	\$74/day (patient) \$133/day (employer)	Denton et al ¹⁴

^a Adapted from Shander, et al¹⁶

To compound the medical-related costs, there are also significant logistical complications to donor-derived RBC transfusion. Units of RBCs must be kept refrigerated during storage which limits their availability in the developing world and in field operations

(e.g., combat, response to natural disasters, etc.). Even when RBCs are readily available, standard practice limits transfusions to clinical settings to allow for monitoring and treatment of potential complications such as those described above. In addition, donor supplied RBCs have a shelf life of 42 days, at which time a significant lysis of erythrocytes has occurred, thereby increasing the risk of transfusion-related adverse events.¹⁷ Due to the short shelf-life of donated blood, local shortages are still common and keeping a well-stocked blood supply can be challenging.¹⁸ To reduce the amount of wasted units, hospitals must balance their supply by predicting demand. However, this can leave them vulnerable with a short supply that is inadequate to meet the need in mass emergency situations.

These medical, economic, and practical deficits of donor-derived RBCs, illustrate the importance of alternatives to donated blood. Although pre-donated autologous blood mitigates many of the transfusion-related risks, whether it is worth the enormously increased cost compared to allogenic blood is still clear.¹⁶ A viable blood substitute that functions similarly to RBCs while avoiding the medical complications associated with allogenic blood transfusions would therefore address an important medical need.

While the components of whole blood perform many functions, we will focus on the oxygen transport function of blood to inform the development of oxygen-carrying therapeutics. Within that narrowed view, the ideal “blood substitute” would have similar oxygen carrying ability as whole blood while minimizing the problems associated with RBC transfusion. Two main classes of oxygen carrying therapeutics have been

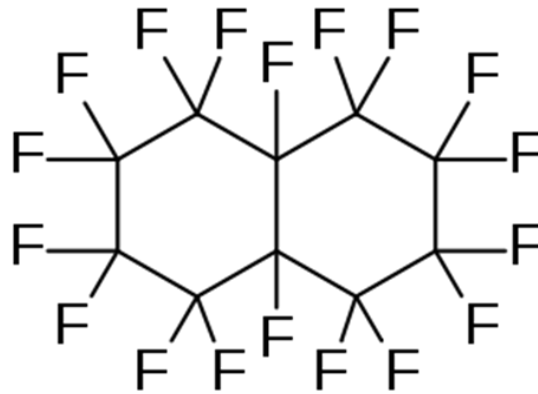
developed for commercialization: perfluorocarbon emulsions and hemoglobin-based oxygen carriers (HBOCs).

1.1.1 Types of RBC Substitutes

Perfluorocarbon Emulsions

Perfluorocarbons (PFCs) are analogues of linear, cyclic, and polycyclic hydrocarbons in which all of the hydrogens have been replaced with fluorine. These compounds are known for being very inert due to the highly stable carbon-fluorine bond and have received considerable interest for commercial applications. Poly(tetrafluoroethylene) or commonly known as Teflon, is one such polymerized PFC that has seen wide industrial and consumer use.

Biologically relevant PFCs are usually 8-10 carbons in length, such as perfluorodecalin or perflubron (bromoperfluoro-*n*-octane), and are colorless, odorless liquids with densities about twice that of water (Figure 1). These inert liquids have the ability to physically dissolve large quantities of gases, including O₂. In addition to being chemically inert, these molecules are highly resistant to enzymatic attack due to the electron-rich fluorine “shield” surrounding the carbon backbone. Their relatively low cost, abundance, and low reactivity towards biomolecules, have prompted considerable interest in developing them as oxygen-carrying therapeutics. In fact, PFC liquids have been successfully used for liquid ventilation in neonatal care.¹⁹ However, due to the linear relationship between O₂ partial pressure and concentration of dissolved O₂, biotherapeutic applications of PFCs require a 100% oxygen environment.



Perfluorodecalin

Figure 1. Chemical structure of a biologically relevant PFC that been investigated for use as a therapeutic oxygen carrier.

In their pure form, PFCs are unsuitable for direct intravenous (IV) transfusions due to their hydrophobicity, which renders them insoluble in aqueous buffers.²⁰ To circumvent this, PFCs must be prepared with emulsifiers such as egg yolk phospholipids or chemical surfactants.¹⁷ Some commercially developed PFC emulsions have been approved but applications have been limited to oxygenation of heart tissues during angioplasty or preservation of transplanted human organs for transportation.²¹ While clinical trials of PFC emulsions as intravenous oxygen carriers have been performed, the linear O₂ “binding” affinity required patients to breath supplemental oxygen for extended periods of time for effects to be observed.²⁰ Due to the inherent difference in oxygen binding characteristics, they are not as effective in O₂ transport as RBCs and therefore do not make a suitable resuscitation fluid for critical care.

Hemoglobin-based Oxygen Carriers

Hemoglobin-based oxygen carriers (HBOCs) are the most well-studied of the potential RBC substitutes. The advantage of chemically modifying hemoglobin (Hb) for

use as an oxygen carrying therapeutic is that, in contrast to perfluorocarbons, the oxygen affinity is inherently going to be most similar to that of whole blood. In addition, a highly pure solution could be formulated with antioxidants to extend the shelf life without refrigeration, making HBOCs much more desirable than current RBCs.³ Like the other potential RBC substitutes, these would not have a specific blood type and therefore could be administered universally in emergency care. HBOCs are generally considered to have the highest potential for an RBC substitute resulting in extensive research and development efforts in both corporate and public settings. There are two major categories of HBOCs: acellular and cellular.

1.2 Hemoglobin-Based Oxygen Carriers

1.2.1 Cellular HBOCs

Liposome-encapsulated Hbs (LEHs) are intended to imitate RBCs, in which Hb is kept out of the blood plasma via encapsulation within a lipid bilayer, thereby reducing the toxicity associated with cell-free Hb. In addition, the encapsulation makes adding allosteric effectors to LEHs possible. For example, 2,3-bisphosphoglycerate (2,3-BPG) and methemoglobin reductase could be co-encapsulated to, respectively, optimize O₂ affinity and oxidation propensities.²² However, LEHs were found to have short circulatory half-lives due to removal by the reticuloendothelial system and shear-induced destruction within the blood stream.²³ Other methods of generating pseudo-cellular Hbs, such as encapsulation within hydrogel particles²⁴ or polymersomes²⁵, have been explored but are still in initial research phases.

1.2.2 Acellular HBOCs

To use cell-free Hb as a therapeutic oxygen bridge, significant re-engineering of the protein is required. Once removed from the erythrocyte, tetrameric Hb (64 kDa) is able to dissociate into α - β dimers (32 kDa), which are rapidly eliminated from circulation through renal filtration and extravasation into tissues²⁶ (Figure 2). Since the 1970s, HBOC design has been primarily focused on generating higher molecular weight species through intra-molecular crosslinking, polymerization, or conjugation in order to address the associated effects of cell-free Hb³ (Table 2).

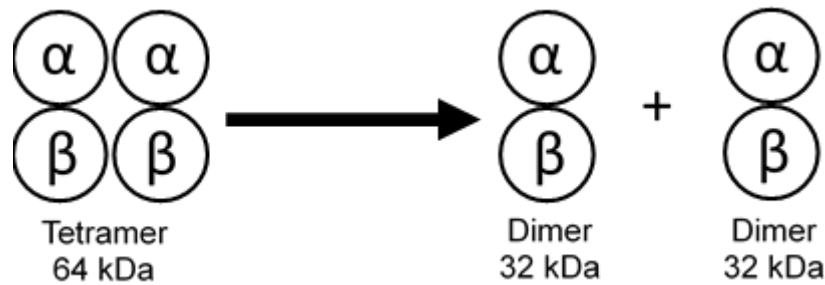
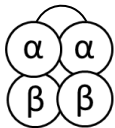
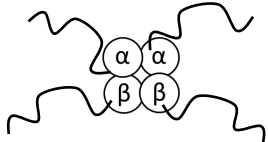
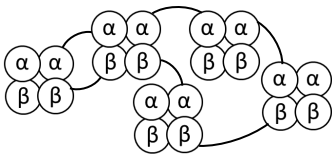


Figure 2. Tetrameric Hb dissociates into obligate heterodimers outside the high-concentration environment of the red-blood cell. As a result, cell-free Hb has a short circulatory half-life and is rapidly removed from the vasculature through renal filtration.

Table 2. A brief overview of the three HBOC types described here.

HBOC Type	Generic Structure	Product Examples ^a
Crosslinked Hb		HemAssist (DCLHb) Optro (rHb1.1)
PEG Conjugated		PHP Hemospan (MP4)
Polymerized Hb		PolyHeme Hemopure (HBOC-201) Hemolink

^a A description of the products and their properties are provided in Table 3

The starting material for most HBOC preparations is commonly obtained from otherwise wasted sources, such as expired human blood or non-human mammalian blood from the meat packing industry.²² Stroma free-Hb (SFH), or stroma poor Hb, is obtained through the filtration and purification of lysed red blood cells. Due to the starting material, SFH invariably contains other red cell protein contaminants that can become a part of the crosslinked HBOCs.²⁷ In contrast, methods to produce recombinant Hb in bacterial systems have generated a new potential source for Hb and have made it easier to modify Hb through site-directed mutagenesis.²⁸

Extensive clinical examinations have been carried out with acellular HBOCS, and several HBOC formulations have made it into clinical Phase III testing. However, to date, no HBOC has been approved for human use in the US.³ A descriptive summary of relevant commercial HBOC formulations is given in Table 3.

Table 3. Summary of HBOCs and their properties and clinical development.

Proprietary Name and Company	General Description	Chemical Modification	Physiochemical Properties			Development Phase and Indications
			MW (kDa)	P50 (mmHg)	n ^a	
HemAssist (DCLHb) Baxter Healthcare	Diaspirin crosslinked	Bis(3,5-dibromosalicyl)-fumarate	64	30	2.7	Phase II/III vascular surgery ²⁹ , orthopedic surgery ³⁰ and hemorrhagic shock ^{31, 32} Terminated
Optro (rHb1.1) Somatogen	Recombinantly crosslinked	Asn108β → Lys, Gly	64	34	2.35	Phase I/II elective surgery ³¹ Acquired by Baxter, Terminated
rHb2.0 Somatogen ^b	Recombinantly crosslinked, PEGylated, and heme-pocket mutated	rHb1.1, with undisclosed modifications	NR ^c	34	1.1	Animal Studies Acquired by Baxter, Terminated
Hemospan (MP4) Sangart	PEGylated	PEG-5000 maleimide	95	6	1.2	Phase II orthopedic surgery ³³ Terminated
PHP Apex Life Sciences	PEGylated and crosslinked	Pyridoxyl-5'-phosphate and Polyethylene glycol	~187	24	NR	Phase II/III, hemorrhagic shock ^{34, 35} Recent phase III trials in Europe found increased morbidity
Hemopure (HBOC-201) Biopure	Polymerized and bovine sourced	Glutaraldehyde	64-500	38	1.3	Phase III trauma ³⁶ and orthopedic surgery ^{30, 37} Approved in South Africa and Russia, ongoing phase III trials in US
Oxyglobin Biopure	Polymerized and bovine sourced	Glutaraldehyde	64-500	38	1.3	Approved for veterinary use in the US
PolyHeme Northfield Laboratories	Polymerized and crosslinked,	Pyridoxyl-5'-phosphate and Glutaraldehyde	64-250	20	1.5-2	Phase II/III trauma ^{38, 39} Defunct
Hemolink Hemosol Inc.	Polymerized and crosslinked	O-raffinose	64-500	34	1.15	Phase II/III cardiac surgery ^{40, 41} Terminated

^a Measure of cooperativity (Hill coefficient) HbA₀: n = 2.9; rHb0.0: n = 2.6.

^b Produced by Somatogen under the Baxter Healthcare Corporation

NR = Not Reported

1.2.3 A History of HBOC Commercial Development

Crosslinked Hemoglobins

HemAssist (Baxter Healthcare Corp.) or its non-commercial analogue DBBF-Hb (US Army) is a diaspirin cross-linked hemoglobin (DCLHb) and was one of the first HBOC products to enter clinical trials.⁴² This HBOC contains a (3,5-dibromo-salicyl)-fumarate (DBBF) intra-molecular crosslink between α_1 K99 and α_2 K99 that is designed to restrict tetramer dissociation⁴³ (Table 3). Phase III clinical trials to assess the safety and efficacy of DCLHb as an emergency resuscitation fluid found it increased 28-day mortality rate in patients compared to normal saline infusions.³²

Optro (Somatogen, Boulder, CO) or its analogue rHb1.1, was designed as an intra-molecular crosslinked Hb and engineered using recombinant technology (Table 3). Using a single glycine to bridge the two α -globins (α -Gly- α), this Hb was expressed in *Escherichia coli* (*E. coli*) as a stable 64 kDa tetramer.²⁸ Other commercial HBOCs are obtained from cheaper sources, such as expired human RBCs, but Somatogen showed the benefit of using recombinant technology and protein engineering to express rHb1.1 with the glycine cross link and the low oxygen affinity mutation β N108K. Clinical trials showed Optro to be relatively well tolerated in surgical patients but its development was discontinued due to various adverse effects such as a hypertensive response and elevated pancreatic enzymes.⁴⁴ Somatogen was eventually acquired by Baxter Healthcare and produced rHb2.0, an HBOC generated using both recombinant and chemical methods: genetically engineered to have reduced nitric oxide reactivity and chemically polymerized and derivatized.⁴⁵ However, development of rHb2.0 was terminated by Baxter before making it out of animal studies.

Marquardt and colleagues elaborated further on this technology to generate a recombinant di-Hb comprising a single-chain tetra- α (α_1 -Gly- α_2 -(SerGlyGly) $_4$ - α_3 -Gly- α_4) and four β subunits⁴⁶. They also produced a tetra-Hb by chemically crosslinking di-Hbs containing a K16C mutation in the C-terminal α -subunit with bismaleimido-hexane, generating the first of its kind monodisperse poly-Hb. These Hbs had an improved vascular retention and hypertensive response in animal models when compared to Optro.⁴⁶

Conjugated Hemoglobins

As with other protein therapeutics, conjugation of polyethylene glycol (PEG) or other related polymers to the Hb surface has been investigated. Sangart Inc. developed one such HBOC, Hemospan or MP4, which contained PEG-50 conjugated to the protein surface (Table 3).⁴⁷ This was achieved by the thiolation of surface-exposed lysines with iminothiolane, followed by conjugation of a PEG-50 maleimide. MP4 was also designed with very high oxygen affinity in order to address the hypothesis of premature unloading of oxygen by previous HBOCs may be the cause of the observed adverse events. Following initial clinical trials, Sangart failed to obtain additional funding and Hemospan was discontinued.

Apex Bioscience developed Pyridoxilated-Hb Polyoxyethylene (PHP). This HBOC features both an intra-molecular crosslink using pyridoxal-5'-phosphate to bridge β_1 - β_2 and conjugation to polyoxyethylene (PEG). After the early termination of a clinical trial as an oxygen delivery therapeutic, PHP was explored as a nitric oxide scavenger in cases of septic shock. Phase III trials were conducted in the US and, more recently, in Europe.³⁴

³⁵ However, PHP was not found to be clinically effective as a vasopressor therapy and was associated with increased mortality.

Polymerized Hemoglobins

Increasing molecular weight of Hb through polymerization has been largely successful in optimizing intravascular retention times. Polymerization of purified human and bovine SFH is achieved using bifunctional cross-linkers such as glutaraldehyde which react non-site specifically, forming a Schiff-base with lysine side-chains on the surface of the protein. As a result, these polymers have high molecular weights but are highly polydisperse.²⁷ Two of the most successful examples of poly-Hb HBOCs are Hemopure (Biopure, Cambridge, MA) and PolyHeme (Northfield, Evanston, IL) (Table 3).

Hemopure, or HBOC-201, is a glutaraldehyde polymerized bovine Hb (bHb) that was approved in 2001 for adult surgical patients in South Africa after completing extensive phase III trials.⁴⁸ While generally well tolerated, analysis of phase III trials showed increased morbidity when transfused into patients over 80 years of age or in those predisposed to cardiac problems.⁴⁸ Despite this, Hemopure has since been approved for use in Russia and is currently (at the time of this writing) undergoing a phase III trial in the US that is scheduled to conclude in July 2020 (ClinicalTrials.gov Identifier: NCT01551503). An analogous product, Oxyglobin, has been approved for veterinary use in the US and Europe.

PolyHeme is also glutaraldehyde polymerized but differs from Hemopure in that it is first pyridoxilated, similar to PHP, and sourced from expired human RBCs.²³ This HBOC has undergone extensive phase II and III clinical trials for pre-hospital stabilization in the

cases of trauma.³⁸ Ultimately, after being in development for over a decade, it was not approved due to safety concerns.⁴⁹

Hemolink (Hemosol, Mississauga, ON, Canada) is a crosslinked and polymerized Hb. Similar to PolyHeme, this HBOC is synthesized using a single crosslinker and polymerizing agent, *O*-raffinose. It was proposed that Hemolink owed its lowered oxygen affinity to insertion of *O*-raffinose into the β_1/β_2 cleft, however this has since been disproven (see section 1.3.1). In a phase III randomized trial, Hemolink was employed to reduce the need for allogenic transfusions during cardiopulmonary bypass surgery. After a higher incidence of myocardial damage was reported, Hemosol terminated clinical development.⁵⁰

1.2.4 HBOC-Related Toxicities

Clinical Side-Effects

The US Food and Drug Administration (FDA) has repeatedly denied approval of HBOCs due to concerns over patient safety. Although there are differences in the biochemical and histological changes in patients, the HBOC products tested to date appear to follow the same “clinically relevant” mechanism of toxicity.^{49, 51} These events appear to emanate from the starting material, acellular Hb, which is known to cause several adverse effects including renal toxicity and hypertension.⁵²

Interestingly, the hydrodynamic radius of Hb sits at the cusp of the glomerulus pore radius (30-35 Å) such that it restricts renal filtration of tetrameric-Hb (~30 Å) and allows $\alpha\beta$ dimers (~24 Å) to pass through.²⁶ Thus, renal toxicity can be prevented by stabilizing tetrameric Hb with intra-molecular crosslinkers like the ones found in DCLHb and rHb1.1.

HBOC-related hypertension has been the most commonly reported side effect in pre-clinical and clinical studies of HBOCs.⁵³ It is largely attributed to the scavenging of nitric oxide (NO), an important cellular signaling molecule and a potent vasodilator. In addition to systemic hypertension, NO scavenging decreases blood flow, promotes release of proinflammatory cytokines, and leads to loss of platelet inactivation.⁵⁴ Although no long-term consequences have been definitively attributed to the depletion of NO^{30, 55}, a model study showed that these conditions can lead to systemic physiological changes, organ dysfunction, and death.⁵⁶ In fact, a meta-analysis of the available trial data for 5 different HBOCs showed there is an increased risk for both myocardial infarction (MI) and death associated with these products.⁴⁹ Because the FDA's primary concern about HBOCs was patient mortality and safety, many consider NO scavenging to be the primary challenge to HBOC approval for clinical use.

Mechanism of NO Scavenging

NO plays an important role in physiological processes such as regulating cellular respiration and vascular tone, wound healing, and nervous system signalling⁵⁷. The vasodilation effects of NO arise when it diffuses into the smooth muscle tissue surrounding the blood vessel wall and activates soluble guanylate cyclase, an enzyme that catalyzes the conversion of guanosine triphosphate (GTP) into 3',5'-cyclic guanosine monophosphate (cGMP) and relaxes the smooth muscle tissue.⁵⁸ The NO induced oxidation of acellular oxyHb (Fe²⁺) to metHb (Fe³⁺) proceeds rapidly ($\sim 7 \times 10^9 \text{ M}^{-1}\text{s}^{-1}$)⁵⁹ and irreversibly, such that Hb is widely considered to be an NO sink⁵⁷ (Figure 3).

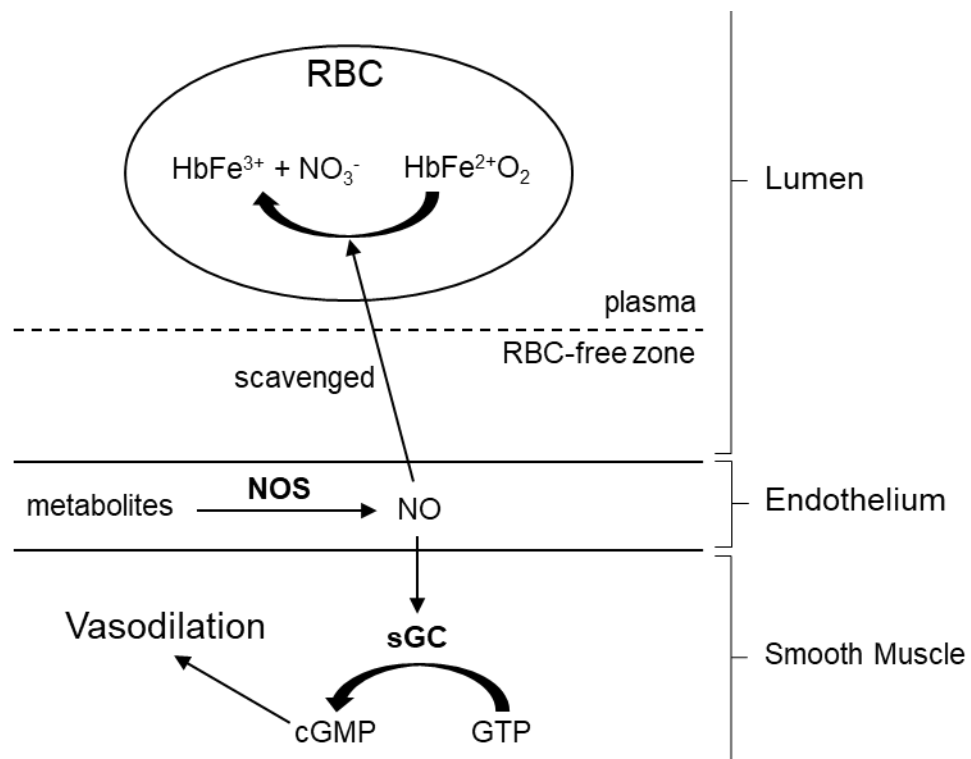


Figure 3. Major pathway of NO-induced vasodilation and NO-scavenging by Hb. Nitric oxide synthase (NOS) metabolizes L-arginine into L-citrulline, producing NO. There is a variety of other enzymatic and non-enzymatic sources of NO in the perivascular region, however NO production within the endothelium is most relevant to scavenging by Hb.

Based on the observation that the NO reaction rate is three orders of magnitude slower with RBC encapsulated Hb vs. free Hb,⁶⁰ it was hypothesized that NO scavenging results from extravasation of low molecular weight Hbs into the endothelium.⁵¹ Similar to preventing renal filtration, the central design consideration for preventing HBOC-mediated hypertension focused on preventing extravasation by increasing the relative size of cell-free Hb through crosslinking or conjugation. While these have seen some success in decreasing renal accumulation and hypertensive effects,⁶¹ a clear understanding of the underlying relationship between these modifications and the observed physiological effects has not been established. For example, transfusion of

glutaraldehyde poly-Hbs, similar in composition to commercial variants, were shown to have an almost 2-fold decrease in the mean arterial pressure (MAP) elevation as was observed with tetrameric hemoglobin.⁶² However, it is unclear whether this was the result of an increase in molecular weight or modification of the protein surface, as a similar attenuated MAP response was observed with non-polymerized Hb conjugated to glutaraldehyde.

Assessing the extravasation model of NO scavenging is further complicated by the polydisperse nature of first-generation HBOCs. For example, Hemopure still elicits a hypertensive response, despite being purified to deplete low molecular weight species.^{17, 51} With a molecular weight range of 87 kDa to 502 kDa and containing 3-4% unmodified tetrameric Hb, it is difficult to determine the species which are responsible for hypertension. This inspired formulations of PolyHeme where tetramer concentration was purposefully depleted to <1%, however, these were still observed to be vasoactive.⁴⁹ Taken together, these data indicate that either the extravasation threshold size is larger than expected, the residual low molecular weight species are responsible for the pressor response, or extravasation is not a prerequisite for NO scavenging.

Though the elimination of tetrameric Hb from HBOC formulations has been the “gold standard” to prevent extravasation, the actual size limitation for this process has not been established unambiguously. In a review by Rippe and Haraldsson,⁶³ the permeability of endothelial capillary walls is controlled by pores of two categories: passive hydrophilic channels with a radius near 40 Å and ‘large pores’ with a 250-300 Å radius. First-generation HBOC formulations such as Hemopure, which would be roughly 60 Å in

diameter on average, may therefore be susceptible to extravasation. Even poly-Hbs with high average molecular weights could have species small enough to escape the vasculature if polydispersity is high.

Although HBOC design efforts have focused on containing Hb within the vasculature, the presumption that extravasation into peripheral tissues is required for NO depletion has been controversial. Computational studies suggest that even when confined to the vasculature, acellular Hb has a NO scavenging ability 500-fold higher than RBCs.⁶⁴ This work used a model based on the Fåhræus effect,⁶⁵ which predicts that RBCs migrate axially in capillaries in the presence of flow and form a flowing RBC-rich core surrounded by a cell-depleted layer⁶⁶ (Figure 3). This RBC-free zone can be as much as 25% of the lumen diameter and acts as a diffusion barrier to NO, effectively allowing the flow of NO back into the smooth muscle tissue to compete with its destruction by oxy-Hb in RBCs.⁶⁷ However, because this effect is dependent on particle size,⁶⁵ acellular Hb does not maintain this barrier and is able to scavenge NO at a greater rate.

Improving HBOC Design

Using Hb-derived therapeutics as oxygen carriers has seen significant setbacks. Preclinical and clinical studies of HBOC toxicities suggest developing the next generation of HBOCs will require controlling the hemodynamic response as related to NO-scavenging. Whether extravasation is required for NO scavenging or not, the evidence suggests a non-vasoactive HBOC would be one with minimal quantities of low MW species (<300kDa), high molecular weights or hydrodynamic radii, and low polydispersity. In fact, several ultrahigh molecular weight poly-Hbs have been developed with average

masses in excess of 15MDa.⁶⁸ One such poly-Hb had an average radius of 250 Å, an average mass of >20MDa, and contained no detectable species <300 Da and was found to be non-extravasating and non-vasoactive in animal models.⁶⁹ However, in these cases the poly-Hb was generated using the same or similar non-specific chemical modifications methodologies that resulted in complex structural and functional changes in first-generation HBOCs which are not easily understood.⁵¹ In addition, a robust purification process was required in order to remove a majority of these lower molecular weight species, which can incur significant costs at the industrial level. Thus, there remains a need to generate HBOCs with well-defined modifications via cost-effective processes.

1.3 Overview of Modern Protein Modification Methodologies

1.3.1 Advances in Protein Engineering

Protein therapeutics have evolved greatly from their origins in animal-sourced medicines such as porcine insulin. Advances in recombinant-DNA technologies and site-directed mutagenesis have allowed for the generation of new or improved drugs and have revolutionized the study of protein science. In addition, the development of protein modification techniques that specifically target nucleophilic side-chains such as lysine or cysteine has advanced our understanding of molecular and cellular biology by enabling researchers to introduce novel chemical functionality into protein targets. This also led to improved biotherapeutics with enhanced physiochemical and pharmacokinetic properties such as PEGylated forms of insulin⁷⁰ or interferon,⁷¹ as well as new cancer treatments that harness the selectivity of monoclonal antibodies to deliver potent cytotoxic small molecules.⁷² However, these protein modification techniques are often limited in their site-selectivity. The relative surface density of modifiable side-chains, most notably lysine,

results in a wide range of possible products. Accordingly, these must be used in applications where either heterogeneity is relatively well tolerated or the target protein is small enough to limit multiple modifications of the same residue type, as is the case for insulin. In contrast, cysteine modifications can be better predicted due to the rarity of exposed free-cysteine residues, or in cases where the target contains exploitable disulfide bridges, such as monoclonal antibodies.

These tools have been used routinely in the development of HBOCs yet, surprisingly little published work describes rigorous biochemical and biophysical characterization of these chemical modifications. Only recently have these HBOCs undergone comprehensive analysis. Meng and colleagues²⁷ found remarkable heterogeneity with poly-Hbs and PEGylated-Hbs with large populations of low molecular weight globin species as a result of these non-specific modifications. They also observed a diverse set of oxygen binding characteristics for these HBOCs that were not predictable based on the modification (i.e. poly-Hbs do not impose a particular effect on oxygen affinity). While groups have made progress in controlling the oxygen binding affinity of glutaraldehyde poly-Hbs⁶⁸, understanding the structure-function relationships of these molecules is difficult. For example, in Hemolink (O-R-PolyHbA₀) it was proposed that raffinose stabilized the low-affinity T-state by crosslinking residues at the 2,3-bisphosphoglycerate (BPG) binding site (β 1Val1, β 1Lys82, and β 2Lys82).⁷³ However, Boykins *et al.*⁷⁴ found that cysteine, not lysine, was the most commonly modified side-chain and the β 1/ β 2 cleft was largely unperturbed, suggesting that the lowered oxygen affinity was the result of an increased energetic barrier to allosteric switching. Furthermore, O-R-PolyHbA₀ was found to be unstable – a characteristic attributed to the

heavily modified protein surface.^{27, 74} From a biochemical perspective, predicting and characterizing the structural and functional impacts of these non-specific chemical modifications remains a challenge.

For biotherapeutics, product heterogeneity can be problematic. For example, in the development of antibody-drug conjugates (ADCs) the drug to antibody ratio can be the dominant factor in altering the pharmacological properties of these therapeutics.⁷⁵ However, the large number of potential conjugation sites and the non-specific modifications can create products that are prone to aggregation and general instability, leading to drugs with increased off-target toxicity and clinical inefficacy.⁷⁶ This has sparked considerable interest in developing methods to improve ADC homogeneity using clever applications of chemical modifications, such as synthesizing a bifunctional maleimide derivative that is able to conjugate payloads via interchain cysteine cross-linking.⁷⁷ Recombinant methods have also been proposed to produce novel monodisperse antibodies using bacterial systems that contain a novel pair of tRNA and its orthogonal aminoacyl-tRNA synthetase, which allows the biosynthetic incorporation of non-canonical amino acids.⁷⁸ Although this technology has powerful implications for the future development of protein therapeutics, it is still in its infancy and remains a complex and expensive approach.

In general, the development of methods that allow precise, site-specific control over protein modifications has been an area of great interest over the last decade. Enzymatic labeling is one such method that has attracted attention as an alternative strategy to more costly approaches of protein conjugation.⁷⁹ This technique uses the high

selectivity of enzymes to site-specifically incorporate labels or chemical handles into protein targets. Enzymes that have been used for this purpose include formylglycine generating enzyme, phosphopantetheinyl transferase, transglutaminase, farnesyltransferase, biotin ligase, lipoic acid ligase, and sortase.⁷⁹ As each enzyme recognizes a specific sequence of amino acids, this approach requires a genetically encoded tag which can limit the available targets to recombinant proteins. Despite this limitation, chemoenzymatic ligation has become an invaluable biochemical tool and has been used to study *ex vivo* and *in vitro* processes such as localization of cell surface proteins through the conjugation of fluorescent probes.⁸⁰

1.3.2 Sortase-Mediated Ligation (SML)

Of particular interest for protein engineering are sortases, a family of transpeptidases found in the cell wall of most gram-positive bacteria.⁸¹ In bacteria, these enzymes function as 'sorters' and decorate the bacterial surfaces with a wide variety of proteins including virulence factors and pili.⁸² Class A sortases (SrtA), the most thoroughly characterized members of the sortase family, are cysteine transpeptidases that recognizes an LPXTG motif (substrate-tag or sortag) and cleave C-terminally to threonine through nucleophilic attack of the peptide carbonyl with the active-site cysteine thiol, releasing the C-terminal fragment (excised fragment). The resulting acyl-enzyme intermediate is then subject to nucleophilic attack from an N-terminal glycine (nucleophile-tag) to form the final ligation product (Figure 4). For the purposes of chemoenzymatic ligation, SrtA homologs from *Staphylococcus aureus* have been developed which lack the N-terminal transmembrane domain that anchors SrtA to the bacterial cell wall allowing these enzymes to be expressed in the soluble fraction.

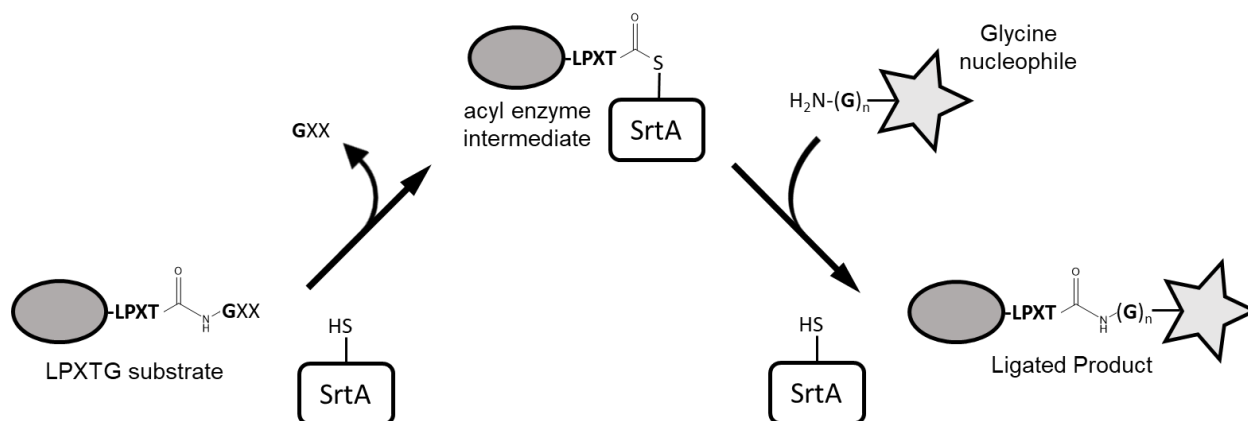


Figure 4. Sortase-mediated ligation as a protein engineering tool. Note that the LPXTG substrate sequence is regenerated in the product resulting in an inherently reversible reaction.

Since its introduction in 2004, sortase-mediated ligation (SML) has been rapidly developed in an effort to generate an enzyme more suitable for protein engineering applications. In order to improve the reaction rate, a directed evolution approach using yeast display was developed and five point-mutations were discovered that resulted in a 120-fold increase in catalytic efficiency and improved affinity for the LPXTG substrate sequence.⁸³ Additional SrtA mutants were developed addressing the limitations imposed by the Ca²⁺-dependence of SML, enabling SrtA to be more suitable for some *in vivo* applications.⁸⁴ More recently, there has been considerable interest in improving ligation efficiency, which suffers from inherent reversibility due to the regeneration of the LPXTG sequence in the product and the N-terminal glycine in the excised fragment. Without a large excess of a reactant, the reaction equilibrium often results in a maximum product accumulation of only 50%. Fortunately, several methodologies have been developed that improve ligation efficiency. One such method reduces the ability for SrtA to recognize the regenerated LPXTG sequence by generating secondary structure at this site in the form of a β -hairpin.⁸⁵ Other methods have been aimed at reducing the nucleophilicity of the excised fragment to hinder the rate of the reverse reaction. One study achieved this by

altering the threonine-glycine peptide bond that is eventually cleaved to form the acyl-enzyme intermediate, such that the excised fragment contains a hydroxyl group at the N-terminus.⁸⁶ Metal-assisted SML (MASML) is a method developed by the Antos lab at Western Washington University, that is able to achieve this without the need to introduce an unnatural peptide bond. By simply expanding the SML recognition sequence to LPXTGGH, they were able to generate an excised fragment (GGH) that uses the N-terminal lone pair to coordinate with Ni²⁺, drastically reducing its nucleophilicity.⁸⁷

These improvements to SrtA, as well as its broad scope of potential protein targets, has enabled SML to be rapidly implemented in a wide range of applications, including the study of biochemical processes such as the NMR-analysis of proteins with poor solubility,⁸⁸ and the improvement of biomaterials by efficiently immobilizing proteins to solid supports.⁸⁹ Moreover, SrtA has emerged as a promising method to improve the pharmacokinetic, solubility, and efficacy of biotherapeutics. For example, sortagged single-domain antibody fragments (or nanobodies) have been efficiently conjugated to cytotoxic payloads using SML, generating next-generation ADCs that are structurally defined and have improved efficacy.⁹⁰

Among the numerous applications of SML, perhaps the most powerful is the selective modification of proteins with bioorthogonal functionality. Such chemical handles include pairs of non-native, non-perturbing functional groups that are inert to biological media and are able to undergo chemoselective reactions under relatively mild conditions. However, protein labeling via bioorthogonal ligation is limited by the non-site selective methods often used to introduce these functional groups. While significant progress has

been made with amber codon suppression, which would allow for the incorporation of non-endogenous synthetic amino acids into recombinant proteins, this technology has yet to become an industrial tool for biotherapeutic development. Instead, SML offers affordable and efficient site-selective modification or functionalization of a wide range of protein targets with methods that are end-user friendly.

1.4 Project Goals and Overview

Protein engineering strategies have improved drastically since the last HBOC to enter phase II/III clinical trials was developed, almost two decades ago. These have already seen applications in the production of improved biotherapeutics with medical significance. However, to date these have yet to be applied to the development of oxygen carrying therapeutics. Therefore, the goal of this project was to demonstrate the feasibility of using modern protein engineering methodologies in the development of next generation HBOCs. Specifically, we propose a two-part approach to generate ultra-high molecular weight Hbs with low polydispersity. First, we propose to introduce bioorthogonal functionality into Hb in a site-specific manner using SML. Then, we aim to decorate a functionalized dendritic scaffold with Hbs utilizing the bioorthogonal reactive groups. These dendritic scaffolds are readily available from commercial sources and provide a convenient method to control the final polymer size.

This thesis describes the expression and characterization of sortagged recombinant-Hbs (rHbs). We designed two α -globins either as an acyl donor, containing a C-terminal MASML-expanded sequence and His-tag, or as an acyl acceptor, with a nucleophilic N-terminal glycine. These modified α -globins were coexpressed with either wt β -globin or a circularly permuted variant to generate sortase-ready rHbs. In this work, we have demonstrated that these rHbs can be modified as both acyl donors and acceptors in a direct protein-protein conjugation using sortase. In addition, by using a bifunctional oligopeptide containing two N-termini, we have successfully introduced a novel intra-molecular Hb crosslink using SML. This has allowed us to potentially stabilize the Hb tetramer while simultaneously introducing bioorthogonal functionality through the

oligopeptide. Finally, we have demonstrated how these functionalized Hbs can be further modified using secondary bioorthogonal reactions.

2. Preparation of Sortase-Ready Hbs and Peptide Crosslinkers

2.1 Expression, purification, and characterization of sortagged α -globins

To generate Hbs containing recognition sites for SrtA, genes encoding for α -globins containing either an N-terminal glycine nucleophile (GG- α) or C-terminal LPETGGH₆ (α -LPETG) tags were obtained via commercial gene synthesis. Each of these constructs was subcloned into expression vectors containing a circularly permuted β -globin (cp β). In addition, an expression vector containing the genes for α -LPETG and wild-type β -globin (wt β) was obtained. Transformed *E. coli* BL21(DE3) cells were cultured and protein expression was induced via standard molecular biology techniques.

Following cell lysis, initial purification and enrichment steps of the two α -LPETG constructs were achieved using IMAC resin chelated with Ni²⁺, as possessed a His₆ affinity tag (Figure 5). Additional purification for these proteins was generally not required, however anion-exchange chromatography (AEX) was performed as needed (Figure 5). To purify GG- α , as it did not contain a His₆-tag, IMAC resin chelated with Zn²⁺ was used, following our standard procedure for purification of rHbs.⁹¹ AEX purification was required to achieve high levels of homogeneity with this protein (Figure 5). Initial verification of mass and purity was performed by SDS-PAGE. As expected, α -LPETG appears at higher molecular weights compared to GG- α due to the LPETG and His₆-tags present in α -LPETG (Figure 5). While α -LPETG and cp β migrated differentially, GG- α and cp β co-migrated through the gel, complicating analysis of GG- α modifications (See section 3.1).

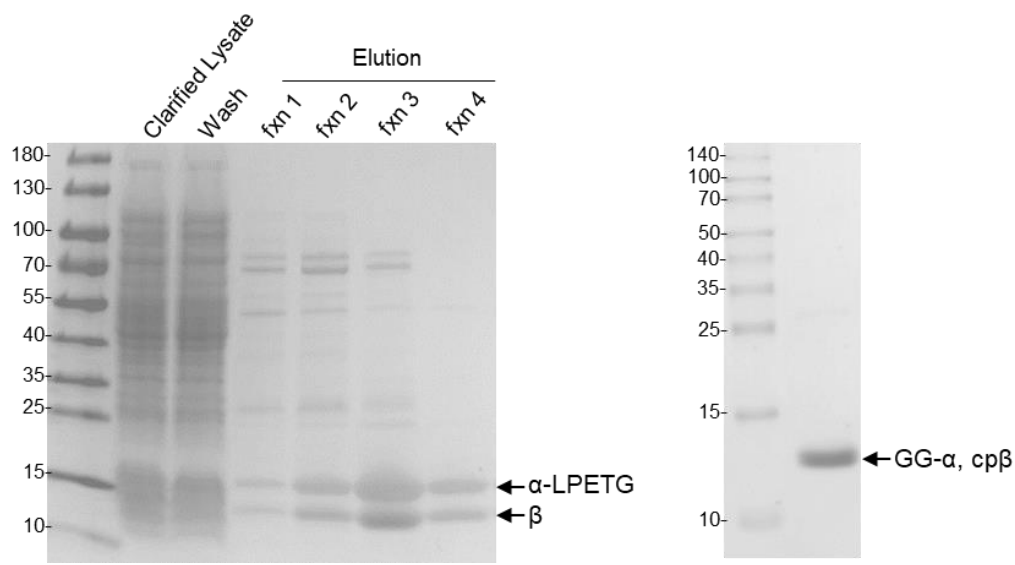


Figure 5. Purification of sortagged-Hbs analyzed by SDS-PAGE. (Left) Ni-IMAC purification of α -LPETG/ β . The column was washed with buffer containing 50 mM imidazole. Eluent was collected in fractions with increasing purity. (Right) AEX purification of GG- α /cp β .

During initial attempts at His₆-tag purification of α -LPETG/cp β a continuous red colored effluent was observed during a wash step containing high concentrations of imidazole (100 mM) and discarded. The sample obtained after the final elution proved to be moderately unstable in solution at 4°C, as evidenced by a significant amount of protein aggregation onto the sides of the container. A minor early eluting peak was observed during AEX that contained isolated α -LPETG globin as well as a major peak containing the expected species α -LPETG and cp β (Figure 6). We suspect that the high salt concentrations present in the final wash step disrupted the α_1 - β_1 interface resulting in elution of cp β while the His₆-tagged α -LPETG remained bound to the resin. This last wash step was omitted from later purifications. Samples purified in this manner were often highly homogenous and no further purification was required following IMAC. Expression

yields were calculated following IMAC and found to be approximately 40 mg of α -LPETG/ β , 25 mg of α -LPETG/ $\text{cp}\beta$, and 15 mg of GG- α / $\text{cp}\beta$ per liter of cell culture.

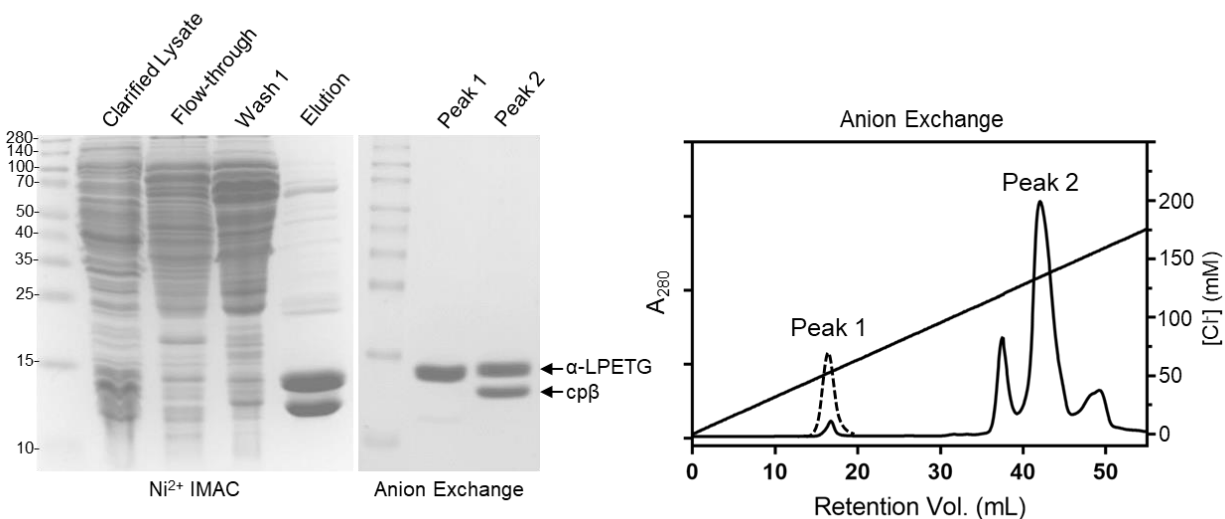


Figure 6. AEX purification of α -LPETG/ $\text{cp}\beta$ following Ni-IMAC. (Left) SDS-PAGE of α -LPETG/ $\text{cp}\beta$ purification. (Right) Anion exchange (AEX) chromatogram of α -LPETG/ $\text{cp}\beta$ following Ni-IMAC. Gradient of NaCl was used to elute samples (linear solid line, right axis). Solid A₂₈₀ trace shows early eluting minor peak containing isolated α -LPETG (Peak 1) and major peak containing both α -LPETG and $\text{cp}\beta$ (Peak 2). Dotted line is an example of the relative peak height prior omission of wash step in Ni-IMAC, solid line is after wash is omitted.

The masses of α -LPETG/ $\text{cp}\beta$ and α -LPETG/ β were determined by ESI-MS (Table 4). An additional mass peak was observed in the deconvoluted spectrum for α -LPETG/ $\text{cp}\beta$ that was 273 Da lower than the observed mass of α -LPETG. In fact, this species is also visible by SDS-PAGE as a doublet band at α -LPETG. The source of this peak is unclear however, a similar phenomenon has been observed previously by our collaborators who have attributed the mass difference to a C-terminal His₄ rather than the expected His₆-tag. If this is the case, we would expect a decreased binding affinity of the His₄ species to Ni²⁺-NTA IMAC resin. Consistent with this, we have been able to deplete

this in our final samples through refinement of the IMAC purification protocol (data not shown).

Table 4. Observed and expected masses by ESI-MS

Species	Expected (Da)	Observed (Da)
β	15,975	15,978
cp β	16,535	16,533
α -LPETGGH ₆	17,180	17,183
α -LPETGGH ₄	33,354	33,361
GG- α	15,803	ND

ND = Not determined

2.2 Design and Synthesis of GGGK(K)GGG

Crosslinking α -LPETG required the synthesis of a peptide containing two glycine N-termini. Specifically, the N-termini were designed to be a GGG motif as these are used as standard nucleophiles in SML experiments. The final design of the crosslinker is shown in Figure 7. It was synthesized with standard solid-peptide synthesis (SPPS) methodologies using a Rink-amide resin (see 5.3.1). Installing two N-termini was achieved by coupling a bis-Fmoc-lysine as the second residue which allowed elongation to occur from both N $_{\alpha}$ and N $_{\epsilon}$ following deprotection. The peptide was cleaved from the resin using trifluoroacetic acid, prior to a final deprotection step in order to leave both N-termini Fmoc-protected. A two-fold excess of crude peptide was then coupled to either fluorescein isothiocyanate (FITC) or dibenzylcyclooctyne N-hydrozysuccinimide (DBCO-NHS) at the C-terminal lysine and purified by RP-HPLC (see section 5.3.2). Product purity was confirmed by RP-HPLC (Figure 7) and identity was verified by ESI-MS (see Appedix).

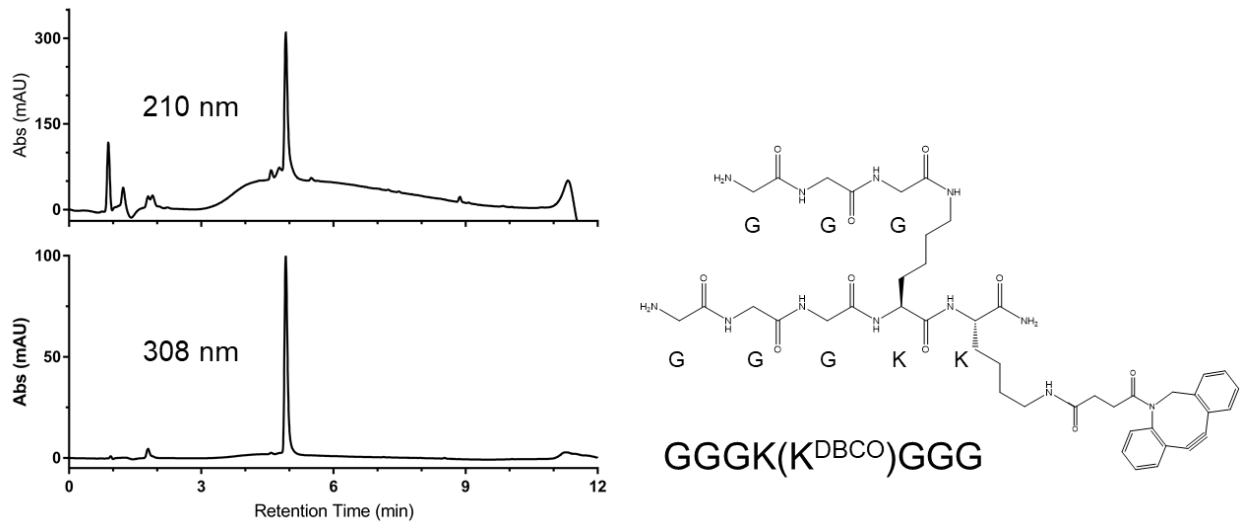


Figure 7. Design and synthesis of GGGK(K^{DBCO})GGG. (Left) HPLC chromatogram of purified DBCO-conjugated crosslinker at 210 nm (total peptide content) and 308 nm (λ_{\max} DBCO). (Right) Final design of crosslinker with conjugation to DBCO. The peptide linker was also conjugated to FITC.

3. Sortase-Mediated Ligation of Sortagged α -subunits

3.1 Ligation of α -LPETG and GG- α by Sortase A

Our initial work focused on generating a di- α construct by directly ligating α -globins using MASML (Figure 8a). To achieve this, equimolar quantities of α -LPETG/cp β and GG- α /cp β were incubated with a fast-acting penta-mutant SrtA for 90 minutes. Final reaction concentrations were 25 μ M in each sortagged α -subunit and 5 μ M SrtA (see 5.4.1 for experimental details). Reaction time-courses were analyzed by SDS-PAGE with SrtA activity quenched at each time point using SDS-PAGE loading buffer. These reactions were performed at 37°C in the presence of 200 μ M Ni²⁺.

As shown in Figure 8b, the ligated product (α -LPETGG- α) can be seen as early as 15 minutes and maximum product yield occurs after 75-90 minutes with total product formation of approximately 70%. However, determination of conversion percentage was complicated by the inability to determine GG- α content due to its co-migration with cp β , as well as inconsistencies in gel loading and lack of a reliable internal standard. Thus, the calculation was based on the proportion of α -LPETG in the product to total α -LPETG using band intensities obtained from densitometry (see Section 5.4.1).

To investigate the effect of nickel-enhancement on the SML of α -globins, side-by-side reactions of α -LPETG and GG- α were conducted with and without Ni²⁺. After incubating for 90 minutes the reactions were analyzed by SDS-PAGE (Figure 8c). In the presence of Ni²⁺, the total accumulation of product was approximately 60% by 90 minutes, while only 50% conversion was achieved in its absence. Similarly, the abundance of remaining α -LPETG was observed to decrease in the presence of Ni²⁺ compared to

without Ni²⁺. However, the proportion of the hydrolyzed product (α-LPET), which results from nucleophilic attack of the acyl-enzyme intermediate by water, was also observed to increase in the presence of Ni²⁺. The position of hydrolyzed product can be clearly observed in the no-nucleophile control reaction (Figure 8c).

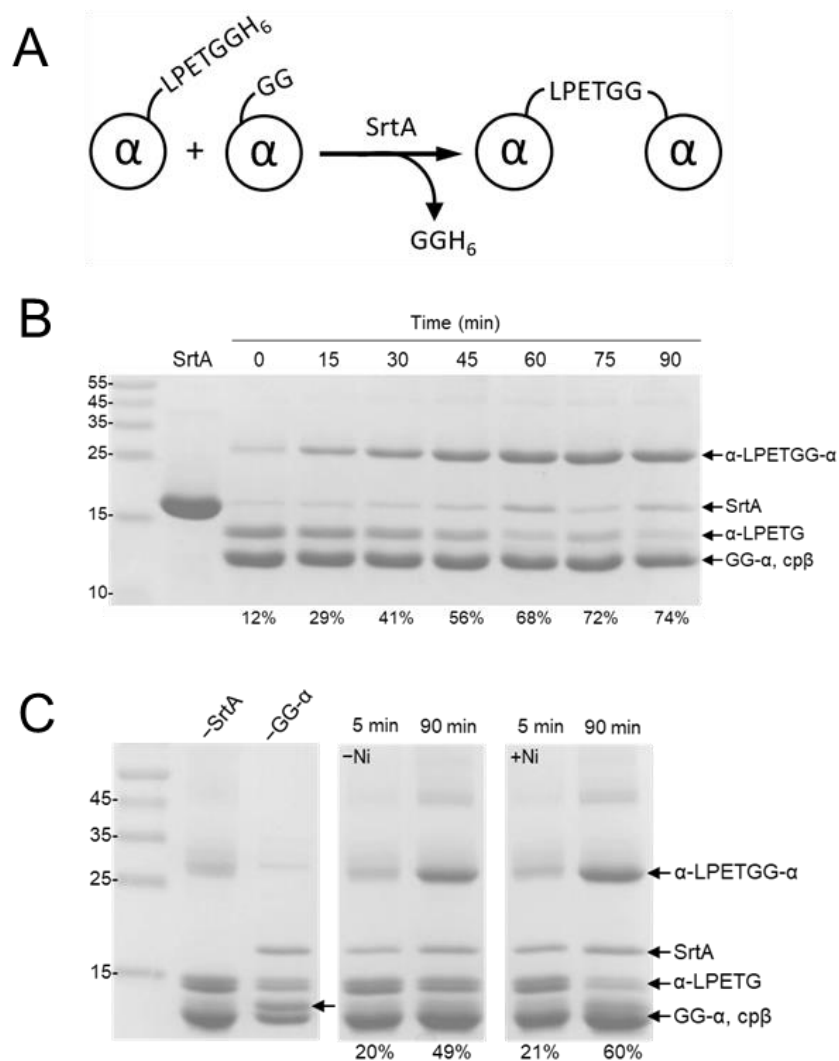


Figure 8. Sortase-catalyzed ligation of α-LPETG and GG-α. **(A)** Depiction of the ligation reaction of α-LPETG and GG-α, generating a di-α species. **(B)** SDS-PAGE analysis of the crosslinking reaction time-course. Values below each lane represent the proportion of α-LPETG in the ligated product. Conditions: 100 μM in heme, 5 μM SrtA, and 200 μM Ni²⁺ (see Section 5.4.1). **(C)** SDS-PAGE analysis of this crosslinking reaction in the absence or presence of 200 μM Ni²⁺. Protein band marked with an unlabeled arrow is hydrolyzed α-LPETG.

Assuming each species existed as a tetramer in solution prior to ligation, 70% conversion would suggest an oligomerized product species (Figure 9a). To investigate the extent of oligomerization of crosslinked α -LPETGG- α /cp β , the reaction mixture was analyzed by native-PAGE (Figure 9b). Recombinant HbA (rHb0.0) was included as a reference standard for the tetramer, considering the tetramer dissociation constant ($K_d = 0.4 - 1.3$ nM) is several orders of magnitude lower than the loading concentration used for this gel (Lane 4). In the SML reaction mixture, the banded smearing at lower relative migrations may suggest the formation of oligomeric states greater than the tetrameric Hb. However, drawing any conclusion from this is difficult given the smearing present throughout all of the lanes. Interestingly, GG- α /cp β migrated the furthest by native-PAGE, despite having ~4% higher tetramer mass than rHb0.0 and the exact cause is not entirely clear (see Section 4.2.1).

Though native-PAGE analysis was largely inconclusive, it would be possible to shed light on the oligomer status using analytical size-exclusion chromatography techniques. In fact, several studies have established methods for separating α_1/β_1 dimers from tetrameric Hb⁹¹ and tetrameric Hb from di-Hb.⁴⁶ However, since this reaction results in a product population that is polydisperse, if it forms oligomers at all, the potential for generating viable high molecular weight HBOCs is low. Instead, these experiments demonstrate that we are able to generate Hb-like molecules that display substrate or nucleophile tags that are reasonably accessible and reactive in SML.

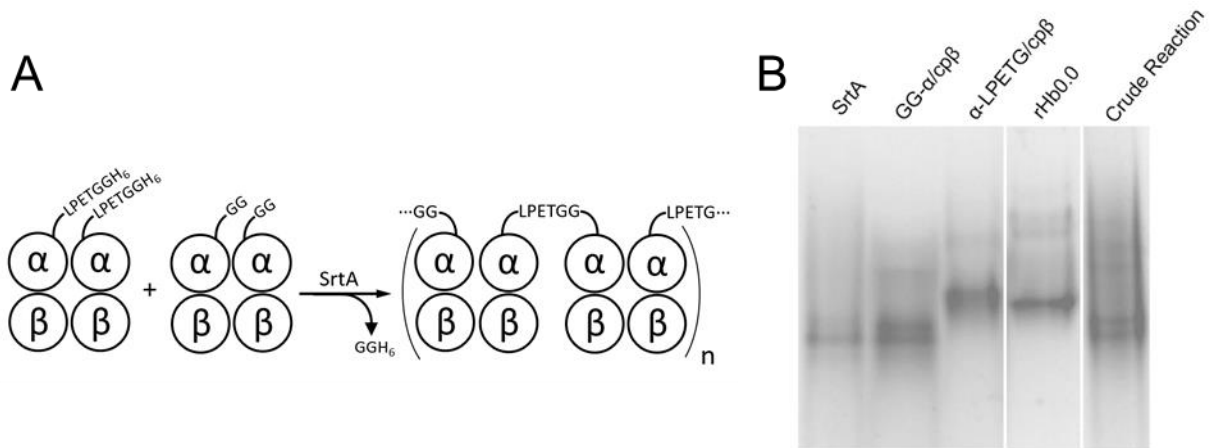


Figure 9. Analysis of oligomerization state of ligated α -LPETG/cp β and GG- α /cp β . (A) Depiction of theoretical Hb-polymerization as catalyzed by sortase. (B) Native-PAGE of the crude reaction mixture following SML. Recombinant HbA was included as a tetrameric reference.

3.2 Crosslinking α -LPETG in a C-to-C Ligation by Sortase A

As outlined previously, our primary goal was to functionalize Hb with a bio-orthogonal “click” handle as a way to generate a polymeric HBOC. To these ends, we used SML to install a functionalized oligopeptide as an intra-molecular crosslinker between adjacent species of α -LPETG. While it would be convenient to crosslink α -LPETG and GG- α using a peptide containing a glycine N-terminus and a “LPETG” C-terminus, this strategy is complicated by a range of competing SML reactions, namely direct α -LPETG/GG- α ligation. Thus, in order to reliably bridge adjacent α -globins using SML, it was required to design a homobifunctional peptide that is reactive in SML (see section 2.2). This could be accomplished with either the substrate- or nucleophile-tagged α -globin by using a crosslinker with the complementary sortag. However, it was decided to move forward with α -LPETG over GG- α due to an increased expression yield, the convenience of a His₆-tag purification, a simpler crosslinker design/synthesis, and the ease of analysis by SDS-PAGE due to separation of the α -LPETG and β bands.

3.2.1 Conjugation of α -LPETG and Gly-PEG4-Gly

We sought to establish the feasibility of a di- α with a α_1 C-terminus to α_2 C-terminus ligation by using Gly-PEG4-Gly as a “model” crosslinker (Figure 10a). Reactions were performed at various ratios of linker:Hb ranging from 1:1 to 20:1, in order to find the optimum stoichiometry. After 90 minutes, SrtA activity was quenched with SDS loading buffer and analyzed via SDS-PAGE (Figure 10b). Regardless of the linker:Hb ratios, a higher molecular weight band appears corresponding to the crosslinked product (α -PEG4- α). Unsurprisingly, α -LPETG is depleted further at higher equivalences of crosslinker, but this is accounted for by an increase in the single-addition product (α -PEG4) rather than the crosslinked product. The variations in gel loading and presence of a species with a similar molecular weight to the product confounded the determination of product yields.

We also ran this reaction in the presence or absence of 200 μ M Ni^{2+} in order to study the metal-enhancement effect on the production of crosslinked product (Figure 10c). Total conversion was calculated using band intensities and expressed as the proportion of crosslinked product to all α -species. The presence of Ni^{2+} had little impact on α -PEG4- α accumulation, with product conversion varying by less than 5% across the linker:Hb ratios tested here. However, the enhancement effect of Ni^{2+} is not entirely clear as this does not consider single-addition product formation, which cannot be reliably determined by SDS-PAGE analysis.

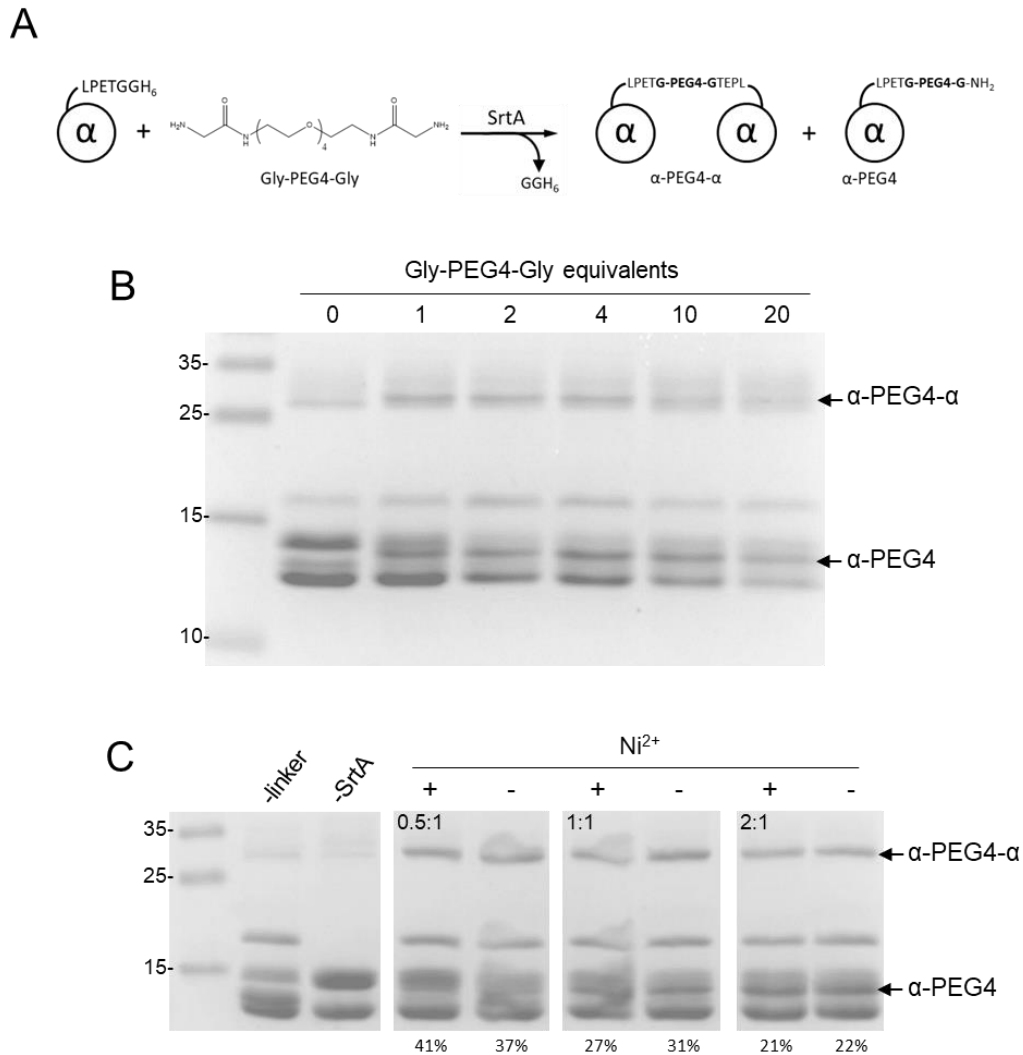


Figure 10. SDS-PAGE analysis of α -LPETG crosslinking using SML. (A) Depiction of the C-terminal to C-terminal ligation strategy using a homo-bifunctional model linker. (B) Reaction end points after 90 minutes at varying linker:Hb ratios. Arrows indicate the crosslinked and single-addition products. (C) Crosslinking reactions in the presence or absence of 200 μ M Ni²⁺ at the indicated linker:Hb ratios. Values below each lane indicate product conversion proportions.

Overall, total product yield was unacceptably low, with a maximum of approximately 40% using a 1:1 linker:Hb ratio and 25% at 4:1. We plan to optimize reaction conditions to determine factors for improving yields. Despite the low yields observed, we established that sortase can be used to crosslink sortagged Hbs. This led

us to investigate the crosslinking of α -LPETG subunits using a functionalized oligopeptide.

3.2.2 Conjugation of α -LPETG and GGGK^{GGG}K^{FITC}

In order to initially study the reactivity of the synthesized homo-bifunctional oligopeptide in the SML crosslinking of α -LPETG, we utilized GGGK(K^{FITC})GGG. We first investigated the optimal linker:Hb ratios to corroborate the results using the Gly-PEG4-Gly model linker. Reactions using 1, 2, and 4 equivalents of GGGK(K^{FITC})GGG to Hb were set up and end points were analyzed by SDS-PAGE. The gel was imaged by both UV fluorescence and Coomassie staining using a Bio-Rad Gel Analyzer. Coomassie staining did not yield quantifiable results however, FITC fluorescence allows us to observe clear incorporation of the peptide into α as both the single-addition (α -GGGK(K^{FITC})GGG) and crosslinked (α -GGGK(K^{FITC})GGG- α) products (Figure 11a). Unlike Gly-PEG4-Gly (MW = 352 Da), which resulted in overall decrease in molecular weight for the single addition product, ligation of GGGK(K^{FITC})GGG (MW = 1004 Da) is slightly more massive than the excised fragment (GGH₆, MW = 955 Da). While it would be expected for species of similar masses (Δ MW = +49 Da) to overlap in SDS-PAGE, α -GGGK(K^{FITC})GGG is observed to migrate differentially to α -LPETG. Due to the overall poor quality of the gel and impurities in the starting material, quantification of product yield could not be accurately determined. Although analysis is complicated by a higher molecular weight species in the absence of SrtA, the appearance of an overlapping fluorescent band in the presence of SrtA indicates formation of a distinct product that incorporates GGGK(K^{FITC})GGG.

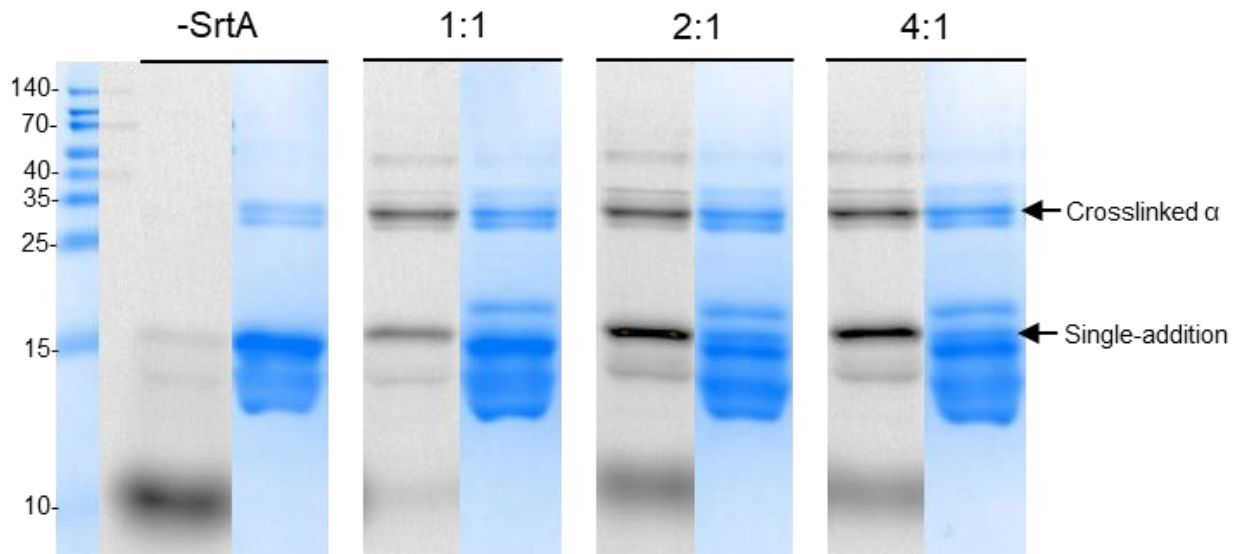


Figure 11. SDS-PAGE analysis of the sortase-mediated crosslinking of α -LPETG at 1, 2, and 4 equivalents of $G_3K(K^{FITC})G_3$. At each linker:Hb ratio, as indicated above the gel, is shown both UV-fluorescence (left) and CBB staining (right).

In the reactions mentioned here, we have been using a penta-mutant SrtA that has a considerably higher catalytic efficiency compared to the wild-type. To investigate the effects of these mutations on the formation of the crosslinked product, reactions were conducted using wtSrtA. The reaction conditions were also altered slightly to match those in other reported uses of wtSrtA: concentration of enzyme was increased to 10 μ M and the reaction was incubated at 37°C for 5 hours. The time-course of the reaction was monitored by SDS-PAGE and samples were treated in the same manner reported above. As expected the reaction was considerably slower than those with the mutant sortase (Figure 12). Formation of the single-addition product was robust compared to the crosslinked product with approximately 50% product distribution between the two. Hydrolysis was also observed to be considerably lower with the wild-type enzyme, consistent with previous reports.⁸³

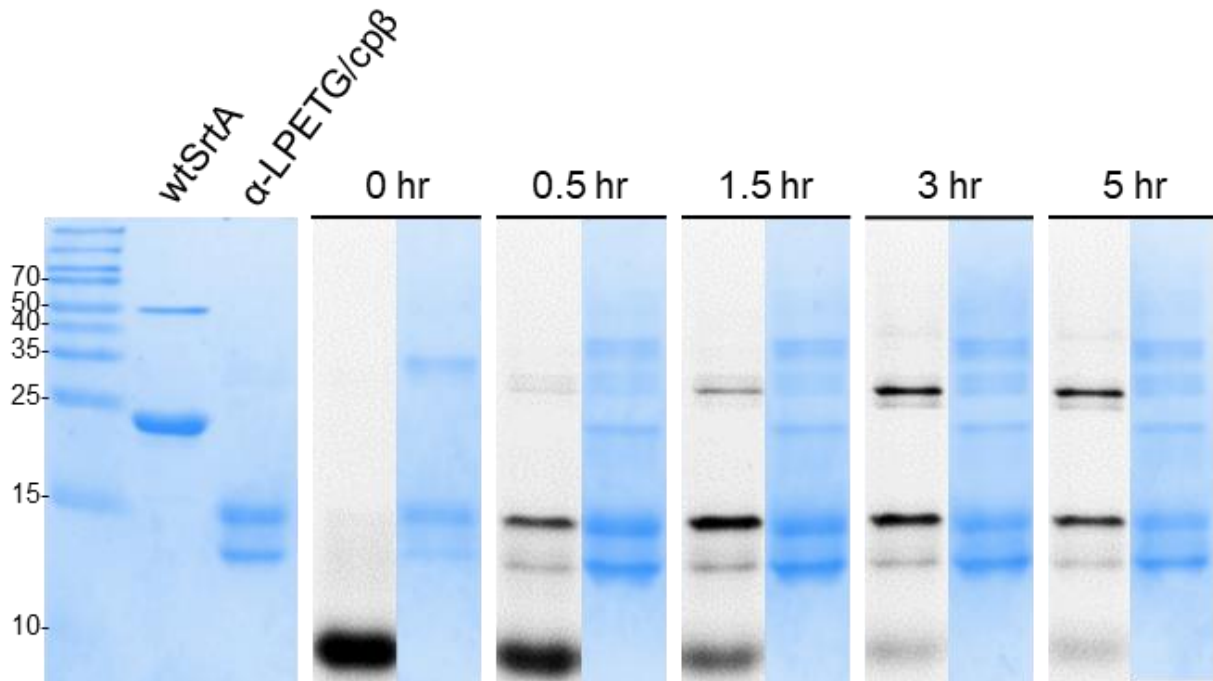


Figure 12. Reaction time-course analysis by SDS-PAGE of wtSrtA catalyzed crosslinking of α -LPETG with 0.5 mol equivalence of GGGK(K^{FITC})GGG. At each time point, indicated above the gel, is shown under both fluorescence (left) and CBB staining (right).

3.2.3 Conjugation of α -LPETG and GGGK(K^{DBCO})GGG

Once it was established that α -LPETG could be crosslinked with a novel C-terminus to C-terminus linkage using our synthetic peptide crosslinker, we aimed to DBCO functionalize these Hbs. Based on previous crosslinking experiments, GGGK(K^{DBCO})GGG was combined with α -LPETG/ β in stoichiometric proportions and reacted with penta-mutant SrtA for 120 min. Reaction progress was monitored by SDS-PAGE (Figure 13). The crosslinked product, α -GGGK(K^{DBCO})GGG- α was observed by SDS-PAGE at approximately 32 kDa after 30 minutes. In addition, a 16 kDa band was observed below the starting material that is consistent with the decreased mass of the single-addition product (α -GGGK(K^{DBCO})GGG, Δ MW = -50 Da).

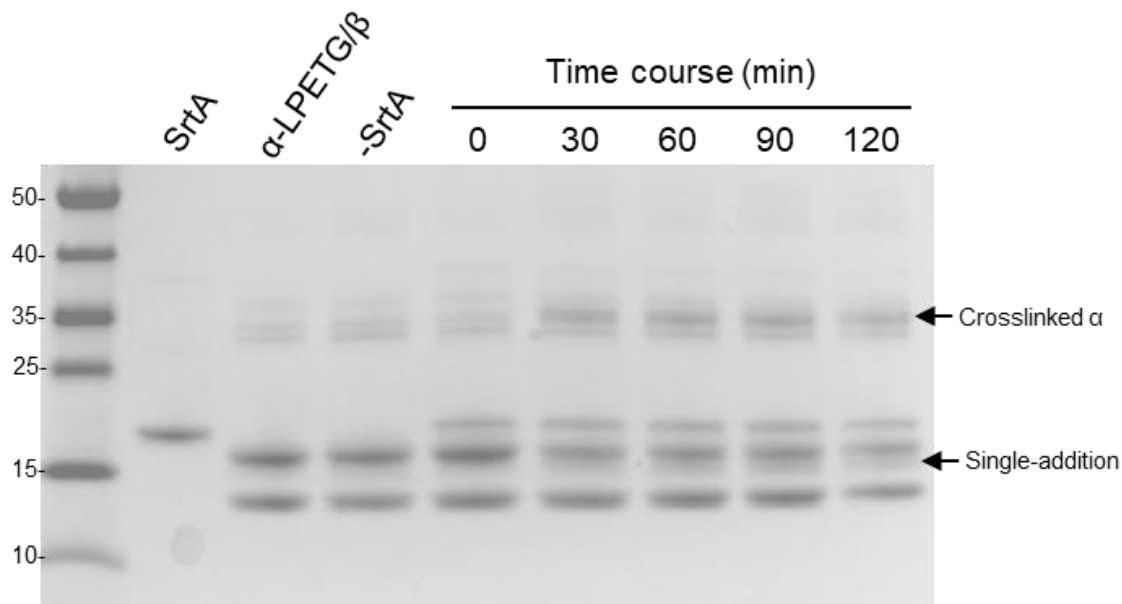


Figure 13. Reaction time-course analysis by SDS-PAGE of sortase-mediated crosslinking of α -LPETG with 0.5 mol equivalence of GGGK(K^{DBCO})GGG. This reaction time-course was also analyzed by ESI-MS at 30 min intervals for 2 hours starting at 10 min. Reconstructed masses were generated from the mass spectra at each time point. Each of the relevant species could be identified: hydrolyzed α (α -LPET), single-addition product (α -GGGK(K^{DBCO})GGG) unmodified α -LPETG, the intended crosslinked product (α -GGGK(K^{DBCO})GGG- α), and the β -subunit. The observed masses closely agreed with the expected masses (Table 5). To determine reaction progress, the peak areas of each α -species in the reconstructed mass spectrum were taken. The reaction reached completion quickly, with a maximum product conversion of 55-60% achieved by 40 min (Figure 14c). While a total product conversion just over 50% is not ideal, it was high enough to generate DBCO functionalized Hb in quantities sufficient for subsequent modification reactions.

Table 5. Expected and ESI-MS observed masses for α -LPETG crosslinking reaction.

Species	Expected (Da)	Observed (Da)
β	15,975	15,978
α -LPETGGH ₆ ^a	17,180	17,183
α -G ₃ K(K-DBCO)G ₃ - α	33,354	33,361
α -G ₃ K(K-DBCO)G ₃	17,128	17,131
α -LPET	16,244	16,246

^a The His₄ species was also observed (M_e = 16,909 Da)

In the future we will work to optimize reaction conditions to maximize the yield. However, the hydrolysis and single-addition products were observed at very low levels throughout the reaction. Maximum single-addition product was only 6% of total α and occurred at 10 minutes into the reaction, while dropping to <1% by 40 min (Figure 14c). Also, hydrolysis of the starting material was not observed until after 40 minutes and increased to one-half of 1% by 100 min. Thus, it is not clear how much product yield can be improved.

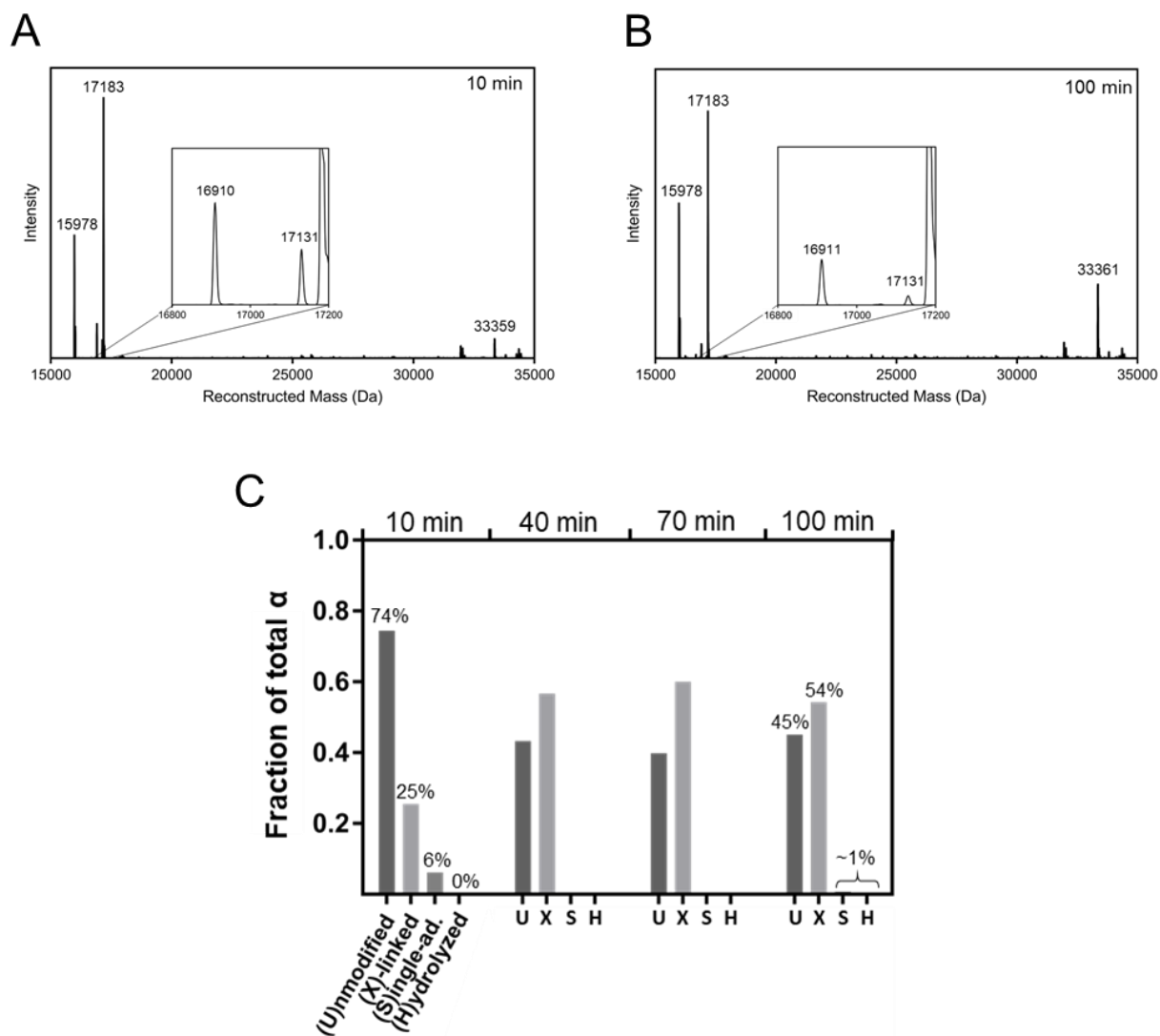


Figure 14. ESI-MS time-course data for the sortase-mediated crosslinking of α -LPETG using GGGK(K^{DBCO})GGG. (A) Reconstructed mass spectrum of the crude reaction mixture at 10 min and (B) 100 min. Inset: Portion of the mass spectrum as shown, both are of the same range. Expected masses are shown in Table 5. (C) Each identified α -globin species as a fraction of total α at each time point. Calculated using ESI-MS reconstructed peak areas as shown in A and B.

3.2.4 Purification of crosslinked α -LPETG

The crude reaction mixture was quickly purified in order to avoid irreversible degradation of products to the hydrolyzed form by SrtA. Fortunately, the His₆-tag present on the starting material is excised during the SrtA catalyzed transpeptidation reaction with

the peptide crosslinker. Therefore, we separated the crosslinked product from the His₆-tagged starting material and SrtA using Ni-NTA chromatography.

In order to purify the crosslinked product, the total reaction volumes were scaled up to final volumes ranging from 1 to 10 mL and otherwise the reaction conditions were identical to previous tests. In this example, a crude chromatogram was generated that clearly shows two distinct Hb-species, one eluting at low levels of imidazole (peak 1) and another at high imidazole concentrations (peak 2) (Figure 15a). As expected, peak 1 is enriched in crosslinked product as compared to the crude reaction and peak 2 (Figure 15b). These findings are supported by the ESI-MS data where the crosslinked product in peak 1 represents the majority of the α -species (Figure 15c). In addition, the starting material and SrtA have been depleted in the purified sample (peak 1) to approximately 5% each and quantities as low as 1% have been recorded.

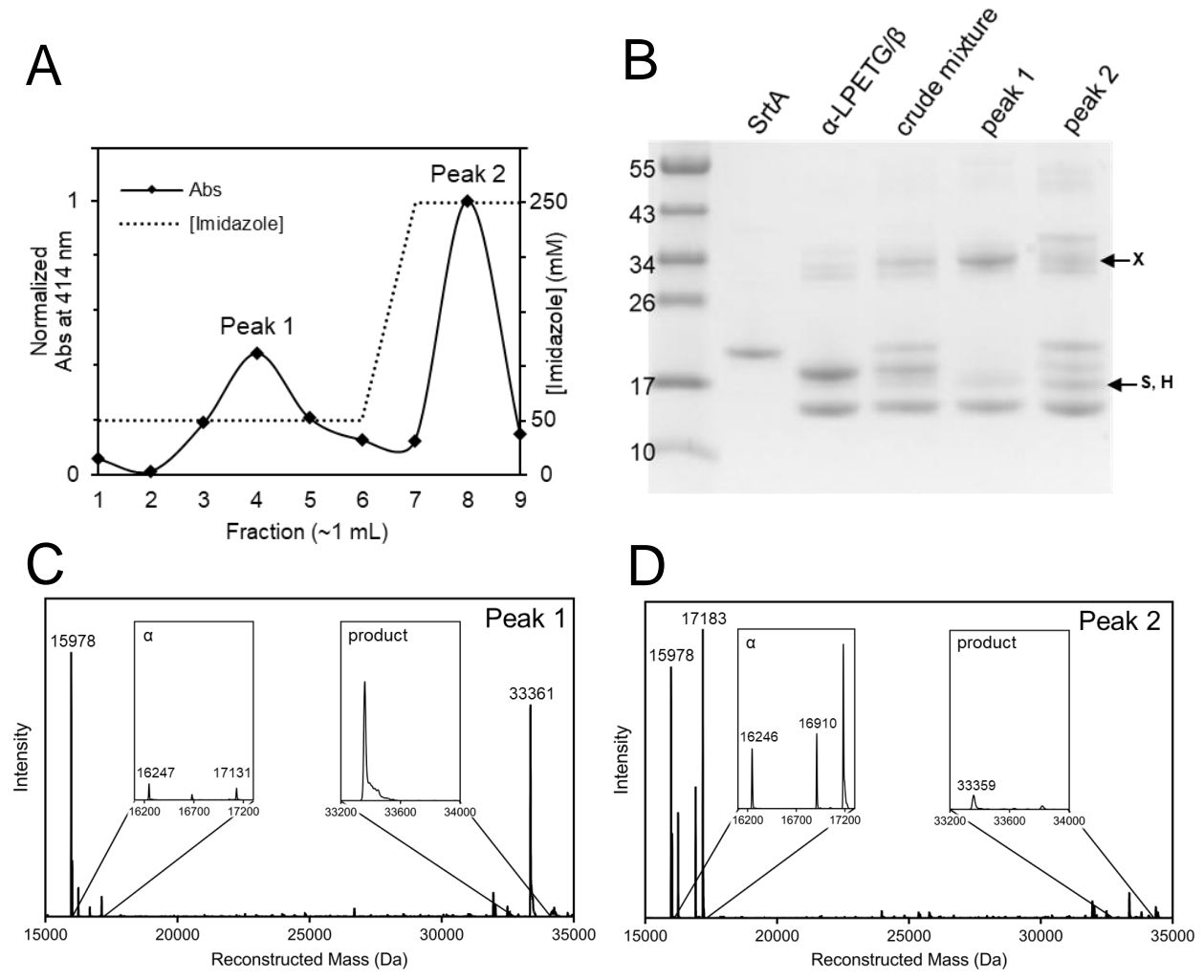


Figure 15. Purification of crosslinked and functionalized α from crude reaction mixture. (A) Normalized Soret band absorbance ($\lambda_{\max} = 414$ nm) of fractions collected during Ni-IMAC purification of crude SML mixture. (B) SDS-PAGE analysis of purified fractions. (C) and (D) ESI-MS analysis of peaks 1 and 2 from crude reaction purification.

Table 6. Typical ESI-MS abundances of α -species in purified fractions of SML mixture.

Species	Peak 1	Peak 2
α -LPETGGH _{6/4}	4% ^a	75%
α -G ₃ K(K ^{DBCO})G ₃ - α	91%	10%
α -G ₃ K(K ^{DBCO})G ₃	2%	0% ^b
α -LPET	2%	15%

^a Only observed as His₄ species
^b Not observed

Both SDS-PAGE and ESI-MS show peak 2 contains His₆-tagged SrtA, unreacted α -LPETG, and hydrolyzed α -LPET in addition to some high molecular weight species. Although hydrolyzed α -LPET does not possess a His₆-tag, its presence in peak 2 is unsurprising as α -LPETG would eventually be hydrolyzed by SrtA due to the absence of any glycine nucleophiles. The observed high molecular weight species by SDS-PAGE are consistent with the starting material. However, on average, ESI-MS suggests crosslinked product makes up approximately 10% of the α -species in peak 2 (Table 6).

3.3 Bioorthogonal Reactivity of Crosslinked Hbs

3.3.1 Probing for DBCO-modified species

To further identify any DBCO containing species, 6-carboxyfluorescein (6-FAM) azide was added in two-fold molar excess to samples of peak 1 and peak 2, as well as purified starting material as a control. After 30 minutes the samples were analyzed by SDS-PAGE and ESI-MS (Figure 16). Similar to the crosslinking experiments using FITC conjugated linkers, the gels were imaged by both fluorescence and CBB staining. After

the addition of 6-FAM azide to peak 1, conjugation is to the crosslinked and single-addition products observed by SDS-PAGE. Interestingly, the 6-FAM conjugated species migrate differentially from the non-conjugated ones despite only increasing the molecular weight by ~1%, resulting in the doubling of the crosslinked product band after CBB staining (Figure 16a). The observed mass for the crosslinked 6-FAM conjugate is consistent with the expected mass for this product (MW = 33,354 Da), as determined via ESI-MS (Figure 16b). The increased sensitivity from fluorescence imaging also allowed us to observe DBCO-modified species in peak 2, while their presence is not obvious in the CBB staining. The total protein content of peak 2 appears unchanged with the exception of the expected increased abundance of hydrolyzed α -LPET as SrtA is still present in this fraction.

This experiment shows that our DBCO-oligopeptide incorporates and crosslinks α -LPETG as intended and confirms that DBCO is accessible and reactive in the crosslinked product.

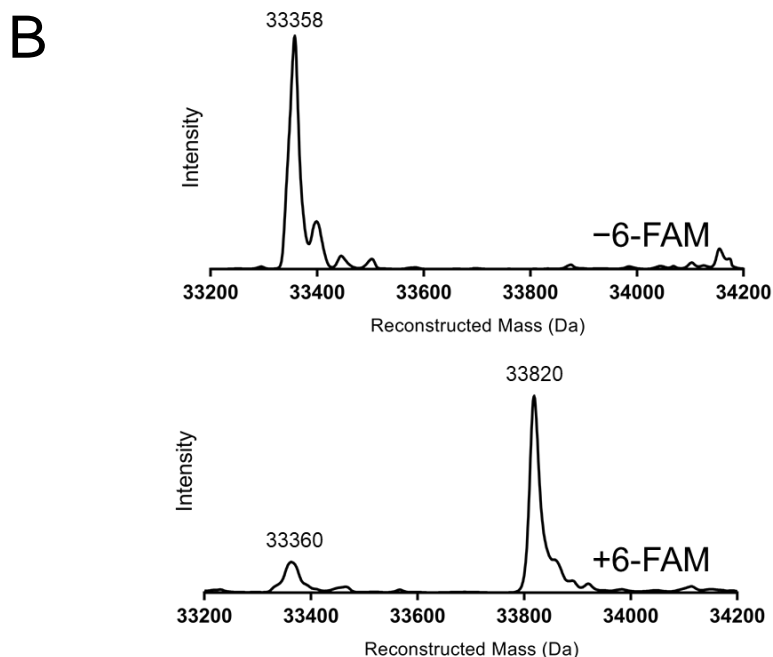
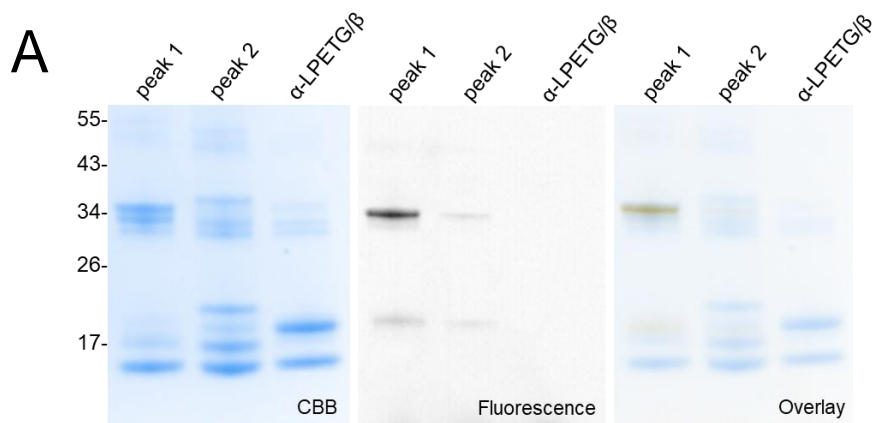


Figure 16. Bioorthogonal conjugation of 6-FAM and DBCO modified Hbs. **(A)** Identification of DBCO-modified Hbs by addition of 6-FAM azide in purified fractions of sortase-mediated crosslinking reactions. Peak 1 and 2 refer to fractions collected during purification (Figure 15). **(B)** ESI-MS of 6-FAM conjugation to crosslinked and DBCO-modified α species in peak 1. Adduct mass of +462 Da aligns closely with the expected adduct mass ($\Delta MW = +458$ Da).

3.3.2 Oligomerization of DBCO-modified Hb

As outlined in Section 1.4, the end goal of this project is to establish a method for generating polymeric Hb of defined molecular weight. To that end, this body of work was

aimed at characterizing Hb-oligomerization using azide functionalized PEGs. Purified α -GGGK(K^{DBCO})GGG- α was combined with an azido-PEG5-azide, a homo-bifunctional PEG azide linker, in 1-, 5-, 20-, 50-, and 100-fold excess. Azido-PEG5-azide required dilution in DMSO due to its limited solubility in water, so a DMSO-control was included. Following incubation for 2 hours, reaction products were analyzed by SDS-PAGE (Figure 17a). While there is variance in the loading or staining of these reactions, no change of protein content is observed. The product of this reaction would be a tetra- α species with an approximate molecular weight of 67 kD and no banding is present at this mass. However, an additional high molecular weight species was observed around 50 kDa, present even in the absence of azido-PEG5-azide. To ensure DBCO reactivity, a two-fold excess of 6-FAM azide was reacted with this sample of α -GGGK(K^{DBCO})GGG- α . Interestingly, in addition to the expected single-addition and crosslinked fluorescent α species, a fluorescent band was observed near the molecular weight of this 50 kDa band (Figure 17b).

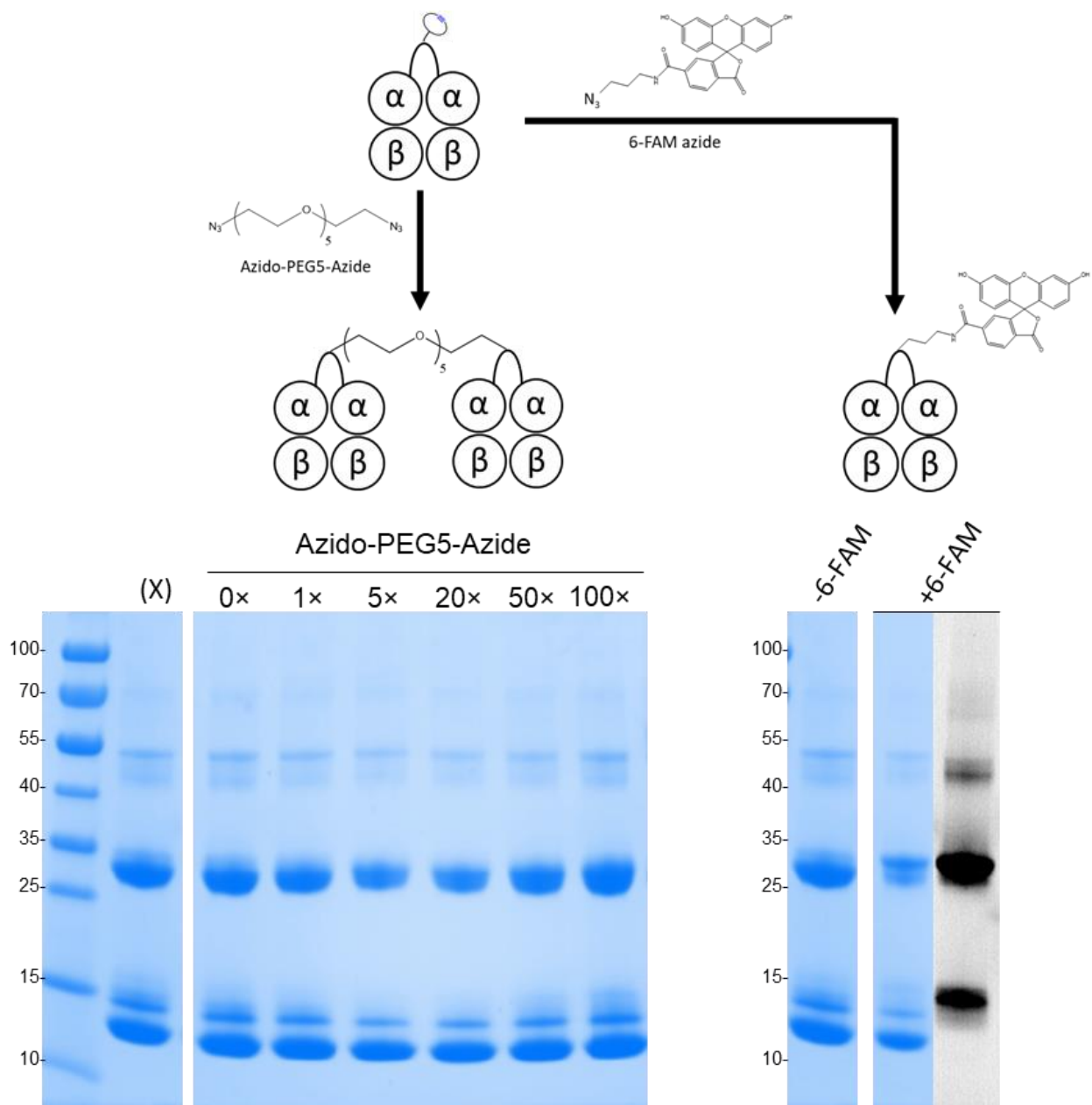


Figure 17. Reaction of α -GGGK(K^{DBCO})GGG- α and azido-PEG5-azide. (Top) Reaction scheme for crosslinking α -GGGK(K^{DBCO})GGG- α by azido-PEG5-azide or conjugation of 6-FAM azide. (Bottom left) CBB stained SDS-PAGE gel of reaction with various molar excesses of the linker. The “0x” lane is a DMSO control. (Top right) SDS-PAGE gel of 6-FAM azide added to the same α -GGGK(K^{DBCO})GGG- α sample in top left gel. Side by side lanes are CBB stained and fluorescence image of the same lane.

As an alternative scaffold, a 4-arm PEG-10k azide was obtained and combined with α -GGGK(K^{DBCO})GGG- α in 20, 50, and 100-fold excesses and analyzed by SDS-

PAGE after two hours (Figure 18). Most noticeably, the large molecular weight PEG had interesting effects on the protein migration patterns. While it appears as though the changes in banding might be the result of a change in protein composition, the cross-lane streaking between the 20x and 50x lanes suggests otherwise. Still, a high molecular weight band around 60 kDa is observed in 50-fold and 100-fold excess of the 4-arm PEG azide that is not present in reactions lacking the PEG azide. In addition, there is noticeable separation of the ~33 kDa crosslinked product bands which may indicate a change in protein composition for the crosslinked species. However, this could simply be anomalous migration for these two samples.

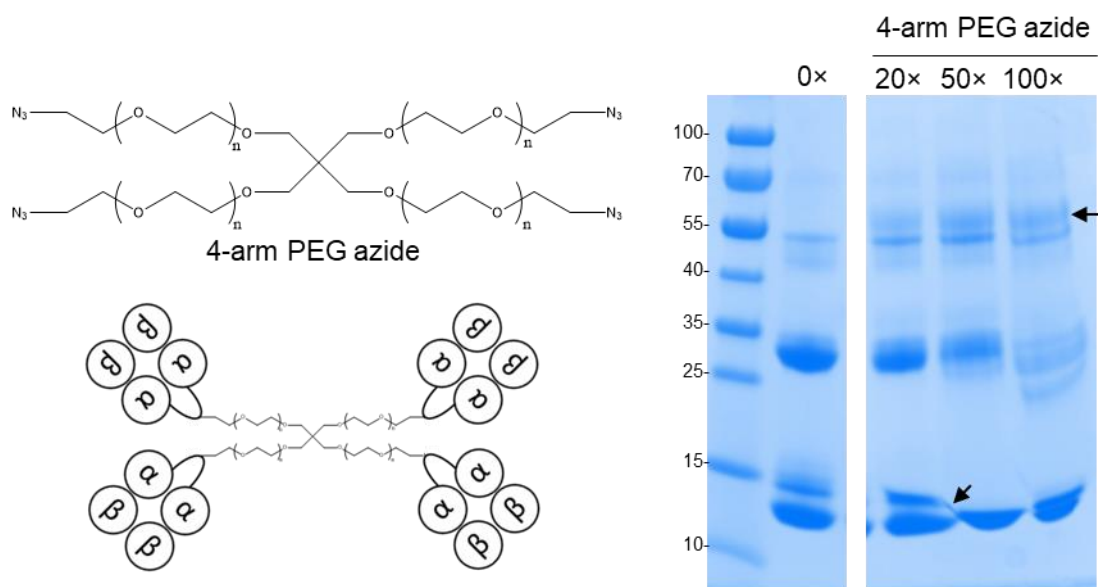


Figure 18. Inter-molecular crosslinking experiments using α -G₃K(K^{DBCO})G₃- α and 4-arm PEG azide. (Left) Schematic representation of 4-arm PEG azide and the intended product. (Right) SDS-PAGE analysis of α -GGGK(K^{DBCO})GGG- α and 4-arm PEG azide reaction performed at various molar excesses of the multi-branched linker, as indicated at the top of each lane.

Further analysis of these reactions and optimization of conditions will be needed in order to achieve successful intermolecular crosslinking of the Hbs.

4. Discussion

4.1 Implication of Termini Modification in Sortagged-Hbs

Expressing Hb with a C-terminal His₆-tag resulted in considerable improvements in initial purity following IMAC compared to the conventional zinc affinity approach of Hb purification. While this is largely unsurprising, there are important structural implications that can result from the modification of globin termini. Work done in our lab found that relocation of the β -subunit termini to the α_1/β_1 interface resulted in a loss of cooperativity and increased oxygen affinity.⁹¹ One possible explanation is the conversion of the C-terminal carboxyl which has been converted into an amide in order to achieve circular permutation of the β -subunit. The C-terminus of β (β His146) is a part of an important electrostatic interaction with α Lys40 that stabilizes the low O₂ affinity T-state conformation of Hb.⁹² Similarly, the α -termini interact with each other in a salt-bridge in the T-state. While the α termini have been modified before with success in rHb1.1, this was done using a single glycine residue which may allow this region of the protein to maintain a similar conformation as the native protein. Therefore, it is possible that modifying the α -N- or C-terminus with a long flexible linker may have some effect on the oxygen binding properties of the molecule.

Furthermore, while the difference in migration by native-PAGE between α -LPETG/cp β and GG- α /cp β is likely the result of the charged His₆-tag, the migration of rHb0.0 may suggest this difference could be the result of a change in their conformational states. In fact, the tendency for Hbs containing cp β to dissociate has been suggested to be the result of increased steric bulk within the β_1/β_2 cleft, favoring the dimer conformation.⁹¹ Since adjacent α -subunits interact in a similar manner, the addition of a

large poly-Gly tag at the α N-terminus could result in a similar disruption of this interaction resulting in the observed change in relative hydrodynamic sizes. However, additional analysis using analytical ultra-centrifugation (AUC), size-exclusion chromatography (SEC), or dynamic light scattering will be required to determine this.

4.2 Functionalizing and Crosslinking Sortagged-Hbs

Two methods of α -crosslinking were described in this work, 'direct' crosslinking, where α -globins act as either acyl-donors or acceptors, and 'indirect' crosslinking using a bifunctional oligopeptide nucleophile and α -LPETG. While both of these methods result in a crosslinked di- α subunit there are distinct differences which are discussed below.

4.2.1 Implications of Tetrameric Hb on Crosslinking

The products of the direct and indirect crosslinking appear very similarly when denatured for SDS-PAGE. However, the direct method generates a crosslinked α via an inter-molecular reaction, rather than the expected intra-molecular reaction involved in the final ligation used for the indirect methods. A consequence of this is the possibility of Hb oligomerization in the products, as seen by native-PAGE analysis. But despite over 70% conversion, there appeared to remain a significant portion of smaller Hb species in solution, which may indicate there is some level of rearrangement of tertiary structure in these oligomers. As discussed previously, these cp β -containing Hbs have a reduced capacity to form the tetramer. Analytical SEC experiments suggest that at the concentrations in this reaction (50 μ M in heme) the tetramer would only account for approximately 20% of total heme.⁹¹ In addition, recent AUC analysis of cp β -containing Hbs found a tetramer \rightarrow heterodimer dissociation constant values in the low μ M range (K_d

≈ 5 μM). Thus, it remains possible that rather than forming higher order oligomers, the α-LPETGG-α product has a potential to rearrange into obligate tetramers.

This rearrangement may also help explain the high conversion levels of in direct crosslinking experiments. Generally, it is expected to achieve 50% product conversion using SML without using a reactant excess or the metal-assisted methods mentioned previously. However, even in the absence of Ni²⁺, we were able to observe conversion levels approaching 70%, suggesting an equilibrium shifted towards products. One study found the sortase-mediated circularization of GFP had an excellent conversion (>90%), as a result of the structural proximity of the acyl-enzyme intermediate and the nucleophilic N-terminus⁹³ (Figure 19). Similarly, the N- and C- terminus of adjacent α-globins are in close proximity within the tetramer and could confer resistance to cleavage by sortase. If these Hb products do, in fact, rearrange and form a stabilized tetramer, it could result in an enhancement of product accumulation. While this is speculative, this provides a reasonable explanation to the surprisingly high conversion rate for this unoptimized reaction.

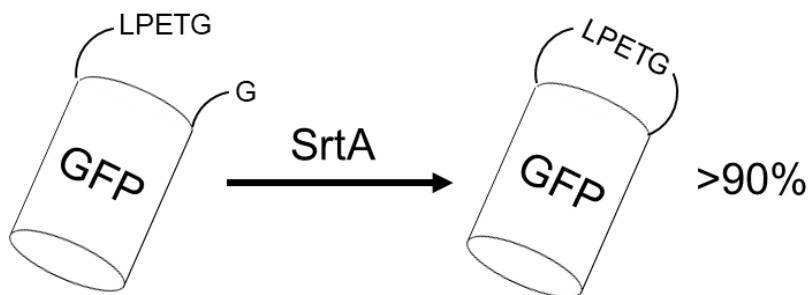


Figure 19. Circularization of GFP by Antos *et al.*⁹³ These investigators were able to circularize GFP with a C-terminal LPETG and N-terminal Gly with high efficiency (>90%).

4.2.2 Indirect Crosslinking and Functionalizing Hb

This goal of this work was to functionalize Hb through the SML of a peptide containing a “click” handle with the sortagged α -globin. As mentioned in section 1.3.2, chemoenzymatic ligation of reaction handles has become common practice. However, conventional methods of doing this rely on ligation of a simple functionalized oligopeptide (e.i. not bifunctional, such as GGK^{DBCO}). For our purposes, this would create a suboptimal situation in which each Hb tetramer would display two bioorthogonal reaction handles, complicating future conjugation reactions. This work shows that we were able to avoid this by crosslinking α -globins with a single functionalized peptide via SML. This way, we successfully showed that Hb could be site-specifically modified exactly once, which could restrict the dissociation of Hb into α_1/β_1 heterodimers – a required trait in HBOC design.

However, we had predicted that this crosslinking would be enhanced by the colocalization of reacting groups when two α/β dimers form a tetramer. Unfortunately, the high product conversion levels observed using direct crosslinking did not translate well to the indirect methods. We observed 60-70% maximum product formation for direct ligation, while only ~50% of the di- α product formed with indirect ligation. One possible explanation for this is that the bifunctional peptide crosslinks α -subunits via a C- to C-terminal ligation, rather than the N- to C-terminal ligation in a direct crosslinking reaction. Adjacent C-termini are approximately 30 Å apart while this is only 3 Å for adjacent α N- and α C- termini (Figure 20). While 30 Å could easily be spanned by the 35 amino acids between ligated α -subunits in α -GGGK(K^{DBCO})GGG- α , this extra distance could significantly reduce the effective concentration of the reactive groups in the second crosslinking event compared to that in the case of the direct couple reaction.

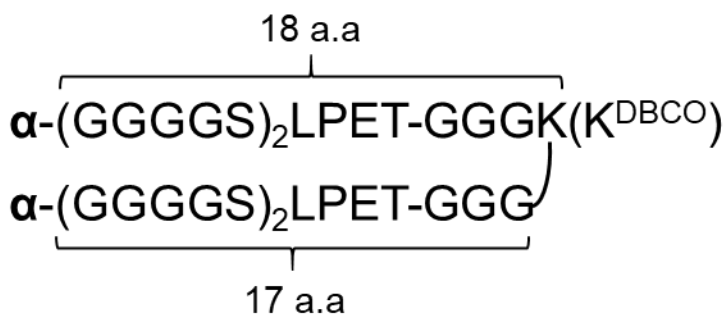
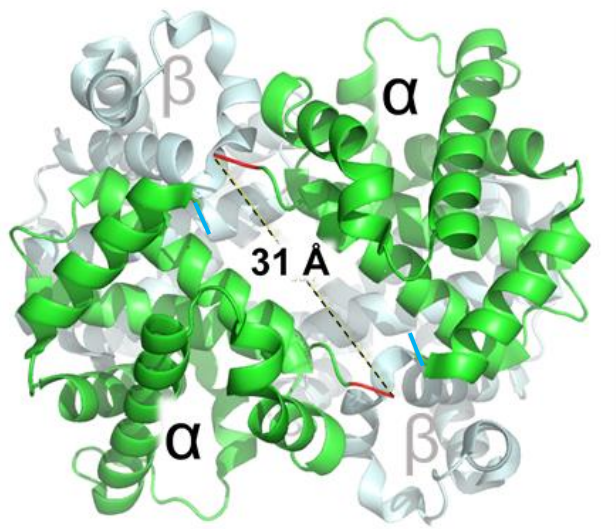


Figure 20. C-to-C fusion of adjacent α -subunits in tetrameric Hb. (Top) Relative positions of α termini at the α_1/α_2 interface in tetrameric Hb. C-termini (red) are separated by 30 Å, while N-termini (blue) associate near adjacent α C-termini. PDB ID: 2DN1. (Bottom) The number of amino acids on each subunit that would span the distance between the termini.

Despite the reduced yield of product formation for indirect crosslinking, the association of α/β dimers appears to influence the formation of the crosslinked product once the single-addition product is formed. The relative fluorescence in SDS-PAGE experiments following conjugation of 6-FAM to the purified products, showed a strong preference for crosslinked α product over the single-addition (Figure 16a). This is supported by ESI-MS analysis, where in crude reaction mixtures, the single-addition product only accounted for ~1% of total α -species and crosslinked product reached

upwards of 50%. Anecdotally, more single-addition was observed using sortagged-Hbs containing cp β (1-2%) as compared to wt β (~0.4%), which could be the result of a difference in the tetrameric Hb populations. Whether this is significant or not requires additional investigation.

4.2.3 Byproduct Formation

Sortase-catalyzed hydrolysis is one of the best-characterized side reactions in SML.⁹⁴ As mentioned previously, hydrolysis is irreversible and serves as a substrate sink in this reaction, but suppression of hydrolytic products can be expected with increasing nucleophile concentrations. However, for the crosslinking experiments shown here, an excess of nucleophile was not ideal due to an increase in the formation of the single-addition product (Figure 10). Despite a stoichiometric ratio of nucleophile, <1% of total α was found to be hydrolyzed at maximum product formation and only reached approximately 1% of total α after an additional hour. Furthermore, we were able to retain high yields of product and prevent further hydrolysis of crosslinked and single-addition products by rapid separation of the final reaction mixture from SrtA.

The same could not be said of the remaining unreacted α -LPETG, which co-eluted with SrtA during Ni-IMAC. While this meant a loss of ~40-50% of the starting material, for our purposes product retention was the main consideration and no further attempt to separate SrtA was made. It is likely that this material could be separated from SrtA using other purification techniques such as SEC or AEX before or after Ni-IMAC. SrtA activity could also be reduced using chelating agents, such as EDTA, as Ca²⁺ is a required

cofactor for SML. However, this was not done in this study in order to perform Ni-IMAC. Further analysis will be required to minimize wasted starting material.

While SDS-PAGE and ESI-MS did not suggest appreciable amounts of SrtA in the purified fraction of crosslinked product, an increased proportion of the hydrolytic product (~5%) was observed in the purified fraction as compared to the crude mixture, which could suggest a residual amount of sortase; thus, further purification of this fraction may be required.

Sortase has also been reported to react with ϵ -amino groups of lysines to form intermolecular crosslinked side-products.⁹⁵ This process has also been found to be accelerated with penta-mutant SrtA as a result of its lowered affinity for the glycine nucleophile.^{83, 96} For protein-peptide reactions, this product is relatively easy to identify as it almost doubles the mass of the target protein. In the work presented here, identification of this species was obscured by the expected crosslinked product and additional contaminating species in the starting material. However, the fluorescent band near 50 kDa following the conjugation of 6-FAM azide to the purified crosslinked product provides some evidence suggesting an additional crosslinking event may have occurred (Figure 17b). Due to the nature of this crosslinking reaction, a side-product could be expected that would result in a 49 kDa tri- α that would retain DBCO functionality (Figure 21). Four lysines can be found on the adjacent α/β heterodimer (α Lys7, α Lys11, β Lys59, β Lys61) that are within 20 Å of the α_1 C-terminus (Figure 21). Given that the α C-termini are separated by ~30 Å, it is plausible that this undesired side reaction could give rise to the observed 50 kDa species.

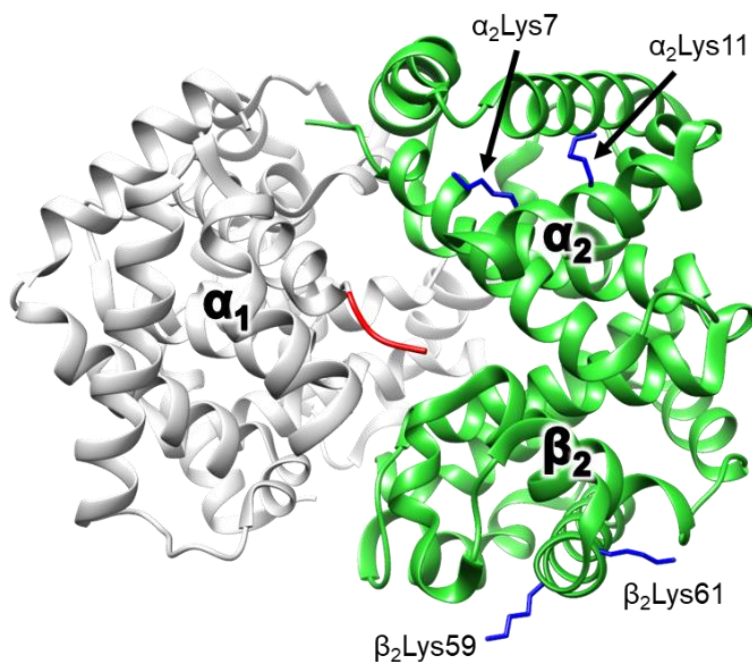
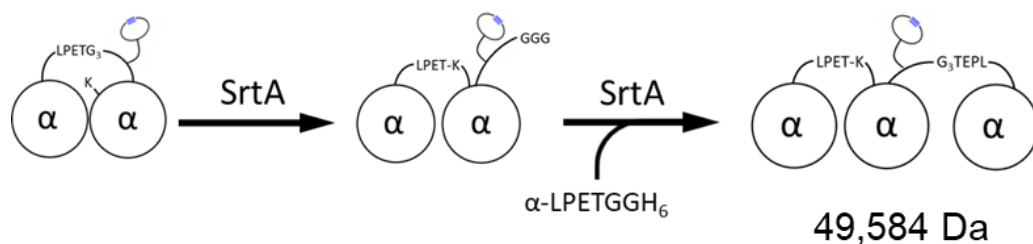


Figure 21. Hypothetical additional crosslinking event catalyzed by sortase where a lysine ϵ -amine acts as a nucleophile. (Top) Hypothetical route to achieve the 49 kDa fluorescent species as observed by SDS-PAGE following 6-FAM azide conjugation. (Bottom) Possible sources of lysine ϵ -amine nucleophiles for side-product formation. Labeled are lysine residues (blue) on the adjacent α/β heterodimer within 20 Å of the α_1 C-terminus (red).

4.3 Improving the Bioorthogonal Reactivity of DBCO-Hbs

This work successfully demonstrated the reactivity of DBCO-conjugated Hbs through the conjugation of 6-FAM azide. However, these Hbs did not show reactivity with bifunctional or 4-arm PEG azides. While it is not entirely clear why this was the case, some potential explanations are discussed here.

Whether these PEG azides were functional under the conditions used here was not tested. Using a DBCO-conjugated fluorescent probe would likely be sufficient to establish their reactivity with the strained cyclooctyne. This probe could also assist in the identification of multi-branched PEGs that are partially decorated in Hb. Furthermore, the homo-bifunctional PEG5 azide used in this study was only partially soluble in water and required dilution into DMSO prior to its use. The reaction volumes used here made it difficult to determine if this PEG reagent was 'oiling' out of solution. Additional optimization of these reactions will be required to draw any conclusions from these experiments.

4.4 Conclusions and Future Directions

4.4.1 Dendritic Biotherapeutics

There are some limitations with using high molecular weight or multi-branched PEGs for this application. Polymers of sufficient sizes are prone to intra- and inter-molecular entanglement, which can limit accessibility to their active sites.⁹⁷ In addition, PEGs are known for their ability to improve biotherapeutic potency with steric shielding effects and distinctive hydration layers⁹⁸ which could also limit accessibility to multiple reactive sites. In general, ligation efficiency would be expected to decrease with increasing molecular weight. Using conditions that are known to disrupt entanglement and hydration of these polymers, such as altering pH or ionic strength, could have beneficial increases in reactivity.⁹⁷

Dendrimers are another type of multi-branched polymer that may yield different results as high levels of surface decoration may not be required to have a beneficial impact on the circulatory retention time and vasoactive effects of HBOCs. One study

reported that conjugating three to five antibodies to a sixth-generation dendrimer resulted in an increase in particle radius from 60 Å to 350 Å.⁹⁹ In addition, the ability of dendrimers to trap small hydrophobic molecules has been well documented¹⁰⁰ and could result in reduced heme-based toxic effects with cell-free Hb. With this in mind, even with low levels of Hb conjugation to a large dendrimer could result in a non-vasoactive, less toxic HBOC.

4.4.2 DBCO-Azide “Click” Chemistry and Hbs

Some additional considerations must be given to the use of DBCO as a bioorthogonal reaction handle for Hb. Cyclooctynes have been reported to react with free-thiols via the thiol-yne mechanism.¹⁰¹ The presence of βCys93 may result in difficulty maintaining the reactivity of DBCO prior to azide ligation. This side-reaction may also be accelerated with Hb, considering the thiol-yne mechanism is free radical and Hb is a known free-radical generator.¹⁰² Thus, it may be advisable to pre-oxidize this cysteine before modifying Hb, as this has been shown to mitigate thiol-yne adducts,¹⁰³ or replace them via site-directed mutagenesis.

4.4.3 Final Thoughts

Chemoenzymatic methodologies for producing fusion proteins have been previously reported^{83, 96} and can offer relief when traditional genetically encoded fusions are not tolerated.¹⁰⁴ However, creating protein fusions where both N- or C-termini need to be maintained for function or stability remains a significant challenge. Although protein-protein conjugates with unnatural N-to-N or C-to-C fusions have previously been generated using sortase,¹⁰⁵ the work presented in this thesis describes a novel one-pot

synthesis of homodimeric proteins with C-to-C ligations with the ability to introduce additional functionality via SML.

In summary, this body of work demonstrates proof-of-concept that Hb can be site-specifically crosslinked and functionalized using modern methodologies, potentially providing an alternative strategy for modifying Hbs in the development of oxygen carrying therapeutics.

5. Experimental

5.1 Expression and Purification of Hbs

5.1.1 Gene Synthesis

The α -LPETG gene encode a C-terminal His₆-tag, the SrtA_{Staph} “substrate” sequence (LPETG) and a 10 amino acid (GGGGS)₂ linker. The GG- α gene was designed to encode for the SrtA_{Staph} “nucleophile” tag followed by a similar nine amino acid linker. These genetic constructs were synthesized and subcloned into an expression vector containing a circularly permuted β -globin (cp β). In addition, a wt- β construct was synthesized and subcloned into an expression vector containing α -LPETG. These genes were synthesized, cloned, and optimized by Genscript (Piscataway, New Jersey) (Appendix). All Hb variants used in this study contained point-mutations which have been shown to increase the yield of soluble Hb in bacterial expression systems (α G15A, β G16A, β H116I, β K82D).^{106, 107}

Full amino acid sequence of GG- α (initiator methionine absent following purification):

GGGGSGGGGSLSPADKTNVKA AWAKVGAHAGEYGA EALERMFLSFPTTKTYFPHFD
LSHGSAQVKGHGK K VADALTNVAH VDDMPNALSALS DLHAHKLRVDPVNFKLLSHC
LLVTLAAHLPAEFTPAVHASLDKFLASVSTVLT SKYR

Full amino acid sequence of α -LPETG:

MLSPADKTNVKA AWAKVGAHAGEYGA EALERMFLSFPTTKTYFPHFDLSHGSAQVKG
HGK K VADALTNVAH VDDMPNALSALS DLHAHKLRVDPVNFKLLSHCLLVTLAAHLPA
EFTPAVHASLDKFLASVSTVLT SKYRGGGGSGGGGSLPETGGHHHHH

Full amino acid sequence of cp β :

MEFTPPVQAAYQKVVAGVANALAHKYHGSGGQGGGVH LTPEEKSAVTALWAKVNVD
EVGGEALGRLLVVYPWTQRFFESFGDLSTPDAVMGNPKVKAHGKKVLGAFSDGLAHL
DNLDGTFATLSELHCDKLHVDPENFRLLGNVLCVLA IHFGK

Full amino acid sequence of β -(G16A, H116I, K82D):

MVHLTPEEKSAVTALWAKVNVDEVGGEALGRLLVVYPWTQRFFESFGDLSTPDAVMG
NPKVKAHGKKVLGAFSDGLAHLNLDGTFATLSELHCDKLHVDPENFRLLGNVLVCVL
AIHFGKEFTPPVQAAYQKVVAGVANALAHKYH

5.1.2 Transformation

All Hb expression vectors were combined with *E. coli* BL21(DE3) cells to make the desired transformed bacterial expression strains. A total of 50 μ L of chemically competent cells were added to 1 μ L of the expression vector (50-100 ng/mL). Following a 30-minute incubation, the cells were heat-shocked at 42 °C for 45 seconds, allowed to recover on ice for 2 minutes, then bathed with 950 μ L of Luria-Bertani broth (LB), and allowed to incubate for 45 minutes. The cells were then plated onto tetracycline selection plates (25 μ g/mL) and incubated at 37 °C for 24 hours. Single colonies were selected and used to inoculate 10 mL of LB-tet (25 μ g/mL), which was allowed to grow overnight at 37 °C. Expression strain seedstocks were made from the overnight culture by dilution (1:1 v/v) with 50% (v/v) glycerol/water, followed by flash freezing of 1 mL aliquots in liquid nitrogen.

5.1.3 Expression

Recombinant Hbs were expressed in 1 L cultures of Terrific Broth (TB) and tetracycline (25 μ g/mL) in 2.8 L Fernbach flasks. A starter culture was made by inoculating 10 mL of LB-tet (25 μ g/mL) with 1 μ L of seedstock or a single selection-plate colony and grown for 12-14 hours at 37°C with shaking at 200 rpm. Following inoculation of each 1 L culture with a 10 mL overnight culture, they were allowed to grow to an optical density at 600 nm (OD₆₀₀) of about 1.8 to 2.0 at which point protein production was induced with 1 mM isopropyl β -D-1 thiogalactopyranoside (IPTG) and allowed to grow for 5 hours. A

supplemental heme solution (per 1 L growth: 0.05 g porcine hemin, Alfa Aesar, 98+% pure; 5 mL of 200 mM NaOH) was made and portioned into hourly additions over the induction period. Cells were harvested by centrifugation at 6,000 × g for 10 min. Cell pellets were collected and flash frozen in liquid nitrogen then stored at -80 °C.

5.1.4 Purification of His-tagged Hbs (α -LPETG/cp β , α -LPETG/ β)

Frozen cell pellets were thawed and resuspended in 30 mL of lysis buffer (250 mM NaCl, 50 mM Tris-HCl, 10 mM imidazole, pH 8.5). Cells were lysed by sonication for 90 seconds with a Branson Instruments, Inc. Sonifier (model 450) equipped with a 1.8 cm diameter horn using 50% duty cycle and a power output of 6. The crude lysate was clarified by centrifugation at 20,000 × g for 30 min. The insoluble fraction was discarded and the clarified lysate was filtered through a 0.45 μ m filter. The lysate was then added to 3-10 mL of Ni-NTA chromatography resin (HisPur, Thermo Scientific) and unbound protein was washed from the column with 8 column volumes (CV) of 20 mM Tris-HCl, 0.5 M NaCl, 10mM imidazole, pH 8.5. The column was then washed with 4 CV 20 mM Tris-HCl, 0.1 M NaCl, 50 mM imidazole, pH 8.5 followed by 2 CV 20 mM Tris-HCl, 0.1 M NaCl, 100 mM imidazole, pH 8.5 to remove any proteins with non-specific binding (the latter step was later omitted). The bound protein was eluted with 20 mM Tris-HCl, 0.1 M NaCl, 250 mM imidazole, pH 8.5. Alternatively, fast-flow chelating sepharose (GE Life Sciences) loaded with Ni²⁺ was used for some purifications. To prepare the column, the resin was washed with 5 CV of water to remove the 20% ethanol storage solution. The column was then equilibrated with 0.5 CV 0.2 M NiSO₄ and any loosely bound ions were removed with 5 CV of an acidic sodium acetate buffer (50 mM NaOAc, pH 4.5). The column was then equilibrated with lysis buffer prior to loading clarified lysate.

5.1.5 Purification of non-tagged Hbs (GG- α)

Frozen cell pellets were thawed and resuspended in 30 mL of lysis buffer (17 mM NaCl, 50 mM Tris-HCl, pH 8.5). Cells were lysed by sonication and clarified in the same manner described above. Then Zn²⁺ (zinc acetate) was added to the clarified lysate up to a final concentration of 4 μ M to precipitate non-Hb zinc binding proteins. The exact concentration of zinc acetate varied and was determined empirically by addition of varying concentrations (0 – 4 μ M) of zinc acetate to separate aliquots of the clarified lysate followed by centrifugation at 14,000 \times g. The samples were then inspected for a red colored pellet that indicates precipitated hemoglobin. The highest concentration of Zn²⁺ that does not result in Hb precipitation was added to the bulk clarified lysate. The precipitated proteins were removed by centrifugation at 40,000 \times g for 20 min. The Zn-treated lysate was then filtered through a 0.45 μ m filter and added to fast-flow chelating sepharose (GE Life Sciences) equilibrated with Zn²⁺ by addition of 2 CV of 20 mM Zn(OAc)₂ followed by 5 CV of 0.2 M NaCl. Unbound proteins were removed with 8 CV of 20 mM Tris-HCl, 0.5 M NaCl, pH 8.5 and proteins with unspecific binding were removed with 2 CV of 250 mM Tris-HCl, pH 8.5 and 6 CV of 20 mM Tris-HCl pH 8.5. Protein was eluted with 20 mM Tris-HCl, 15 mM ethylenediaminetetraacetic acid (EDTA), pH 8.5.

5.1.6 Anion-exchange chromatography

Further purification was performed as needed on an ÄKTA Explorer chromatography system using a Mono-Q 10/100 GL (GE Life Sciences) strong anion exchanger. Samples were prepared by desalting in 15-mL Amicon Centricon concentrators with 10,000 Da molecular weight cut-off (MWCO) or by dialysis. Samples were concentrated to <1 mL and filtered by centrifugation in a tabletop microfuge using

Costar Spin-X 2.0 mL 0.22 μm cellulose acetate tube filters at 14,000 RPM for 1 minute. The Mono-Q column was equilibrated with Cl^- using: 5 CV of 20 mM Tris-HCl, pH 8.5; 5 CV of 20 mM Tris-HCl, 0.5 M NaCl, pH 8.5; and 5 CV of 20 mM Tris-HCl pH 8.5. The protein was loaded in equilibration buffer at a flow rate of 4 mL/min, then eluted using a gradient from 100% 20 mM Tris-HCl pH 8.5 to 100% 20 mM Tris-HCl, 0.5 M NaCl, pH 8.5 over 20 CV. Eluent was monitored using absorbance at 280 nm. All peaks that appeared red in color were collected and hemoglobin content was confirmed with UV-Vis spectroscopy.

5.1.7 Determination of Protein Concentration

The concentration of hemoglobin in the samples was determined by UV-Vis spectroscopy using a Thermo Scientific Nanodrop 1000 spectrophotometer. The Soret band in the 414-416 nm range for oxy-hemoglobin was used for quantitation ($\epsilon_{414} = 125,000 \text{ M}^{-1} \text{ cm}^{-1}$).¹⁰⁸

5.1.8 Gel Electrophoresis

Purity was estimated by sodium dodecylsulfate polyacrylamide gel electrophoresis (SDS-PAGE) and densitometry. The efficacy of each purification step was determined by SDS-PAGE and only fractions that had the highest level of purity were used for subsequent purification steps. Samples were prepared by incubating approximately 9 μg of protein with 2x Laemmli Sample Buffer (Bio-Rad). The gels used in this study were either produced in-house (stacking: 5% (w/v) polyacrylamide; resolving: 15% (w/v) polyacrylamide) or obtained commercially (Bio-Rad TGX 4-20% (w/v) polyacrylamide). Electrophoresis buffer contained 25 mM Tris-HCl, 250 mM glycine, and 0.1% (w/v) SDS.

Bands were visualized by incubating the gel with a Coomassie Brilliant Blue staining solution (50% (v/v) methanol, 10% (v/v) glacial acetic acid, 0.1% (w/v) Coomassie Brilliant Blue R250) for one or more hours followed by a 1:3:4 glacial acetic acid:methanol:water solution until the gel was sufficiently destained. The percent purity was calculated by densitometry using a Bio-Rad Gel Doc EZ Gel Documentation System.

5.2 Staphylococcus aureus Sortase A

All sortase (Srt) variants used in this study were provided courtesy of the Antos Lab (Western Washington University, Bellingham, WA). These were expressed as either N-terminal or C-terminal His₆ fusions derived from *S. aureus* SrtA and lack the N-terminal 59-residue transmembrane domain (SrtA_{Δ59-Staph}). These enzymes were provided in purified form via Ni-NTA IMAC. The two variants used in this study were either the wild-type SrtA_{Δ59-Staph} or penta-mutant SrtA_{Δ59-Staph}, and their sequences are provided.

Wild-type SrtA_{Δ59-Staph}

```
GSSHHHHHHSSGLVPRGSHMQAKPQIPKDKSKVAGYIEIPDADIKEPVYPGPATPEQL  
NRGVSFAEENESLDDQNISIAGHTFIDRPNYQFTNLKAAKKGSMVYFKVGNETRKYKM  
TSIRDVKPTDVGVLDEQKGKDKQLTLITCDDYNEKTGVWEKRKIFVATEVK
```

Penta-mutant SrtA_{Δ59-Staph}

```
MQAKPQIPKDKSKVAGYIEIPDADIKEPVYPGPATREQLNRGVSFAEENESLDDQNISIA  
GHTFIDRPNYQFTNLKAAKKGSMVYFKVGNETRKYKMTSIRNVKPTAVEVLDEQKGKD  
KQLTLITCDDYNEETGVWETRKIFVATEVKLEHHHHHH
```

5.3 Preparation of Oligopeptide Crosslinkers

5.3.1 Peptide Synthesis

Bifunctional crosslinker peptide was synthesized using manual Fmoc solid phase peptide synthesis (SPPS). An Extract Clean SPE 15 mL reservoir was loaded with 0.2 mmol of Fmoc-protected Rink amide MBHA resin (AnaSpec Inc.). Resin was washed three times with ~10 mL *N*-Methyl-2-pyrrolidone (NMP) and mixed by rocking for 10 minutes. Deprotection was accomplished by incubating resin two times with an 80:20 NMP/piperidine solution at room temperature for approximately 20 minutes with shaking. The piperidine was then removed from the column using pure NMP (3x10 mL, 10 min each). Peptide coupling was achieved by incubation with a solution containing a three-fold molar excess of the Fmoc protected amino acid (Chem-Impex Int'l Inc.), a three-fold excess of 2-(1H-benzotriazol-1-yl)-1,1,3,3-tetramethyluronium hexafluorophosphate (HBTU) (Chem-Impex Int'l Inc.), a five-fold excess of *N,N*-Diisopropylethylamine (DIPEA) (Chem-Impex Int'l Inc.), and approximately 5 mL of NMP. The coupling reaction was incubated for 1 hour or overnight at room temperature with shaking. Coupling was monitored with a Kaiser test, which probes for free-amines. Once a negative result was achieved, the resin was washed (NMP, 3x10 mL, 10 min each), deprotected (80:20 NMP/piperidine, 2x10 mL, 20 min each), and the next amino acid coupled in the same manner as above.

The finished peptide was cleaved from the resin by two-30 minute treatments with approximately 5 mL of 95:2.5:2.5 trifluoroacetic acid (TFA):triisopropyl silane (TIPS):H₂O. The cleaved peptide was concentrated on a rotary evaporator then precipitated from 40 mL of diethyl ether at -80°C. Precipitated peptides were collected by centrifugation and

dried under vacuum for 48 hours. Yield was approximated by weight and ~1 mM stock was made using NMP to dissolve the peptide.

5.3.2 Peptide Modification and Purification

Crude (Fmoc-GGG)₂KK was then conjugated with dibenzylcyclo-octyne (DBCO). The reaction mixtures combined a half molar equivalent of DBCO N-hydroxysuccinimide ester (DBCO-NHS), a three-fold molar excess of DIPEA, and the crude peptide in NMP ($V = 100 \mu\text{L}$, $[\text{peptide}] = \sim 500 \mu\text{M}$). The reaction was monitored by HPLC (Thermo Scientific Dionex UltiMate 3000 chromatography system) and ESI-MS (Advion expression^L CMS). HPLC was performed using a Phenomenex Kinetex 2.6 μm , 100 Å C18 column (2.1 x 100 mm) with MeCN (0.1% TFA)/H₂O (0.1% TFA) as the mobile phase. Flow rate = 0.4 mL/min. Gradient: 0-0.5 min: 10% MeCN (0.1% TFA); 0.5-8 min: linear gradient to 90% MeCN (0.1% TFA); 8-10 min: hold 90% MeCN (0.1% TFA); 10-13 min 10% MeCN (0.1% TFA). Once the peptide modifier was no longer detected, the peptide was deprotected by adding piperidine up to 20% (v/v). Deprotection was monitored by HPLC-MS in the same manner as above. Example mass spectra of these two steps are provided in the Appendix.

Once deprotection was achieved, semi-preparative purification of peptides was performed using a Phenomenex Kinetex 5 μm 100 Å C18 column (10 x 250 mm) fitted with a Phenomenex SecurityGuard SemiPrep Guard cartridge. Flow rate = 4 mL/min. Gradient: 0-0.5 min: 10% MeCN (0.1% TFA); 0.5-8 min: linear gradient to 90% MeCN (0.1% TFA); 8-10 min: hold 90% MeCN (0.1% TFA); 10-13 min 10% MeCN (0.1% TFA) at 10 μL injection volumes. The expected product had a retention time of 7.35 min and

was collected. Product identification and purity were verified by analytical HPLC and ESI-MS (Appendix A). MeCN was removed via rotary evaporation and water was removed via lyophilization. Dehydrated peptide was dissolved in DMSO to a final concentration of 0.1 – 1 mM. Concentrations of peptide were determined by UV-Vis analysis following a 10-fold dilution into water or buffer and using the appropriate molar extinction coefficients (6-FAM: $\lambda_{\max} = 495 \text{ nm}$, $\epsilon_{495} = 75,000 \text{ M}^{-1}\text{cm}^{-1}$; DBCO: $\lambda_{\max} = 308 \text{ nm}$, $\epsilon_{495} = 11,800 \text{ M}^{-1}\text{cm}^{-1}$).

5.4 Sortase-Mediated Ligation Reactions

In general, sortase-mediated crosslinking reactions were performed on an analytical scale (volume = 10-100 μL), unless product purification was intended, in which case reaction volumes were 1 – 10 mL. Reactions were performed in 50 mM Tris, 150 mM NaCl, and 10 mM CaCl_2 (pH 7.5), added via a 10x stock solution. Unless otherwise specified, all references to crosslinking reactions carried out with “SrtA” refers to the penta-mutant SrtA_{Staph}. Stock solution of SrtA were in 50 mM Tris, 150 mM NaCl, pH 7.5 and Hb stock solutions were in 20 mM Tris, pH 8.5. Concentrations of Hb are reported in terms of heme equivalents (assuming one heme per globin subunit).

5.4.1 SML of α -LPETG and GG- α

Reactions had the basic composition of 5 μM SrtA, 50 μM α -LPETG, 50 μM GG- α , and 0 or 200 μM NiSO_4 . The addition order was always consistent: water and buffer were added first, followed by Hb samples, then the reaction was initiated by addition of SrtA. Mixing was achieved by gentle manual flicking after the addition of each component followed by pulse centrifugation in a tabletop microfuge as necessary. Reactions were

carried out in 0.6 mL microcentrifuge tubes without shaking at either room temperature or 37 °C (incubator).

5.4.2 Crosslinking α -LPETG with Peptide Crosslinker

Unless specified otherwise, peptide crosslinking reactions contained 5 μ M SrtA, 50 μ M α -LPETG, 12.5 – 125 μ M crosslinker, and 0 or 200 μ M NiSO₄. These reactions were also 3 – 8% (v/v) DMSO, due to the presence of DMSO in the crosslinker stock solution. Dilutions were made as needed to keep final DMSO concentrations below 10%. Molar equivalents of added crosslinker are reported as ratios to tetrameric Hb ($[\text{Hb}] = \frac{[\text{heme}]}{4}$). Similar to direct crosslinking experiments, reactions were carried out in 0.6 mL microcentrifuge tubes without shaking at either room temperature or 37 °C, and reagent addition order was always consistent: water and buffer were added first, followed by α -LPETG and crosslinker, then the reaction was initiated by addition of SrtA.

5.4.3 Crosslinked Product Purification

In general, product purification was done in a similar manner as described for His-tagged Hbs. A column of Ni-NTA chromatography resin (HisPur, Thermo Scientific) was prepared and equilibrated with 20 mM Tris-HCl, 0.5 M NaCl, 10mM imidazole, pH 8.5. Reactions were purified after incubation for either 90 or 120 min. The crude reaction mixtures were prepared by adding imidazole to a final concentration of 50 μ M using a 1 M stock, then loaded onto the column. The column was then washed with 20 mM Tris-HCl, 0.1 M NaCl, 50 mM imidazole, pH 8.5 until the product band had eluted. The remaining bound protein was eluted with 20 mM Tris-HCl, 0.1 M NaCl, 250 mM imidazole, pH 8.5. Bound and unbound Hb amounts were monitored visually and fractionating was

done by hand. Hb content was determined by absorbance at 414 nm. After fractions were appropriately pooled, the product fraction was concentrated using 4 mL Amicon Centricon concentrators (10k MWCO) to a final concentration of 100 – 400 μ M as determined by UV-Vis. Crosslinked samples were stored at 0 – 4°C (short-term) or -80°C (long-term).

5.4.4 ESI-MS and SDS-PAGE analyses of SML reactions

SDS-PAGE analysis of reactions was performed by removing 5-10 μ L portions of the crude reaction mixture and adding them to the appropriate amount of 2x Laemmli Sample Buffer (Bio-Rad) in order to stop enzymatic activity. Samples were stored at 4°C until all time-point were collected and final loading volume was 10 – 15 μ L. Final loading volumes for other experiments were determined individually based on heme concentrations (4 – 8 μ g final Hb loading). SDS-PAGE was performed using either hand-poured gels (5% stacking, 20% resolving) or TGX 4-20% gradient gels (Bio-Rad). Quantification of band intensities was performed using a Bio-Rad Gel Doc EZ Gel Documentation System. Band intensities were normalized to SrtA for calculation of product conversion, when applicable.

HPLC-MS analysis was performed using a Phenomenex Aeris 3.6 μ m, WIDEPORE C4 200 Å LC column (10 × 2.1 mm) fitted with a Phenomenex SecurityGuard Analytical Guard cartridge. Flow rate = 0.3 mL/min. Gradient: 0-0.5 min: 10% MeCN (0.1% TFA); 0.5-8 min: linear gradient 10% to 90% MeCN (0.1% TFA); 8-10 min: 90% MeCN (0.1% TFA); 10-14 min 10% MeCN (0.1% TFA) at 1 - 3 μ L injection volumes. ESI-MS data was collected using a 500-1800 Da mass range. Averaged mass spectra were generated from the corresponding chromatogram peaks using MNova (MestreLab

Research, Ver 10.0). Reconstructed masses and peak volumes were generated from the averaged mass spectra using the maximum entropy algorithm in Analyst (SCIEX, Ver 1.4).

5.5 Bioorthogonal Ligation Reactions

5.5.1 6-FAM Azide Conjugation

These conjugation reactions were prepared by adding a three-fold molar excess of the azide reagent relative to tetrameric hemoglobin concentrations (assuming one molar equivalent of DBCO per Hb tetramer). Diluted stock solutions of 6-FAM azide (Lumiprobe Life Science Solutions) were prepared to 1 mM in DMSO and added to 0.6 mL microcentrifuge tubes containing 20 – 50 μ L of sample. Final concentrations of Hb samples were 50 – 200 μ M in heme. Reactions were incubated at room temperature for 30 minutes to 2 hours. SDS-PAGE samples were prepared as described in Section 5.4.4. Analysis by ESI-MS was performed using the same method as described in Section 5.4.4 and excess 6-FAM azide was removed prior to HPLC separation using 0.5 – 3 mL dialysis cassettes (Slide-A-Lyzer 10K MWCO, ThermoFisher Scientific).

5.5.2 PEG-Azide Conjugation

1,17-Diazido-2,6,9,12,15-pentaoxaheptadecane (Azido-PEG5-azide), was obtained from Sigma-Aldrich. A 10 mM (v/v) stock solution of the oily liquid was made by dilution with DMSO and additional stocks were made as needed to keep final volume of the linker added to coupling reactions within the range of 1-10 μ L. The final total volume of DMSO was kept constant in every set of experiments. Final Hb concentrations were 40 – 300 μ M in heme (10 – 75 μ M Hb). Reactions were incubated at room temperature

or 37°C for 1 – 3 hours. SDS-PAGE samples were prepared as described in Section 5.4.4. 4-ARM PEG azide was obtained from Creative PEGWorks. Coupling reactions were carried out in the same manner for Azido-PEG5-azide, except stock solutions were made with water rather than DMSO.

Literature Cited

- [1] AuBuchon, J. P., Birkmeyer, J. D., and Busch, M. P. (1997) Safety of the blood supply in the United States: opportunities and controversies, *Annals of internal medicine* 127, 904-909.
- [2] McCullough, J. (2003) Progress Toward a Pathogen-Free Blood Supply, *Clinical Infectious Diseases* 37, 88-95.
- [3] Chen, J. Y., Scerbo, M., and Kramer, G. (2009) A review of blood substitutes: examining the history, clinical trial results, and ethics of hemoglobin-based oxygen carriers, *Clinics (Sao Paulo)* 64, 803-813.
- [4] Stramer, S. L., Linnen, J. M., Carrick, J. M., Foster, G. A., Krysztof, D. E., Zou, S., Dodd, R. Y., Tirado-Marrero, L. M., Hunsperger, E., Santiago, G. A., Munoz-Jordan, J. L., and Tomashek, K. M. (2012) Dengue viremia in blood donors identified by RNA and detection of dengue transfusion transmission during the 2007 dengue outbreak in Puerto Rico, *Transfusion* 52, 1657-1666.
- [5] Snyder, E. L., Stramer, S. L., and Benjamin, R. J. (2015) The safety of the blood supply--time to raise the bar, *The New England journal of medicine* 372, 1882-1885.
- [6] Vincent, J. L., Baron, J. F., Reinhart, K., Gattinoni, L., Thijs, L., Webb, A., Meier-Hellmann, A., Nollet, G., and Peres-Bota, D. (2002) Anemia and blood transfusion in critically ill patients, *Jama* 288, 1499-1507.
- [7] Zallen, G., Offner, P. J., Moore, E. E., Blackwell, J., Ciesla, D. J., Gabriel, J., Denny, C., and Silliman, C. C. (1999) Age of transfused blood is an independent risk factor for postinjury multiple organ failure, *American journal of surgery* 178, 570-572.
- [8] Moore, F. A., Moore, E. E., and Sauaia, A. (1997) Blood transfusion. An independent risk factor for postinjury multiple organ failure, *Archives of surgery (Chicago, Ill. : 1960)* 132, 620-624; discussion 624-625.
- [9] Taylor, R. W., O'Brien, J., Trottier, S. J., Manganaro, L., Cytron, M., Lesko, M. F., Arnzen, K., Cappadoro, C., Fu, M., Plisco, M. S., Sadaka, F. G., and Veremakis, C. (2006) Red blood cell transfusions and nosocomial infections in critically ill patients, *Crit Care Med* 34, 2302-2308; quiz 2309.
- [10] Toner, R. W., Pizzi, L., Leas, B., Ballas, S. K., Quigley, A., and Goldfarb, N. I. (2011) Costs to hospitals of acquiring and processing blood in the US: a survey of hospital-based blood banks and transfusion services, *Applied health economics and health policy* 9, 29-37.
- [11] Cremieux, P. Y., Barrett, B., Anderson, K., and Slavin, M. B. (2000) Cost of outpatient blood transfusion in cancer patients, *Journal of clinical oncology : official journal of the American Society of Clinical Oncology* 18, 2755-2761.

- [12] Etchason, J., Petz, L., Keeler, E., Calhoun, L., Kleinman, S., Snider, C., Fink, A., and Brook, R. (1995) The cost effectiveness of preoperative autologous blood donations, *The New England journal of medicine* 332, 719-724.
- [13] Cantor, S. B., Hudson, D. V., Jr., Lichtiger, B., and Rubenstein, E. B. (1998) Costs of blood transfusion: a process-flow analysis, *Journal of clinical oncology : official journal of the American Society of Clinical Oncology* 16, 2364-2370.
- [14] Denton, T. A., Diamond, G. A., Matloff, J. M., and Gray, R. J. (1994) Anemia therapy: individual benefit and societal cost, *Semin Oncol* 21, 29-35.
- [15] Vamvakas, E. C., and Carven, J. H. (1998) Allogeneic blood transfusion, hospital charges, and length of hospitalization: a study of 487 consecutive patients undergoing colorectal cancer resection, *Archives of pathology & laboratory medicine* 122, 145-151.
- [16] Shander, A., Hofmann, A., Gombotz, H., Theusinger, O. M., and Spahn, D. R. (2007) Estimating the cost of blood: past, present, and future directions, *Best practice & research. Clinical anaesthesiology* 21, 271-289.
- [17] Riess, J. G. (2001) Oxygen carriers ("blood substitutes")--raison d'etre, chemistry, and some physiology, *Chem Rev* 101, 2797-2920.
- [18] Whitaker, B. I. (2011) The 2011 National Blood Collection and Utilization Survey Report, p 98, US Department of Health and Human Services, Bethesda, Maryland.
- [19] Greenspan, J. S., Wolfson, M. R., and Shaffer, T. H. (2000) Liquid ventilation, *Semin Perinatol* 24, 396-405.
- [20] Spahn, D. R. (1999) Blood substitutes. Artificial oxygen carriers: perfluorocarbon emulsions, *Crit Care* 3, R93-97.
- [21] Lowe, K. C. (2006) Blood substitutes: from chemistry to clinic, *Journal of Materials Chemistry* 16, 4189-4196.
- [22] Sanders, K. E., Ackers, G., and Sligar, S. (1996) Engineering and design of blood substitutes, *Curr Opin Struct Biol* 6, 534-540.
- [23] Moradi, S., Jahanian-Najafabadi, A., and Roudkenar, M. H. (2016) Artificial Blood Substitutes: First Steps on the Long Route to Clinical Utility, *Clinical medicine insights. Blood disorders* 9, 33-41.
- [24] Patton, J. N., and Palmer, A. F. (2005) Photopolymerization of Bovine Hemoglobin Entrapped Nanoscale Hydrogel Particles within Liposomal Reactors for Use as an Artificial Blood Substitute, *Biomacromolecules* 6, 414-424.
- [25] Rameez, S., Alost, H., and Palmer, A. F. (2008) Biocompatible and biodegradable polymersome encapsulated hemoglobin: a potential oxygen carrier, *Bioconjug Chem* 19, 1025-1032.
- [26] Urbaitis, B. K., Razynska, A., Corteza, Q., Fronticelli, C., and Bucci, E. (1991) Intravascular retention and renal handling of purified natural and intramolecularly

- cross-linked hemoglobins, *The Journal of laboratory and clinical medicine* 117, 115-121.
- [27] Meng, F., Kassa, T., Jana, S., Wood, F., Zhang, X., Jia, Y., D'Agnillo, F., and Alayash, A. I. (2018) Comprehensive Biochemical and Biophysical Characterization of Hemoglobin-Based Oxygen Carrier Therapeutics: All HBOCs Are Not Created Equally, *Bioconjug Chem*.
- [28] Hoffman, S. J., Looker, D. L., Roehrich, J. M., Cozart, P. E., Durfee, S. L., Tedesco, J. L., and Stetler, G. L. (1990) Expression of fully functional tetrameric human hemoglobin in *Escherichia coli*, *Proc Natl Acad Sci U S A* 87, 8521-8525.
- [29] Garrioch, M. A., McClure, J. H., and Wildsmith, J. A. (1999) Haemodynamic effects of diaspirin crosslinked haemoglobin (DCLHb) given before abdominal aortic aneurysm surgery, *British journal of anaesthesia* 83, 702-707.
- [30] Freilich, D., Pearce, L. B., Pitman, A., Greenburg, G., Berzins, M., Bebris, L., Ahlers, S., and McCarron, R. (2009) HBOC-201 vasoactivity in a phase III clinical trial in orthopedic surgery subjects--extrapolation of potential risk for acute trauma trials, *The Journal of trauma* 66, 365-376.
- [31] Sloan, E. P., Koenigsberg, M., Clark, J. M., Weir, W. B., and Philbin, N. (2014) Shock index and prediction of traumatic hemorrhagic shock 28-day mortality: data from the DCLHb resuscitation clinical trials, *The western journal of emergency medicine* 15, 795-802.
- [32] Sloan, E. P., Koenigsberg, M., Gens, D., Cipolle, M., Runge, J., Mallory, M. N., and Rodman, G., Jr. (1999) Diaspirin cross-linked hemoglobin (DCLHb) in the treatment of severe traumatic hemorrhagic shock: a randomized controlled efficacy trial, *Jama* 282, 1857-1864.
- [33] Olofsson, C. I., Gorecki, A. Z., Dirksen, R., Kofranek, I., Majewski, J. A., Mazurkiewicz, T., Jahoda, D., Fagrell, B., Keipert, P. E., Hardiman, Y. J., and Levy, H. (2011) Evaluation of MP4OX for prevention of perioperative hypotension in patients undergoing primary hip arthroplasty with spinal anesthesia: a randomized, double-blind, multicenter study, *Anesthesiology* 114, 1048-1063.
- [34] Kinasewitz, G. T., Privalle, C. T., Imm, A., Steingrub, J. S., Malcynski, J. T., Balk, R. A., and DeAngelo, J. (2008) Multicenter, randomized, placebo-controlled study of the nitric oxide scavenger pyridoxalated hemoglobin polyoxyethylene in distributive shock, *Crit Care Med* 36, 1999-2007.
- [35] Vincent, J. L., Privalle, C. T., Singer, M., Lorente, J. A., Boehm, E., Meier-Hellmann, A., Darius, H., Ferrer, R., Sirvent, J. M., Marx, G., and DeAngelo, J. (2015) Multicenter, randomized, placebo-controlled phase III study of pyridoxalated hemoglobin polyoxyethylene in distributive shock (PHOENIX), *Crit Care Med* 43, 57-64.
- [36] Sloan, E. P., Koenigsberg, M., Weir, W. B., Clark, J. M., O'Connor, R., Olinger, M., and Cydulka, R. (2015) Emergency Resuscitation of Patients Enrolled in the US

Diaspirin Cross-linked Hemoglobin (DCLHb) Clinical Efficacy Trial, *Prehospital and disaster medicine* 30, 54-61.

- [37] Jahr, J. S., Mackenzie, C., Pearce, L. B., Pitman, A., and Greenburg, A. G. (2008) HBOC-201 as an alternative to blood transfusion: efficacy and safety evaluation in a multicenter phase III trial in elective orthopedic surgery, *The Journal of trauma* 64, 1484-1497.
- [38] Gould, S. A., Moore, E. E., Hoyt, D. B., Ness, P. M., Norris, E. J., Carson, J. L., Hides, G. A., Freeman, I. H., DeWoskin, R., and Moss, G. S. (2002) The life-sustaining capacity of human polymerized hemoglobin when red cells might be unavailable, *J Am Coll Surg* 195, 445-452; discussion 452-445.
- [39] Gould, S. A., Moore, E. E., Hoyt, D. B., Burch, J. M., Haenel, J. B., Garcia, J., DeWoskin, R., and Moss, G. S. (1998) The first randomized trial of human polymerized hemoglobin as a blood substitute in acute trauma and emergent surgery, *J Am Coll Surg* 187, 113-120; discussion 120-112.
- [40] Greenburg, A. G., and Kim, H. W. (2004) Use of an oxygen therapeutic as an adjunct to intraoperative autologous donation to reduce transfusion requirements in patients undergoing coronary artery bypass graft surgery, *J Am Coll Surg* 198, 373-383; discussion 384-375.
- [41] Hill, S. E., Gottschalk, L. I., and Grichnik, K. (2002) Safety and preliminary efficacy of hemoglobin raffimer for patients undergoing coronary artery bypass surgery, *J Cardiothorac Vasc Anesth* 16, 695-702.
- [42] D'Agnillo, F., and Alayash, A. I. (2000) Site-specific modifications and toxicity of blood substitutes. The case of diaspirin cross-linked hemoglobin, *Advanced drug delivery reviews* 40, 199-212.
- [43] Nelson, D., Azari, M., Brown, R., Burhop, K., Bush, S., Catarello, J., Chuang, H., Downing, C., Estep, T., Loewen, A., and et al. (1992) Preparation and characterization of diaspirin cross-linked hemoglobin solutions for preclinical studies, *Biomaterials, artificial cells, and immobilization biotechnology : official journal of the International Society for Artificial Cells and Immobilization Biotechnology* 20, 423-427.
- [44] Hayes, J. K., Stanley, T. H., Lind, G. H., East, K., Smith, B., and Kessler, K. (2001) A double-blind study to evaluate the safety of recombinant human hemoglobin in surgical patients during general anesthesia, *J Cardiothorac Vasc Anesth* 15, 593-602.
- [45] Malhotra, A. K., Kelly, M. E., Miller, P. R., Hartman, J. C., Fabian, T. C., and Proctor, K. G. (2003) Resuscitation with a novel hemoglobin-based oxygen carrier in a Swine model of uncontrolled perioperative hemorrhage, *The Journal of trauma* 54, 915-924.
- [46] Marquardt, D. A., Doyle, M. P., Davidson, J. S., Epp, J. K., Aitken, J. F., Lemon, D. D., and Anthony-Cahill, S. J. (2012) Monodisperse 130 kDa and 260 kDa

Recombinant Human Hemoglobin Polymers as Scaffolds for Protein Engineering of Hemoglobin-Based Oxygen Carriers, *J Funct Biomater* 3, 61-78.

- [47] Winslow, R. M. (2004) MP4, a new nonvasoactive polyethylene glycol-hemoglobin conjugate, *Artificial organs* 28, 800-806.
- [48] Jahr, J. S., Moallempour, M., and Lim, J. C. (2008) HBOC-201, hemoglobin glutamer-250 (bovine), Hemopure (Biopure Corporation), *Expert opinion on biological therapy* 8, 1425-1433.
- [49] Natanson, C., Kern, S. J., Lurie, P., Banks, S. M., and Wolfe, S. M. (2008) Cell-free hemoglobin-based blood substitutes and risk of myocardial infarction and death: a meta-analysis, *Jama* 299, 2304-2312.
- [50] Weiskopf, R. B. (2010) Hemoglobin-based oxygen carriers: compassionate use and compassionate clinical trials, *Anesthesia and analgesia* 110, 659-662.
- [51] Alayash, A. I. (2010) Setbacks in blood substitutes research and development: a biochemical perspective, *Clinics in laboratory medicine* 30, 381-389.
- [52] Stowell, C. P., Levin, J., Spiess, B. D., and Winslow, R. M. (2001) Progress in the development of RBC substitutes, *Transfusion* 41, 287-299.
- [53] Alayash, A. I. (2014) Blood substitutes: why haven't we been more successful?, *Trends in biotechnology* 32, 177-185.
- [54] De Caterina, R., Libby, P., Peng, H. B., Thannickal, V. J., Rajavashisth, T. B., Gimbrone, M. A., Shin, W. S., and Liao, J. K. (1995) Nitric oxide decreases cytokine-induced endothelial activation. Nitric oxide selectively reduces endothelial expression of adhesion molecules and proinflammatory cytokines, *Journal of Clinical Investigation* 96, 60-68.
- [55] Alayash, A. I. (2017) Hemoglobin-Based Blood Substitutes and the Treatment of Sickle Cell Disease: More Harm than Help?, *Biomolecules* 7, 2.
- [56] Minneci, P. C., Deans, K. J., Zhi, H., Yuen, P. S., Star, R. A., Banks, S. M., Schechter, A. N., Natanson, C., Gladwin, M. T., and Solomon, S. B. (2005) Hemolysis-associated endothelial dysfunction mediated by accelerated NO inactivation by decompartmentalized oxyhemoglobin, *The Journal of clinical investigation* 115, 3409-3417.
- [57] Zhou, Y., Cabrales, P., and Palmer, A. F. (2012) Simulation of NO and O₂ transport facilitated by polymerized hemoglobin solutions in an arteriole that takes into account wall shear stress-induced NO production, *Biophysical chemistry* 162, 45-60.
- [58] Chen, K., Pittman, R. N., and Popel, A. S. (2008) Nitric oxide in the vasculature: where does it come from and where does it go? A quantitative perspective, *Antioxidants & redox signaling* 10, 1185-1198.
- [59] Eich, R. F., Li, T., Lemon, D. D., Doherty, D. H., Curry, S. R., Aitken, J. F., Mathews, A. J., Johnson, K. A., Smith, R. D., Phillips, G. N., Jr., and Olson, J. S. (1996)

- Mechanism of NO-induced oxidation of myoglobin and hemoglobin, *Biochemistry* 35, 6976-6983.
- [60] Liu, X., Miller, M. J., Joshi, M. S., Sadowska-Krowicka, H., Clark, D. A., and Lancaster, J. R., Jr. (1998) Diffusion-limited reaction of free nitric oxide with erythrocytes, *J Biol Chem* 273, 18709-18713.
- [61] Kim, H. W., and Greenburg, A. G. (2004) Artificial oxygen carriers as red blood cell substitutes: a selected review and current status, *Artificial organs* 28, 813-828.
- [62] Doyle, M. P., Apostol, I., and Kerwin, B. A. (1999) Glutaraldehyde modification of recombinant human hemoglobin alters its hemodynamic properties, *J Biol Chem* 274, 2583-2591.
- [63] Rippe, B., and Haraldsson, B. (1994) Transport of macromolecules across microvascular walls: the two-pore theory, *Physiological reviews* 74, 163-219.
- [64] Alayash, A. I. (2004) Oxygen therapeutics: can we tame haemoglobin?, *Nature reviews. Drug discovery* 3, 152-159.
- [65] Goldsmith, H. L., Cokelet, G. R., and Gaehtgens, P. (1989) Robin Fahraeus: evolution of his concepts in cardiovascular physiology, *The American journal of physiology* 257, H1005-1015.
- [66] Fedosov, D. A., Caswell, B., Popel, A. S., and Karniadakis, G. E. (2010) Blood Flow and Cell-Free Layer in Microvessels, *Microcirculation (New York, N.Y. : 1994)* 17, 615-628.
- [67] Liao, J. C., Hein, T. W., Vaughn, M. W., Huang, K. T., and Kuo, L. (1999) Intravascular flow decreases erythrocyte consumption of nitric oxide, *Proc Natl Acad Sci U S A* 96, 8757-8761.
- [68] Buehler, P. W., Zhou, Y., Cabrales, P., Jia, Y., Sun, G., Harris, D. R., Tsai, A. G., Intaglietta, M., and Palmer, A. F. (2010) Synthesis, biophysical properties and pharmacokinetics of ultrahigh molecular weight tense and relaxed state polymerized bovine hemoglobins, *Biomaterials* 31, 3723-3735.
- [69] Matheson, B., Kwansa, H. E., Bucci, E., Rebel, A., and Koehler, R. C. (2002) Vascular response to infusions of a nonextravasating hemoglobin polymer, *J Appl Physiol (1985)* 93, 1479-1486.
- [70] Caparrotta, T. M., and Evans, M. (2014) PEGylated insulin Lispro, (LY2605541)--a new basal insulin analogue, *Diabetes, obesity & metabolism* 16, 388-395.
- [71] Jevsevar, S., Kunstelj, M., and Porekar, V. G. (2010) PEGylation of therapeutic proteins, *Biotechnology journal* 5, 113-128.
- [72] Ducry, L., and Stump, B. (2010) Antibody-drug conjugates: linking cytotoxic payloads to monoclonal antibodies, *Bioconjug Chem* 21, 5-13.
- [73] Adamson, J. G., Bonaventura, J. B., Er, S. S., Jones, R. T., Langlois, S. F., MacDonald, I. D., Moore, C., Pliura, D. H., Rydall, J. R., Wicks, D. G., Wiffen, D. E., Wojciechowski, P. W., and Wong, L. T. (1998) Production, Characterization,

- and Clinical Evaluation of Hemolink, an Oxidized Raffinose Cross-Linked Hemoglobin-Based Blood Substitute, In *Red blood cell substitutes : basic principles and clinical applications* (Rudolph, A. S., Rabinovici, R., and Feuerstein, G. Z., Eds.), pp 335-351, M. Dekker, New York.
- [74] Boykins, R. A., Buehler, P. W., Jia, Y., Venable, R., and Alayash, A. I. (2005) O-raffinose crosslinked hemoglobin lacks site-specific chemistry in the central cavity: structural and functional consequences of beta93Cys modification, *Proteins* 59, 840-855.
- [75] Mullard, A. (2013) Maturing antibody-drug conjugate pipeline hits 30, *Nature reviews. Drug discovery* 12, 329-332.
- [76] Boswell, C. A., Mundo, E. E., Zhang, C., Bumbaca, D., Valle, N. R., Kozak, K. R., Fourie, A., Chuh, J., Koppada, N., Saad, O., Gill, H., Shen, B. Q., Rubinfeld, B., Tibbitts, J., Kaur, S., Theil, F. P., Fielder, P. J., Khawli, L. A., and Lin, K. (2011) Impact of drug conjugation on pharmacokinetics and tissue distribution of anti-STEAP1 antibody-drug conjugates in rats, *Bioconjug Chem* 22, 1994-2004.
- [77] Behrens, C. R., Ha, E. H., Chinn, L. L., Bowers, S., Probst, G., Fitch-Bruhns, M., Monteon, J., Valdiosera, A., Bermudez, A., Liao-Chan, S., Wong, T., Melnick, J., Theunissen, J. W., Flory, M. R., Houser, D., Venstrom, K., Levashova, Z., Sauer, P., Migone, T. S., van der Horst, E. H., Halcomb, R. L., and Jackson, D. Y. (2015) Antibody-Drug Conjugates (ADCs) Derived from Interchain Cysteine Cross-Linking Demonstrate Improved Homogeneity and Other Pharmacological Properties over Conventional Heterogeneous ADCs, *Mol Pharm* 12, 3986-3998.
- [78] Wals, K., and Ovaa, H. (2014) Unnatural amino acid incorporation in E. coli: current and future applications in the design of therapeutic proteins, *Front Chem* 2, 15.
- [79] Rashidian, M., Dozier, J. K., and Distefano, M. D. (2013) Enzymatic labeling of proteins: techniques and approaches, *Bioconjug Chem* 24, 1277-1294.
- [80] Chen, I., Howarth, M., Lin, W., and Ting, A. Y. (2005) Site-specific labeling of cell surface proteins with biophysical probes using biotin ligase, *Nature methods* 2, 99-104.
- [81] Mao, H., Hart, S. A., Schink, A., and Pollok, B. A. (2004) Sortase-mediated protein ligation: a new method for protein engineering, *J Am Chem Soc* 126, 2670-2671.
- [82] Spirig, T., Weiner, E. M., and Clubb, R. T. (2011) Sortase enzymes in Gram-positive bacteria, *Molecular microbiology* 82, 1044-1059.
- [83] Chen, I., Dorr, B. M., and Liu, D. R. (2011) A general strategy for the evolution of bond-forming enzymes using yeast display, *Proc Natl Acad Sci U S A* 108, 11399-11404.
- [84] Hirakawa, H., Ishikawa, S., and Nagamune, T. (2012) Design of Ca²⁺-independent Staphylococcus aureus sortase A mutants, *Biotechnology and bioengineering* 109, 2955-2961.

- [85] Yamamura, Y., Hirakawa, H., Yamaguchi, S., and Nagamune, T. (2011) Enhancement of sortase A-mediated protein ligation by inducing a β -hairpin structure around the ligation site, *Chemical Communications* 47, 4742-4744.
- [86] Liu, F., Luo, E. Y., Flora, D. B., and Mezo, A. R. (2014) Irreversible sortase A-mediated ligation driven by diketopiperazine formation, *The Journal of organic chemistry* 79, 487-492.
- [87] Row, R. D., Roark, T. J., Philip, M. C., Perkins, L. L., and Antos, J. M. (2015) Enhancing the efficiency of sortase-mediated ligations through nickel-peptide complex formation, *Chem Commun (Camb)* 51, 12548-12551.
- [88] Amer, B. R., Macdonald, R., Jacobitz, A. W., Liauw, B., and Clubb, R. T. (2016) Rapid addition of unlabeled silent solubility tags to proteins using a new substrate-fused sortase reagent, *Journal of biomolecular NMR* 64, 197-205.
- [89] Meldal, M., and Schoffelen, S. (2016) Recent advances in covalent, site-specific protein immobilization, *F1000Research* 5, F1000 Faculty Rev-2303.
- [90] Fang, T., Duarte, J. N., Ling, J., Li, Z., Guzman, J. S., and Ploegh, H. L. (2016) Structurally Defined alphaMHC-II Nanobody-Drug Conjugates: A Therapeutic and Imaging System for B-Cell Lymphoma, *Angewandte Chemie (International ed. in English)* 55, 2416-2420.
- [91] Asmundson, A. L., Taber, A. M., van der Walde, A., Lin, D. H., Olson, J. S., and Anthony-Cahill, S. J. (2009) Coexpression of human alpha- and circularly permuted beta-globins yields a hemoglobin with normal R state but modified T state properties, *Biochemistry* 48, 5456-5465.
- [92] Viappiani, C., Abbruzzetti, S., Ronda, L., Bettati, S., Henry, E. R., Mozzarelli, A., and Eaton, W. A. (2014) Experimental basis for a new allosteric model for multisubunit proteins, *Proc Natl Acad Sci U S A* 111, 12758-12763.
- [93] Antos, J. M., Popp, M. W., Ernst, R., Chew, G. L., Spooner, E., and Ploegh, H. L. (2009) A straight path to circular proteins, *J Biol Chem* 284, 16028-16036.
- [94] Ton-That, H., Mazmanian, S. K., Faull, K. F., and Schneewind, O. (2000) Anchoring of surface proteins to the cell wall of *Staphylococcus aureus*. Sortase catalyzed in vitro transpeptidation reaction using LPXTG peptide and NH(2)-Gly(3) substrates, *J Biol Chem* 275, 9876-9881.
- [95] Mohlmann, S., Mahlert, C., Greven, S., Scholz, P., and Harrenga, A. (2011) In vitro sortagging of an antibody fab fragment: overcoming unproductive reactions of sortase with water and lysine side chains, *Chembiochem* 12, 1774-1780.
- [96] Heck, T., Pham, P.-H., Yerlikaya, A., Thöny-Meyer, L., and Richter, M. (2014) Sortase A catalyzed reaction pathways: a comparative study with six SrtA variants, *Catalysis Science & Technology* 4, 2946-2956.
- [97] Pickens, C. J., Johnson, S. N., Pressnall, M. M., Leon, M. A., and Berkland, C. J. (2018) Practical Considerations, Challenges, and Limitations of Bioconjugation via Azide-Alkyne Cycloaddition, *Bioconjug Chem* 29, 686-701.

- [98] Mu, Q., Hu, T., and Yu, J. (2013) Molecular insight into the steric shielding effect of PEG on the conjugated staphylokinase: biochemical characterization and molecular dynamics simulation, *PLoS one* 8, e68559.
- [99] Xie, J., Wang, J., Chen, H., Shen, W., Sinko, P. J., Dong, H., Zhao, R., Lu, Y., Zhu, Y., and Jia, L. (2015) Multivalent Conjugation of Antibody to Dendrimers for the Enhanced Capture and Regulation on Colon Cancer Cells, *Scientific Reports* 5, 9445.
- [100] Astruc, D., Boisselier, E., and Ornelas, C. (2010) Dendrimers Designed for Functions: From Physical, Photophysical, and Supramolecular Properties to Applications in Sensing, Catalysis, Molecular Electronics, Photonics, and Nanomedicine, *Chemical Reviews* 110, 1857-1959.
- [101] Zhang, C., Dai, P., Vinogradov, A. A., Gates, Z. P., and Pentelute, B. L. (2018) Site-Selective Cysteine–Cyclooctyne Conjugation, *Angewandte Chemie International Edition* 57, 6459-6463.
- [102] Alayash, A. I., and Cashion, R. E. (1995) Hemoglobin and free radicals: implications for the development of a safe blood substitute, *Molecular medicine today* 1, 122-127.
- [103] Nair, D. P., Podgórski, M., Chatani, S., Gong, T., Xi, W., Fenoli, C. R., and Bowman, C. N. (2014) The Thiol-Michael Addition Click Reaction: A Powerful and Widely Used Tool in Materials Chemistry, *Chemistry of Materials* 26, 724-744.
- [104] Popp, M. W., Antos, J. M., Grotenbreg, G. M., Spooner, E., and Ploegh, H. L. (2007) Sortagging: a versatile method for protein labeling, *Nature chemical biology* 3, 707-708.
- [105] Witte, M. D., Cragolini, J. J., Dougan, S. K., Yoder, N. C., Popp, M. W., and Ploegh, H. L. (2012) Preparation of unnatural N-to-N and C-to-C protein fusions, *Proceedings of the National Academy of Sciences* 109, 11993-11998.
- [106] Weickert, M. J., Pagratis, M., Glascock, C. B., and Blackmore, R. (1999) A mutation that improves soluble recombinant hemoglobin accumulation in *Escherichia coli* in heme excess, *Appl Environ Microbiol* 65, 640-647.
- [107] Graves, P. E., Henderson, D. P., Horstman, M. J., Solomon, B. J., and Olson, J. S. (2008) Enhancing stability and expression of recombinant human hemoglobin in *E. coli*: Progress in the development of a recombinant HBOC source, *Biochim Biophys Acta* 1784, 1471-1479.
- [108] Di Iorio, E. E. (1981) Preparation of derivatives of ferrous and ferric hemoglobin, *Methods Enzymol* 76, 57-72.

Appendix

Optimized gene sequence for α -LPETG

GGATCCGAGCTGTTGACAATTAATCATCGGCTCGTATAATGTGTGGAATTGTGAGCGGATAACAATTTCA
CTAAGGAGGTTAATTAATGCTGAGCCCGGCGGACAAGACCAACGTGAAAGCGGCGTGGGCGAAGGTTGGT
GCGCATGCGGGCGAGTATGGTGC GGAGGCGCTGGAACGTATGTTCCCTGAGCTTTCGACCACCAAGACCT
ATTTCCCGCACTTTGACCTGAGCCACGGCAGCGCGCAGGTGAAAGGTCACGGCAAGAAAGTTGCGGATGC
GCTGACCAACGCGGTGGCGCACGTTGACGATATGCCGAACGCGCTGAGCGCGCTGAGCGACCTGCACGCG
CACAAGCTGCGTGTGGACCCGGTTAACTTCAAACCTGCTGAGCCACTGCCTGCTGGTGACCCTGGCGGCGC
ACCTGCCGGCGGAGTTCACCCCGGCGGTTACGCGAGCCTGGATAAGTTTCTGGCGAGCGTGAGCACCGT
TCTGACCAGCAAATATCGTGGTGGCGGTGGCAGCGGTGGCGGTGGCAGCCTGCCGAAACCGGTGGCCAC
CACCACCACCACCTAATAACTGCAG

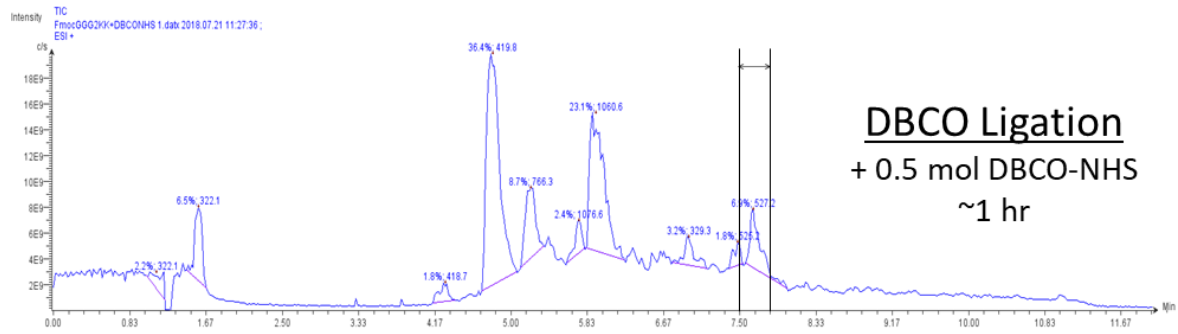
Optimized gene sequence for GG- α

GGATCCGAGCTGTTGACAATTAATCATCGGCTCGTATAATGTGTGGAATTGTGAGCGGATAACAATTTCA
CTAAGGAGGTTAATTAATGGGTGGCGGTGGCAGCGGTGGCGGTGGCAGCCTGAGCCCGGCGGACAAGACC
AACGTGAAAGCGGCGTGGGCGAAGGTTGGTGC GCATGCGGGCGAGTATGGTGC GGAGGCGCTGGAACGTA
TGTTCCCTGAGCTTTCGACCACCAAGACCTATTTCCCGCACTTTGACCTGAGCCACGGCAGCGCGCAGGT
GAAAGGTCACGGCAAGAAAGTTGCGGATGCGCTGACCAACGCGGTGGCGCACGTTGACGATATGCCGAAC
GCGCTGAGCGCGCTGAGCGACCTGCACGCGCACAAGCTGCGTGTGGACCCGGTTAACTTCAAACCTGCTGA
GCCACTGCCTGCTGGTGACCCTGGCGGCGCACCTGCCGGCGGAGTTCACCCCGGCGGTTACGCGAGCCT
GGATAAGTTTCTGGCGAGCGTGAGCACCGTTCTGACCAGCAAATACCGTTAATAACTGCAG

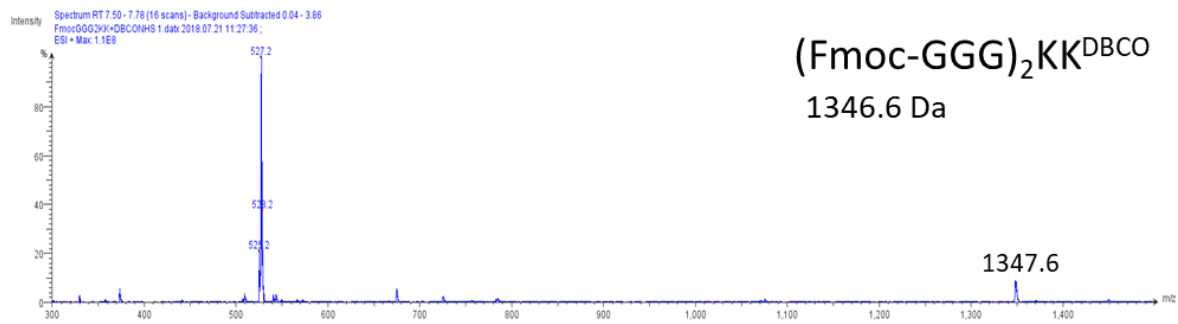
Optimized gene sequence for wt β

CTGCAGTAAGGAGGTAATATATGGTTCACCTGACCCCGGAGGAAAAGAGCGCGGTGACCGCGCTGTGGGC
GAAAGTGAACGTTGACGAGGTTGGTGGCGAAGCGCTGGGTCGTCTGCTGGTTGTGTACCCGTGGACCCAG
CGTTTCTTTGAGAGCTTCGGTGACCTGAGCACCCCGGATGCGGTTATGGGTAACCCGAAGGTGAAAGCGC
ACGGTAAGAAAGTTCTGGGCGCGTTCAGCGATGGTCTGGCGCACCTGGACAACCTGGATGGCACCTTTGC
GACCCTGAGCGAGCTGCACTGCGACAACTGCACGTGGATCCGGAAAACCTTTCGTCTGCTGGGCAACGTG
CTGGTTTTCGTGCTGGCGATCCACTTCGGCAAGGAATTTACCCCGCGGTTTCAGGCGGCGTACCAAAAAG
TTGTTGCGGGTGTGGCGAACGCGCTGGCGCACAAGTATCACTAATAAAGCTT

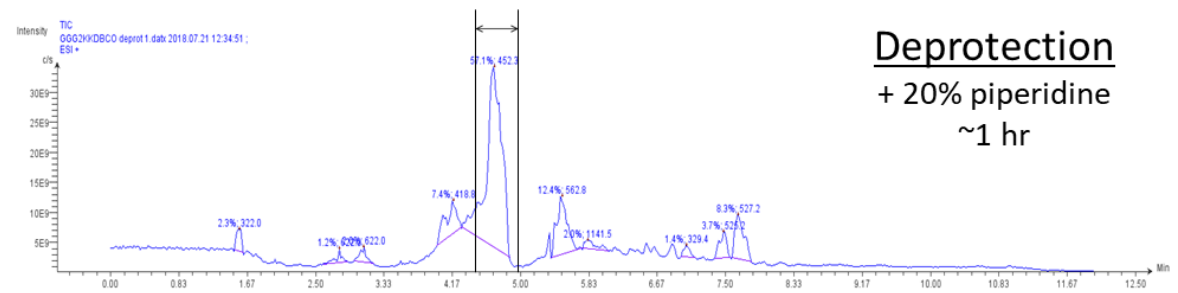
Example total ion chromatogram and mass spectra (of indicated area) from (GGG)₂KK modification with DBCO-NHS.



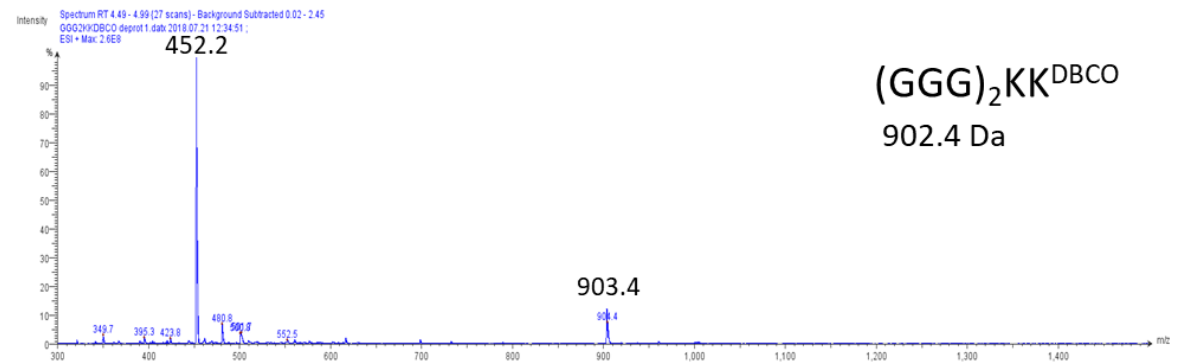
DBCO Ligation
+ 0.5 mol DBCO-NHS
~1 hr



(Fmoc-GGG)₂KK^{DBCO}
1346.6 Da



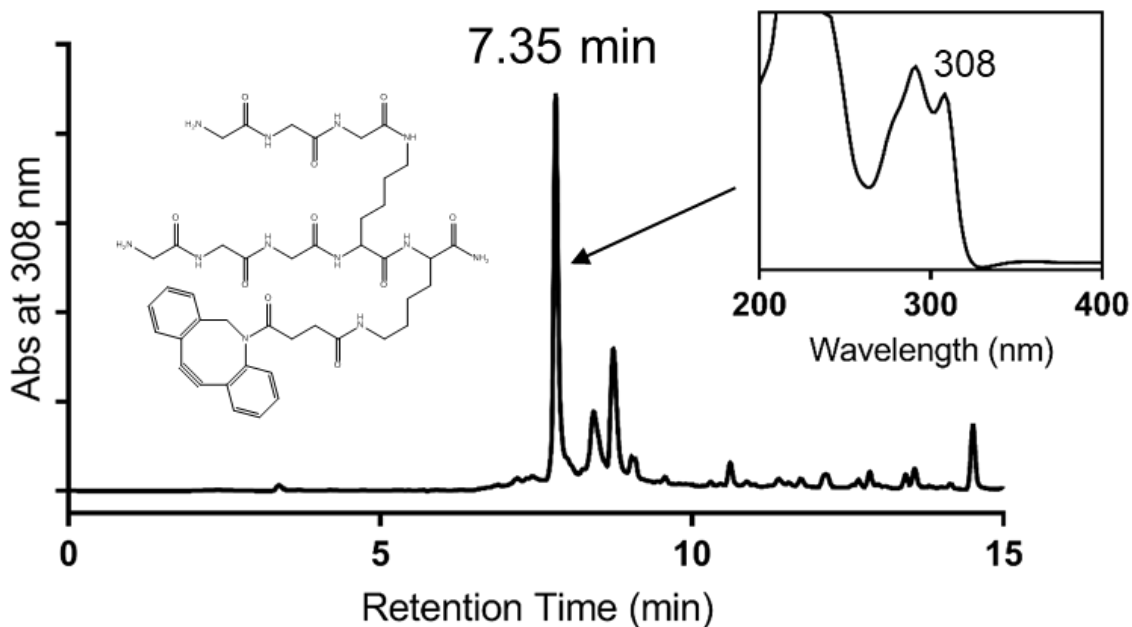
Deprotection
+ 20% piperidine
~1 hr



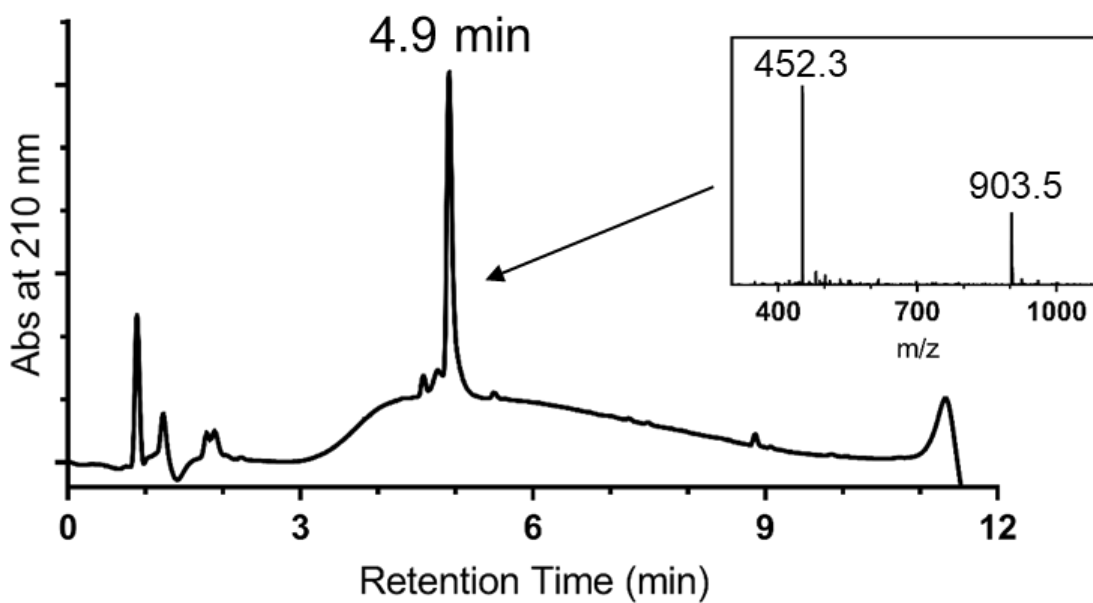
(GGG)₂KK^{DBCO}
902.4 Da

Example chromatogram from (GGG)₂KK-DBCO purification and verification.

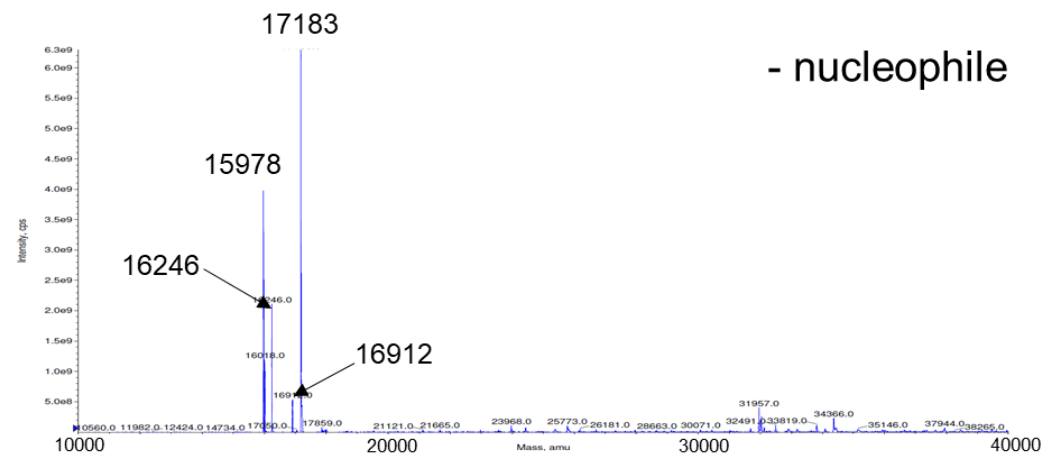
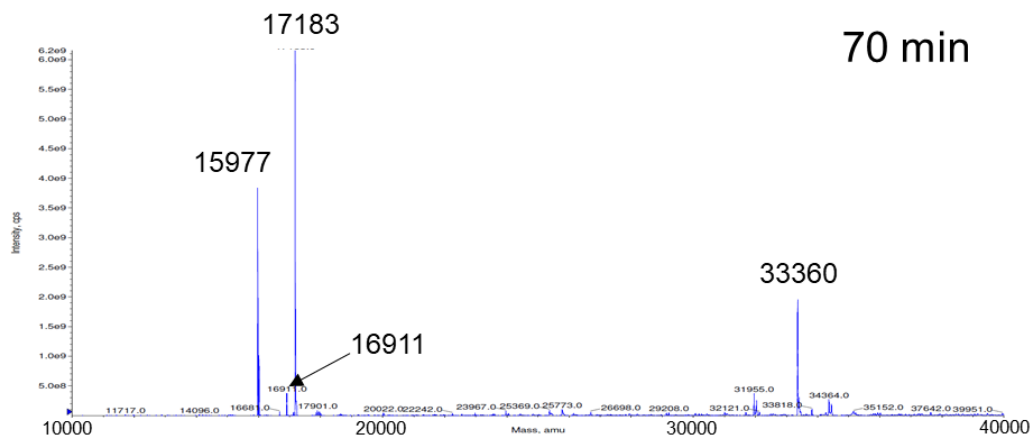
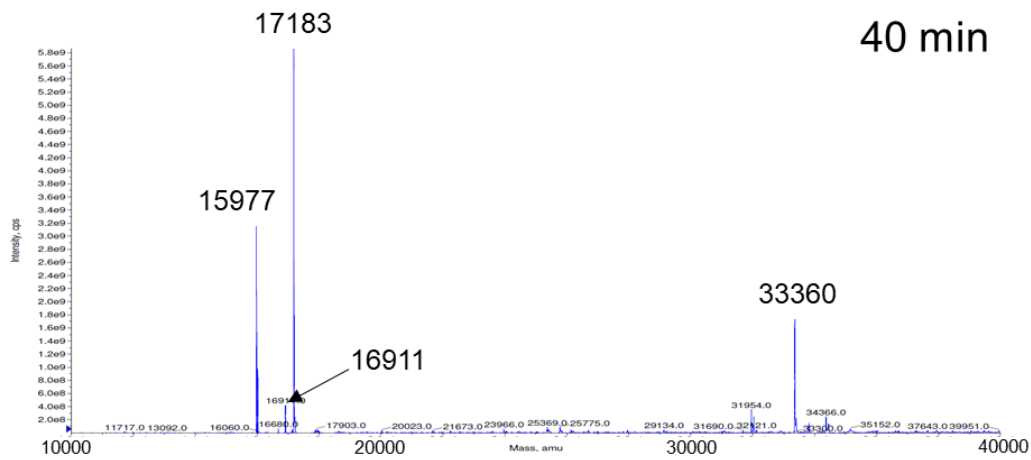
C4 RP-HPLC Purification



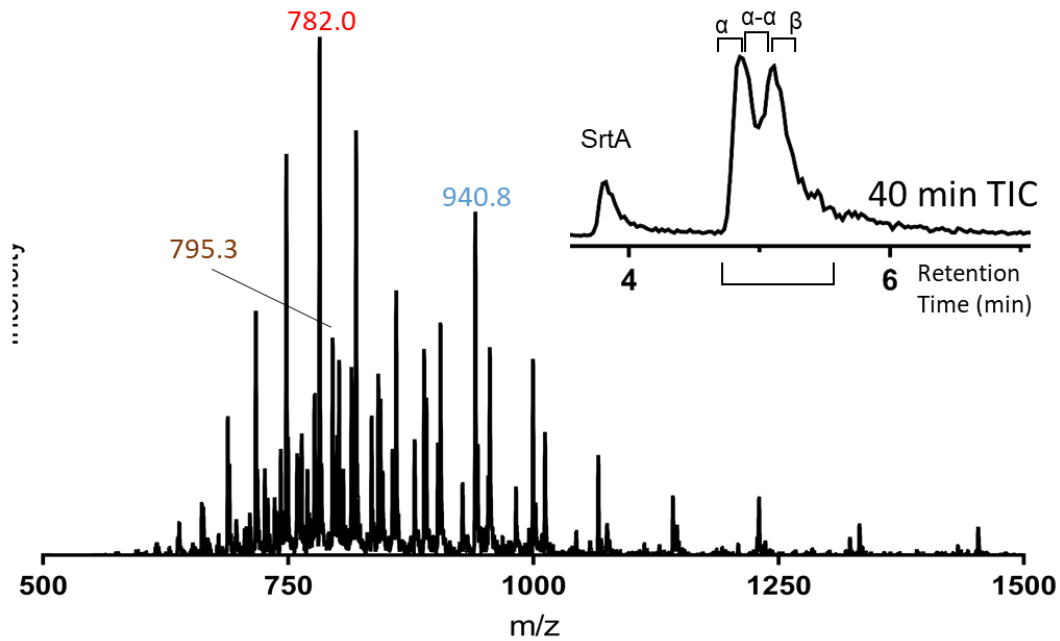
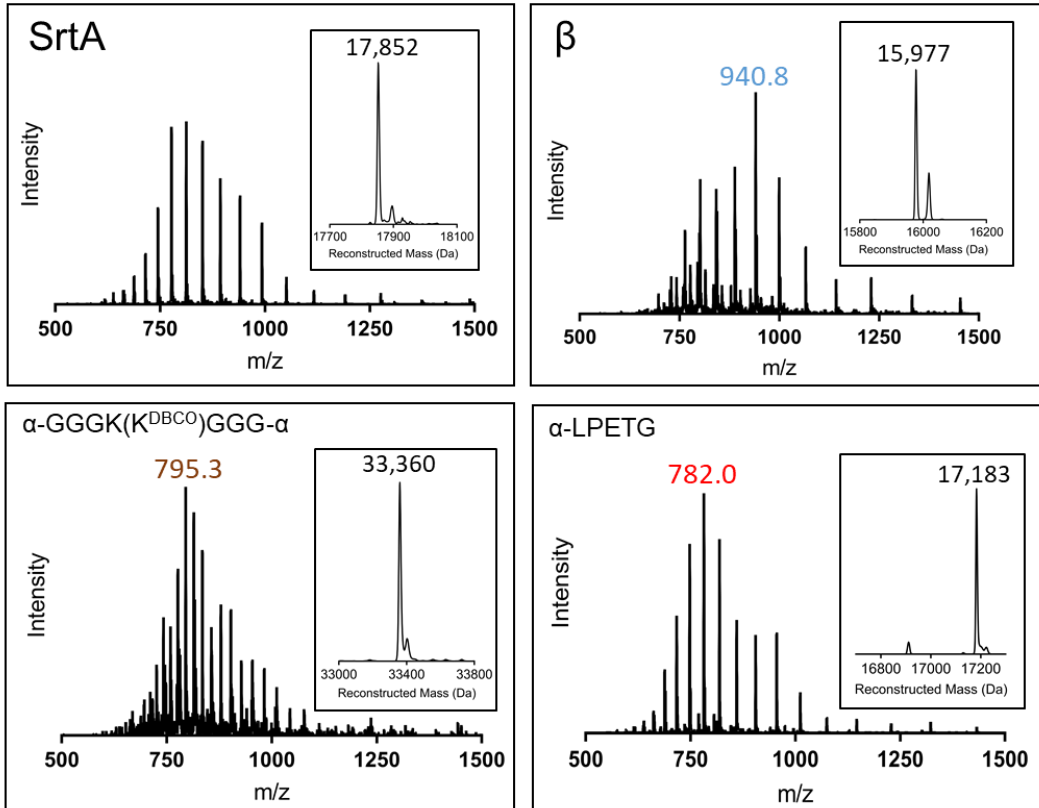
Purity and mass verification by C18 RP-HPLC/MS



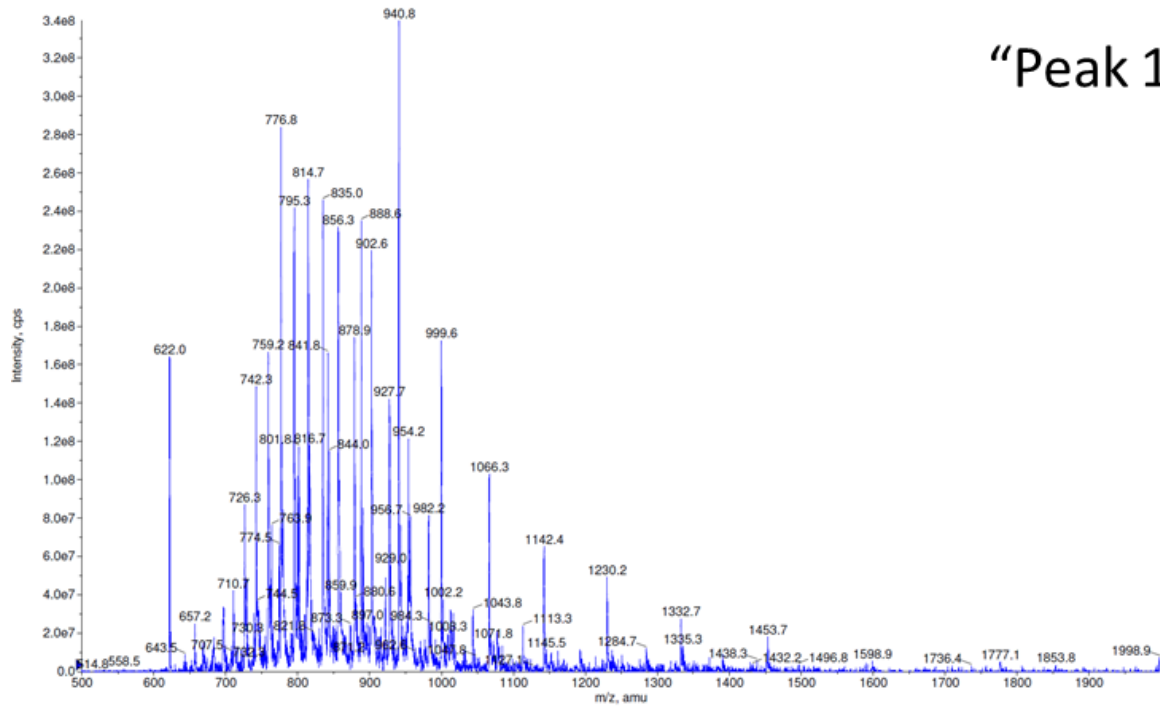
Reconstructed mass data not shown above for the 40- and 70-minute timepoints used in the calculation of crosslinking reaction progress.



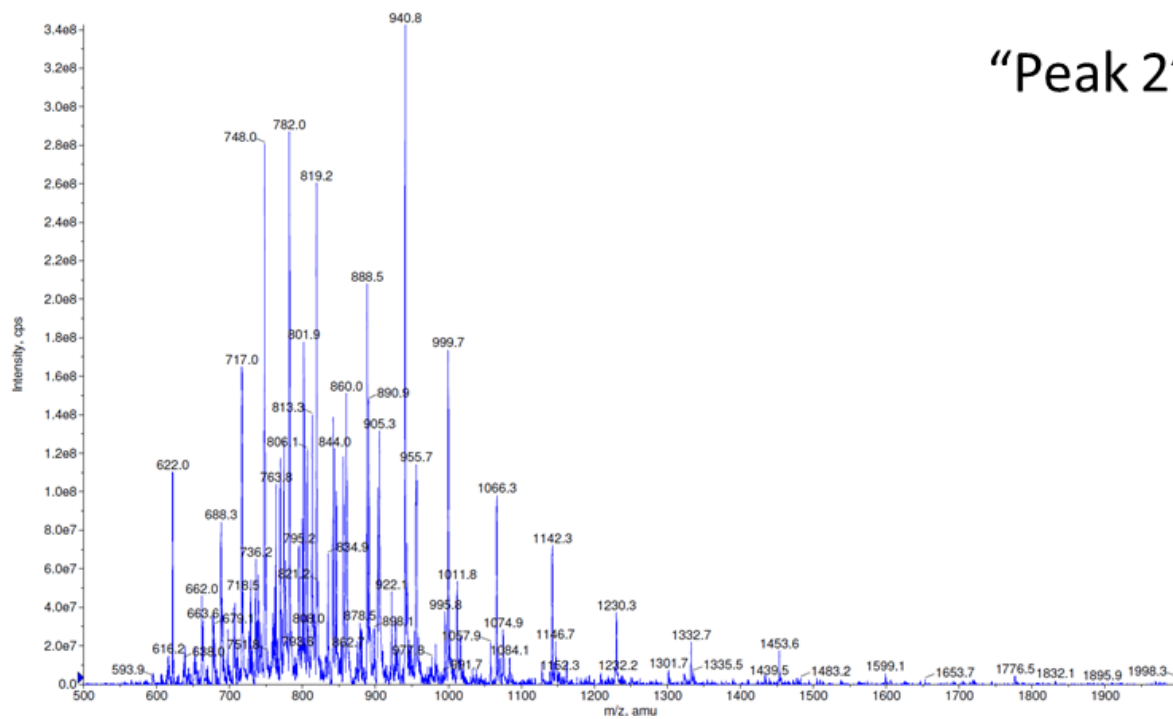
Example of ESI-MS analysis for α -LPETG crosslinking reaction progress at 40 min. The mass spectra for each globin peak can be identified by times indicated on the TIC. The averaged MS for entire Hb peak shown on bottom.



Raw mass spectra for purified fractions of crosslinked α -LPETG. Used for the calculation of reconstructed mass graphs shown in Figure 15c-d.



“Peak 1”



“Peak 2”